Formation and Quantification of ˙OH in Oxidative Water Treatment

Dissertation

zur Erlangung des akademischen Grades eines
Doktors der Naturwissenschaften
– Dr. rer. nat. –

vorgelegt von

Alexandra Fischbacher
geb. Jarocki

geboren in Thorn (Polen)

Institut für Instrumentelle Analytische Chemie
der
Universität Duisburg-Essen

2017

Die vorliegende Arbeit wurde im Zeitraum von Juli 2008 bis Dezember 2017 im Arbeitskreis von Prof. Dr. Torsten C. Schmidt am Institut für Instrumentelle Analytische Chemie der Universität Duisburg-Essen durchgeführt.

Tag der Disputation: 20. April 2018

Gutachter:	Prof. Dr. Torsten C. Schmidt
	Prof. Dr. Malte Behrens
Vorsitzende:	Prof. Dr. Karin Stachelscheid

Abstract

$^{\bullet}$OH are unselective and fast reacting. Water treatment processes leading to $^{\bullet}$OH are called advanced oxidation processes (AOPs). The Fenton process, one of several AOPs, describes the reaction of Fe(II) with hydrogen peroxide. Fe(II) is oxidized to Fe(III) that reacts with hydrogen peroxide to Fe(II) and again initiates the Fenton reaction. One reactive species formed in the Fenton process are $^{\bullet}$OH. Conditions such as pH, the H_2O_2:Fe(II) ratio and ligand concentration may influence the $^{\bullet}$OH yield. It could be shown that at pH < 2.7 and > 3.5 the $^{\bullet}$OH yield decreases significantly. The investigated ligands were pyrophosphate and sulfate. It was found that pyrophosphate forms a complex with Fe(III) that does not react with hydrogen peroxide and thus, terminates the Fenton process and decreases the $^{\bullet}$OH yield. Sulfate also influences the Fenton process but not to the same extent as pyrophosphate. The $^{\bullet}$OH yield is decreased when sulfate is added but even at higher concentrations the Fenton reaction is not terminated. It is necessary to investigate more conditions inhibiting or enhancing the Fenton process to be able to predict and control the reaction.

Another AOP that was dealt with is the peroxone process. It describes the reaction of O_3 with H_2O_2. Hitherto, it has been assumed that the $^{\bullet}$OH yield is unity with respect to O_3 consumption. Three approaches were conducted to investigate the $^{\bullet}$OH per consumed O_3. The first approach included competition experiments. The consumption of trace compounds (*p*-chlorobenzoic acid, *p*-nitrobenzoic acid and atrazine present in trace amounts) has been followed as a function of the O_3 concentration in a solution containing H_2O_2 and tertiary butanol (*t*BuOH) in high excess over the trace compounds. For comparison the experiments were conducted with authentic $^{\bullet}$OH generated by γ-radiolysis. By means of known $^{\bullet}$OH rate constants the competition was adequately fitted. Fitting the peroxone data, however, the consumption of the trace indicators can only be rationalized if the $^{\bullet}$OH yield is near 0.5 (*p*-chlorobenzoic: 0.51; *p*-nitrobenzoic: 0.45; atrazine: 0.6). Beside the competition experiments further evidence for a reduced $^{\bullet}$OH yield (near 0.5) is derived from a product analysis of the reactions of *t*BuOH with $^{\bullet}$OH and dimethyl sulfoxide with $^{\bullet}$OH. The mechanistic interpretation for the low $^{\bullet}$OH yield is as follows. In the reaction of O_3 with HO_2^- an adduct (HO_5^-) is formed that decomposes into $O_3^{\bullet-}$ and $HO_2^{\bullet}$ in competition with 2 O_2 + OH^-. The latter process contributes to a reduced $^{\bullet}$OH yield. From the mechanistic considerations and the experimental data it is concluded that the $^{\bullet}$OH yield per consumed O_3 must be near 0.5. As $^{\bullet}$OH are also formed from the reaction of O_3 with water matrix components the effect of the revised mechanisms on practical implementations cannot be predicted.

Ozone is often used in drinking water treatment. In dependency on the water matrix constituents different undesired by-products may be formed. If the water to be treated contains bromide ozonation of this water leads to bromate formation, as the reaction of bromide with ozone yields bromate. Bromate is regulated in drinking water as it is considered to be carcinogenic. Its formation is a multistep process resulting in the last step from the reaction of ozone with bromite. Although this process seemed to be established, it has been shown that ozone reacts with bromite not as previously assumed via O-transfer but via electron-transfer. Besides bromate, the electron transfer reaction also yields $O_3^{\bullet-}$, the precursor of $^{\bullet}OH$. In the experimental setup $^{\bullet}OH$ were not produced from O_3 self-decomposition but solely by the electron-transfer reaction. The first evidence for the electron transfer reaction is derived from the addition of *t*BuOH as $^{\bullet}OH$ scavenger and measuring formaldehyde, the product from the reaction of *t*BuOH with $^{\bullet}OH$. To confirm the outcome of the first experiments HOBr (formed from the reaction of O_3 and bromide) and bromate yields were measured in systems with and without *t*BuOH. As $^{\bullet}OH$ contribute to bromate formation, higher bromate and HOBr yields were observed in the absence of *t*BuOH than in its presence, where all $^{\bullet}OH$ are scavenged. Based on the presented results, a pathway from bromide to bromate, revised in the last step, was suggested. The revised reaction step may help in modelling bromate formation as it is hitherto very imprecise due to too many included reactions that are not well known.

The quantification of $^{\bullet}OH$ is of great interest and its exact quantification is essential for mechanistic considerations. An established method for the determination of $^{\bullet}OH$ in water is the product analysis of the products from the reaction of *t*BuOH with $^{\bullet}OH$, that is also used in this thesis. The products of this reaction are beside formaldehyde and acetone 2-methyl-2-hydroxypropanol and 2-methyl-2-hydroxypropanal. The latter two are not commercially available and therefore, an indirect quantification of $^{\bullet}OH$ is just possible by an assumed yield of formaldehyde formed per $^{\bullet}OH$. The synthesis of 2-methyl-2-hydroxypropanol was performed by adapting a previously published synthesis. The product of the synthesis was characterized by NMR and GC-MS and 2-methyl-2-hydroxypropanol was identified. One method to synthesize 2-methyl-2-hydroxypropanal is the oxidation of 2-methyl-2-hydroxy-propanol by Dess-Martin periodinane (DMP), l,l,l-triacetoxy-l,l-dihydro-l,2-benziodoxol-3(1H)-one. The product characterization was done by NMR and HPLC-UV after derivatization. The NMR spectra did not show any product and the HPLC chromatogram shows many impurities and therefore, 2-methyl-2-hydroxypropanal could not be identified. To obtain the desired product further oxidation methods have to be applied and as 2-methyl-2-hydroxypropanol is just formed

from one reaction in the cascade of reactions its importance for the quantification of •OH is still unknown.

Zusammenfassung

•OH sind hochreaktiv und reagieren unselektiv. Aus diesem Grund werden sie in der Wasseraufbereitung eingesetzt. Wasseraufbereitungsprozesse, die zur •OH-Bildung führen fasst man unter dem Begriff der erweiterten oxidativen Prozesse (Advanced Oxidation Processes (AOPs)) zusammen. Der Fenton-Prozess, einer von vielen AOPs, beschreibt die Reaktion von Fe(II) mit Wasserstoffperoxid. Dabei wird Fe(II) von Wasserstoffperoxid zu Fe(III) oxidiert, dieses reagiert wiederum mit Wasserstoffperoxid zurück zu Fe(II) und initiiert somit erneut die Fenton-Reaktion. Die gebildete reaktive Spezies sind die •OH. Dabei kann die •OH-Ausbeute von unterschiedlichen Faktoren, wie z.B. dem pH-Wert, dem H_2O_2:Fe(II) - Verhältnis und der Ligandenkonzentration, beeinflusst werden. Die vorliegende Arbeit zeigt, dass bei pH-Werten <2,7 und >3,5 die •OH-Ausbeute signifikant abnimmt. Der Einfluss der beiden Liganden, Pyrophosphat und Sulfat, ist untersucht worden. Es konnte gezeigt werden, dass Pyrophosphat einen Komplex mit Fe(III) bildet, der nicht mit Wasserstoffperoxid reagiert und somit den Fenton-Prozess terminiert und die •OH-Ausbeute verringert. Sulfat hat ebenfalls einen Einfluss auf den Fenton-Prozess, jedoch nicht im gleichen Ausmaß wie Pyrophosphat. Die Zugabe von Sulfat führt zwar zur Verringerung der •OH-Ausbeute, jedoch wird selbst bei höheren Sulfatkonzentrationen die Fenton-Reaktion nicht terminiert. Es ist notwendig mehr Bedingungen zu untersuchen, die den Fenton-Prozess hemmen oder verstärken können, um die Reaktionen besser vorhersagen und steuern zu können.

Ein anderer AOP ist der Peroxon-Prozess. Der Prozess beschreibt die Reaktion von O_3 mit H_2O_2. Bisher galt die Annahme, dass die •OH-Ausbeute bezogen auf den O_3-Verbrauch eins ist. In drei unterschiedlichen Ansätzen ist die •OH-Ausbeute pro verbrauchtem O_3 untersucht worden. Im ersten Ansatz sind Kompetitionsexperimente durchgeführt worden. Der Abbau von Spurenstoffen (*p*-Chlorbenzoesäure, *p*-Nitrobenzoesäure und Atrazin) ist in Abhängigkeit von der O_3-Konzentration verfolgt worden. Neben diesen enthielt die Lösung noch H_2O_2 und einen hohen Überschuss an *tert*-Butanol (*t*BuOH). Zum Vergleich wurden die Experimente mit authentischen •OH, die durch γ-Radiolyse erzeugt wurden, durchgeführt. Mithilfe bekannter Geschwindigkeitskonstanten für die o. g. Spurenstoffe mit •OH konnten die Kompetitionen adäquat angepasst werden. Nach der Datenanpassung kann der Spurenstoffabbau jedoch nur dann sinnvoll erklärt werden, wenn die •OH Ausbeute bei ungefähr 0,5 liegt (*p*-Chlorbenzoesäure: 0,51; *p*-Nitrobenzoesäure: 0,45; Atrazin: 0,6). Neben den Kompetitionsexperimenten liefert die Analyse der Produkte aus den Reaktionen von *t*BuOH mit •OH und Dimethylsulfoxid mit •OH weitere Hinweise auf eine reduzierte •OH-Ausbeute

(ca. 0,5). Die mechanistische Interpretation für die niedrige •OH-Ausbeute ist folgende. Bei der Reaktion von O_3 mit HO_2^- wird ein Addukt (HO_5^-) gebildet, das in $O_3^{\bullet-}$ (•OH-Vorläufer) und $HO_2^\bullet$ oder in Konkurrenz dazu zu $2O_2$ und OH^- zerfällt. Letzterer Zerfall führt zu einer reduzierten •OH-Ausbeute. Aus den mechanistischen Überlegungen und den experimentellen Daten wird geschlossen, dass die •OH-Ausbeute pro verbrauchtem O_3 bei ungefähr 0,5 liegen muss. Da •OH auch aus der Reaktion von O_3 mit Wassermatrixkomponenten entstehen können, kann der Effekt des überarbeiteten Mechanismus auf praktische Implementierungen nicht vorhergesagt werden.

Ozon wird oft in der Trinkwasseraufbereitung eingesetzt. In Abhängigkeit von den Wassermatrixbestandteilen können verschiedene unerwünschte Nebenprodukte gebildet werden. Wenn das zu behandelnde Wasser Bromid enthält, führt die Ozonung zur Bildung von Bromat, das aus der Reaktion von Bromid mit Ozon entsteht. Bromat ist im Trinkwasser reguliert, da es als krebserregend gilt. Dessen Bildung ist ein mehrstufiger Prozess, der im letzten Schritt aus der Reaktion von Ozon mit Bromit resultiert. Obwohl dieser Prozess bereits gut etabliert ist, konnte gezeigt werde, dass Ozon mit Bromit nicht wie bisher angenommen über O-Transfer, sondern über Elektronentransfer reagiert. Neben Bromat liefert die Elektronentransferreaktion auch $O_3^{\bullet-}$, den Vorläufer von •OH. Die Versuche wurden so gestaltet, dass keine •OH aus der Selbstzersetzung von O_3 gebildet werden konnten, sondern ausschließlich aus der Elektronentransferreaktion. Der erste Beweis für die Elektronentransferreaktion ergibt sich aus der Zugabe von *t*BuOH als •OH-Fänger und der Messung des Reaktionsproduktes Formaldehyd. Um das Ergebnis der ersten Experimente zu bestätigen, wurden die HOBr- (gebildet aus der Reaktion von O_3 und Bromid) und Bromatausbeuten in Systemen mit und ohne *t*BuOH bestimmt. Da •OH zur Bromatbildung beitragen, wurden in Abwesenheit von *t*BuOH höhere Bromat- und HOBr-Ausbeuten beobachtet als in Gegenwart von *t*BuOH, das alle gebildeten •OH abfängt. Auf der Grundlage der präsentierten Ergebnisse wurde ein im letzten Schritt (Reaktion von O_3 mit Bromit) überarbeiteter Bromatbildungsmechanismus vorgeschlagen. Der geänderte Reaktionsschritt kann die Modellierung der Bromatbildung verbessern, da sie bisher aufgrund zu vieler unbekannter Reaktionen sehr ungenau ist.

Die Quantifizierung von •OH ist von großem Interesse, denn die exakte Quantifizierung ist essentiell für mechanistische Überlegungen. Eine etablierte Methode zur Quantifizierung von •OH in Wasser ist die Analyse der Produkte aus der Reaktion von *t*BuOH mit •OH, die auch in dieser Arbeit verwendet wird. Die Produkte dieser Reaktion sind neben Formaldehyd und

Aceton, 2-Methyl-2-Hydroxypropanol und 2-Methyl-2-Hydroxypropanal. Da die beiden letztgenannten nicht kommerziell erhältlich sind, ist eine indirekte Quantifizierung von •OH nur möglich, wenn man von einer angenommenen Formaldehydausbeute pro •OH ausgeht. Die Synthese von 2-Methyl-2-hydroxypropanol wurde nach Anpassung einer bereits veröffentlichten Synthese durchgeführt. Das Produkt der Synthese wurde mithilfe von NMR und GC-MS charakterisiert und als 2-Methyl-2-Hydroxypropanol identifiziert. Eine Methode zur Synthese von 2-Methyl-2-Hydroxypropanal ist die Oxidation von 2-Methyl-2-Hydroxypropanol durch das Dess-Martin-Periodinan (DMP), 1,1,1-Triacetoxy-1,1-Dihydro-1,2-Benziodoxol-3(1H)-on. Die Produktcharakterisierung wurde mittels NMR und nach einer Derivatisierung der Produkte mittels HPLC-UV durchgeführt. Während die NMR-Spektren keine Produkte aufzeigten, wurden im Chromatogramm der HPLC-Messungen nur Verunreinigungen sichtbar. Somit konnte 2-Methyl-2-Hydroxypropanal nicht nachgewiesen werden. Um das gewünschte Produkt zu erhalten, müssen andere Synthesen durchgeführt werden. Außerdem wird 2-Methyl-2-Hydroxypropanol nur in einer von einer Kaskade von Reaktionen gebildet. Dessen Bedeutung für die •OH-Quantifizierung muss ebenfalls abgeklärt werden.

Table of Contents

Chapter 1

INTRODUCTION

Parts are redrafted from “Fischbacher, A.; Lutze, H. V.; Schmidt, T. C., Ozone/H_2O_2 and ozone/UV processes. In *Advanced oxidation processes for water treatment*, Stefan, M. I., Ed. IWA publishing: London, UK, 2017; pp 163-194.“, ISBN: 9781780407180,

1.1 WATER TREATMENT

More and more organic micropollutants (OMPs), e.g. pharmaceuticals and pesticides can be identified even in trace concentrations in surface waters due to better analytical opportunities. The sources for these contaminations are besides run-off from agricultural and urban areas the discharge of treated wastewater into rivers, as in wastewater treatment plants many of these organic micropollutants are not sufficient degraded or eliminated (Prasse *et al.*, 2015). The contaminated surface waters may lead to a contamination of drinking water sources with OMPs that can be hardly eliminated by conventional drinking water treatment. Conventional drinking water treatment mostly includes a combination of coagulation, sedimentation, filtration and disinfection. In dependency of the raw water quality the conventional treatment may be preceded by a preoxidation step. Ozone is often applied for preoxidation, but in many cases it is insufficient to degrade OMPs and therefore, stronger oxidation agents are required.

Water treatment processes that lead to highly reactive hydroxyl radicals (•OH) are referred to as Advanced Oxidation Processes (AOPs). These radicals are capable of degrading pollutants that survive other oxidation processes such as conventional ozonation, thus, the implementation of •OH-based water treatment processes represent a viable option in order to meet the low drinking water standards for regulated micropollutants. AOPs are already applied in drinking water production, if the drinking water source is contaminated (Werderitsch, 2013). The application of AOPs in wastewater treatment occurs just in lab- or pilot-scale. Prasse *et al.* (2015) proclaim that AOPs might become of greater importance in the future also in wastewater treatment to avoid point-source contamination of water bodies by discharging insufficient treated wastewater. Even if already applied the mechanisms of several AOPs are not well understood.

1.2 ADVANCED OXIDATION PROCESSES

AOPs are defined as "those which involve the generation of hydroxyl radicals in sufficient quantity to affect water purification" (Glaze et al., 1987). The most common processes are ozone-, hydrogen peroxide- or photo-based or a combination of these, e.g. O_3/H_2O_2 (peroxone process), O_3/UV, UV/H_2O_2, Fe(II)/H_2O_2 (Fenton process), O_3/H_2O_2/UV and others. These processes are mostly applied in drinking water treatment to oxidize ozone-refractory compounds by hydroxyl radicals. As •OH react fast and unselective the reaction rates of •OH with organic compounds are much faster than that of O_3 (Table 1-1). In contrast to other

common oxidants, e.g. O_3 and chlorine, AOPs are applied solely for oxidation and not for disinfection of waters.

Table 1-1: Reaction rate constant ranges for the reactions of several compounds with ozone and hydroxyl radicals

Compound	$k(O_3)$ $M^{-1}\ s^{-1}$	$k(^{\bullet}OH)$ $M^{-1}\ s^{-1}$
Chlorinated alkenes	10^{-1} to 10^{3}	10^{9} to 10^{11}
Phenols	10^{3}	10^{9} to 10^{10}
N-containing organics	10 to 10^{2}	10^{8} to 10^{10}
Aromatics	1 to 10^{2}	10^{8} to 10^{10}
Ketones	1	10^{9} to 10^{10}
Alcoholes	10^{-2} to 1	10^{8} to 10^{9}
Alkanes	10^{-2}	10^{6} to 10^{9}

1.3 HYDROXYL RADICALS

1.3.1 $^{\bullet}$OH REACTION MECHANISMS

Hydroxyl radicals ($^{\bullet}OH$) are fast reactive and unselective electrophilic species. The reduction potential of $^{\bullet}OH$ in neutral solution is reported to be in the range of 1.77-1.91 V ($^{\bullet}OH/OH^{-}$) and in acidic solution 2.59-2.74 V ($^{\bullet}OH$, H^{+}/H_2O) (Buxton et al., 1988). They react with many substrates at near-diffusion-controlled rates. The diffusion-controlled limit is in the order of 10^{9} $M^{-1}\ s^{-1}$ or greater (Atkins, 1998). The three main reaction pathways are H-abstraction, addition to double bonds and electron transfer. At high pH values $^{\bullet}OH$ are present in their deprotonated form (pKa = 11.8) (reaction 1-1). The reaction rates of $O^{\bullet-}$ with organic and inorganic compounds are lower than that of $^{\bullet}OH$. However, due to the high pKa of $^{\bullet}OH$, $O^{\bullet-}$ can be neglected for nearly all aquatic systems.

$$^{\bullet}OH + OH^{-} \rightleftharpoons O^{\bullet-} + H_2O \qquad (1\text{-}1)$$

•OH absorb light below 400 nm (Figure 1-1). At 230 nm their extinction coefficient is 575 M^{-1} cm^{-1} (Figure 1-1) but a direct quantification by UV spectroscopy is almost impossible due to its short lifetime. There are several indirect methods available for •OH quantification, but not all methods can be applied for all systems. One has always to take into account the side reactions that may occur and lead to a deficient •OH yield. The presence of other oxidants, e.g., O_3 excludes some quantification methods (see below).

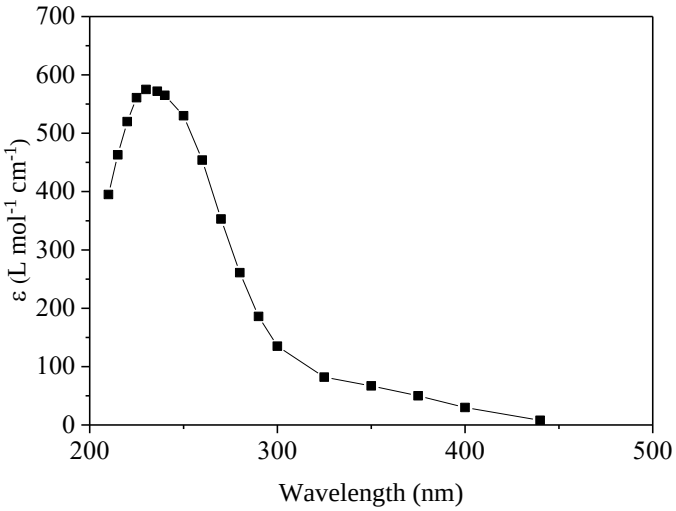

Figure 1-1: Extinction coefficients of •OH in aqueous solution for the wavelength range of 210-440 nm taken from (Czapski and Bielski, 1993)

•OH are generated as reactive species in AOPs but also may occur undesired in systems with prerequisites for •OH generation, e.g. fuel cells that meet the conditions for the Fenton process. The formed •OH degrade the membranes of the fuel cells and hence, decrease their lifetime (Holton and Stevenson, 2013).

1.3.2 •OH REACTION MECHANISMS

1.3.2.1 H-ABSTRACTION

The abstraction of an H by •OH depends on the bond dissociation energy (BDE) of the bond to be broken. Due to different BDEs for C—H bonds, there is a gradient for H abstraction. Tertiary hydrogen ($-\overset{|}{\underset{|}{C}}H$) can be better abstracted than secondary ($H\overset{|}{\underset{|}{C}}H$) than primary ($-CH_3$). An example is shown in Figure 1-2. In ethanol where the BDE for the secondary H is 389.1 – 401.2 kJ mol^{-1} and for the primary H 410 – 423.8 kJ mol^{-1} (Luo, 2007), the secondary H is abstracted to a much greater extent (84.3 %) (reaction 1-2) than the primary H (13.2 %) (reaction 1-3)

(Asmus *et al.*, 1973). As the BDE for the O—H in ethanol is much higher (436 – 441 kJ mol^{-1}) (Luo, 2007) the H abstraction at this position is of minor importance (2.5 %) (reaction 1-4) (Asmus *et al.*, 1973). S—H bonds are mostly weaker than C—H bonds and therefore the H abstraction is diffusion-controlled. Besides the BDE neighboring substituents influence H-abstraction. An electron donating group increases the rate of H-abstraction, while it is decreased by an electron-withdrawing group.

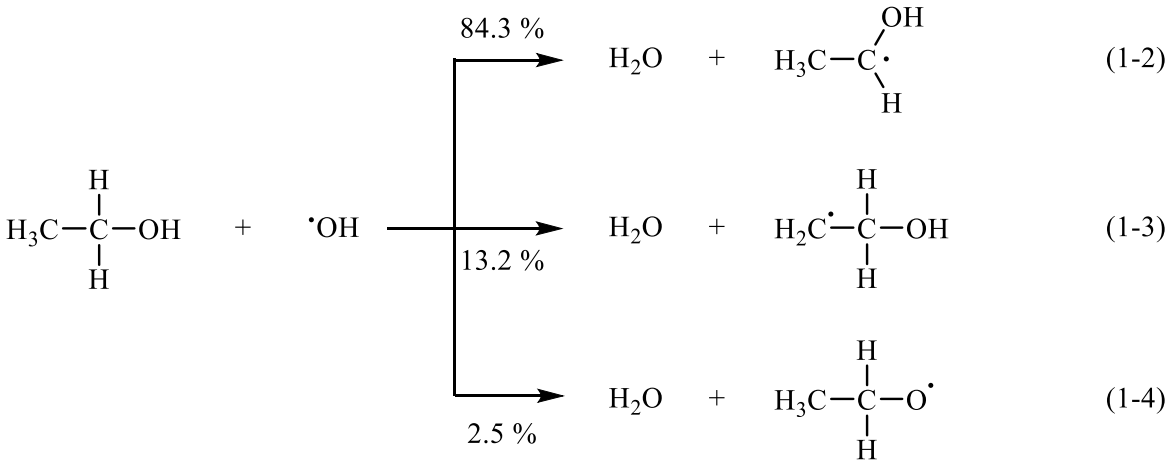

Figure 1-2: H-abstraction reactions of ethanol with •OH

1.3.2.2 ADDITION TO DOUBLE BONDS

Hydroxyl radicals add to C═C, C═N and S═O double bonds but not to C═O double bonds as these bonds have an electron deficit at the C atom, which is the preferred addition position. The addition to a C═C double bond of benzene or benzene derivatives occurs via a short-lived π-complex (reaction 1-5) that immediately collapses into an σ-complex (reaction 1-6). The reaction is near-diffusion-controlled. While the •OH is in the π-complex it is guided to the addition position, which is preferably the electron richest part of the molecule. This can be driven by electron-withdrawing or electron-donating substituents. In benzene derivatives ortho and para position are preferred if electron-donating substituents are present while in presence of electron-withdrawing substituents meta position is favored.

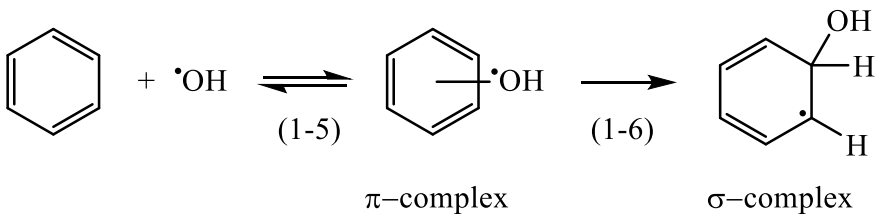

The •OH can also add to lone electron pairs of electron-rich heteroatoms, e.g. amines, sulfides disulfides, halide and pseudo-halide ions. A three-electron intermediate is formed.

1.3.2.3 ELECTRON TRANSFER

The high electron reduction potential of •OH makes an electron transfer in principle possible. However, it is not kinetically favored and therefore, rarely observed in •OH reactions. It is supposed that analogous to the addition reactions in the first step a π-complex is formed. Hence, electron transfer reactions are in competition to addition reactions. Mostly addition is favored, but if positions, which are relevant for the addition of •OH are blocked by bulky substituents, electron transfer may occur.

1.3.3 QUANTIFICATION METHODS

As •OH are very reactive and therefore short lived a direct quantification is almost impossible. Some indirect methods for the quantification of •OH are presented below, e.g. the quantification of the products of the reaction of •OH with *t*BuOH, methanol, DMSO, terephthalic acid and the quantification of •OH yield after their reaction with spin traps by electron spin resonance spectroscopy.

1.3.3.1 THE REACTION OF *t*BUOH WITH •OH

•OH react fast with *t*BuOH ($k = 6 \times 10^8$ M^{-1} s^{-1}) (Buxton *et al.*, 1988). The radical chain reactions take place in presence of O_2 and were described in detail by Schuchmann and von Sonntag (1979) and Flyunt *et al.* (2003) (Figure1-3). The first step is a H-abstraction of the hydrogen from the alcoholic group (5 %) giving a *t*-butoxyl radical (reaction 1-7) that decomposes into acetone and a methyl radical (reaction 1-8) or an abstraction of a primary hydrogen from one of the CH_3 groups yielding an alkyl radical (95 %) (reaction 1-10). The alkyl radical reacts with O_2 giving rise to an alkyl peroxyl radical (reaction 1-11), which decays bimolecularly into a tetroxide (reaction 1-12). The tetroxide may decompose by the Russell-type reaction yielding 2-methyl-2-hydroxypropanol and 2-methyl-2-hydroxypropanal (reaction 1-13) or by the Bennett-type reaction yielding two molecules of 2-methyl-2-hydroxypropanal (reaction 1-14). Two other types of decomposition reactions are possible. In reaction (1-15) the tetroxide decomposes into two molecules formaldehyde and two molecules 2-hydroxyprop-2-yl radical that reacts with O_2 to its peroxyl radical (reaction 1-16) that decomposes into acetone and HO_2• (reaction 1-17). The decomposition of the tetroxide may also yield according to reaction (1-18) two molecules of an oxyl radical, that decomposes into formaldehyde and hydroxyprop-2-yl (reaction 1-19) initiating reaction (1-16) or reacting to acetone and superoxide (reaction 1-20).

The oxyl radical formed in reaction (1-18) may also undergo a cascade of reactions (1-21 – 1-23) yielding 2-methyl-2-hydroxypropanal.

The main products from the reaction of $^{\bullet}OH$ with *t*BuOH are 2-methyl-2-hydroxypropanol, 2-methyl-2-hydroxypropanal, acetone and formaldehyde. As there is no authentic standard for 2-methyl-2-hydroxypropanol and 2-methyl-2-hydroxypropanal the quantification occurs by measuring formaldehyde. The formaldehyde yield represents 30±4 % $^{\bullet}OH$. If O_3 is present the formaldehyde yield represents 50 % of $^{\bullet}OH$, as superoxide formed in reaction (1-20) reacts with O_3 giving rise to additional $^{\bullet}OH$ that contributes to a higher formaldehyde yield.

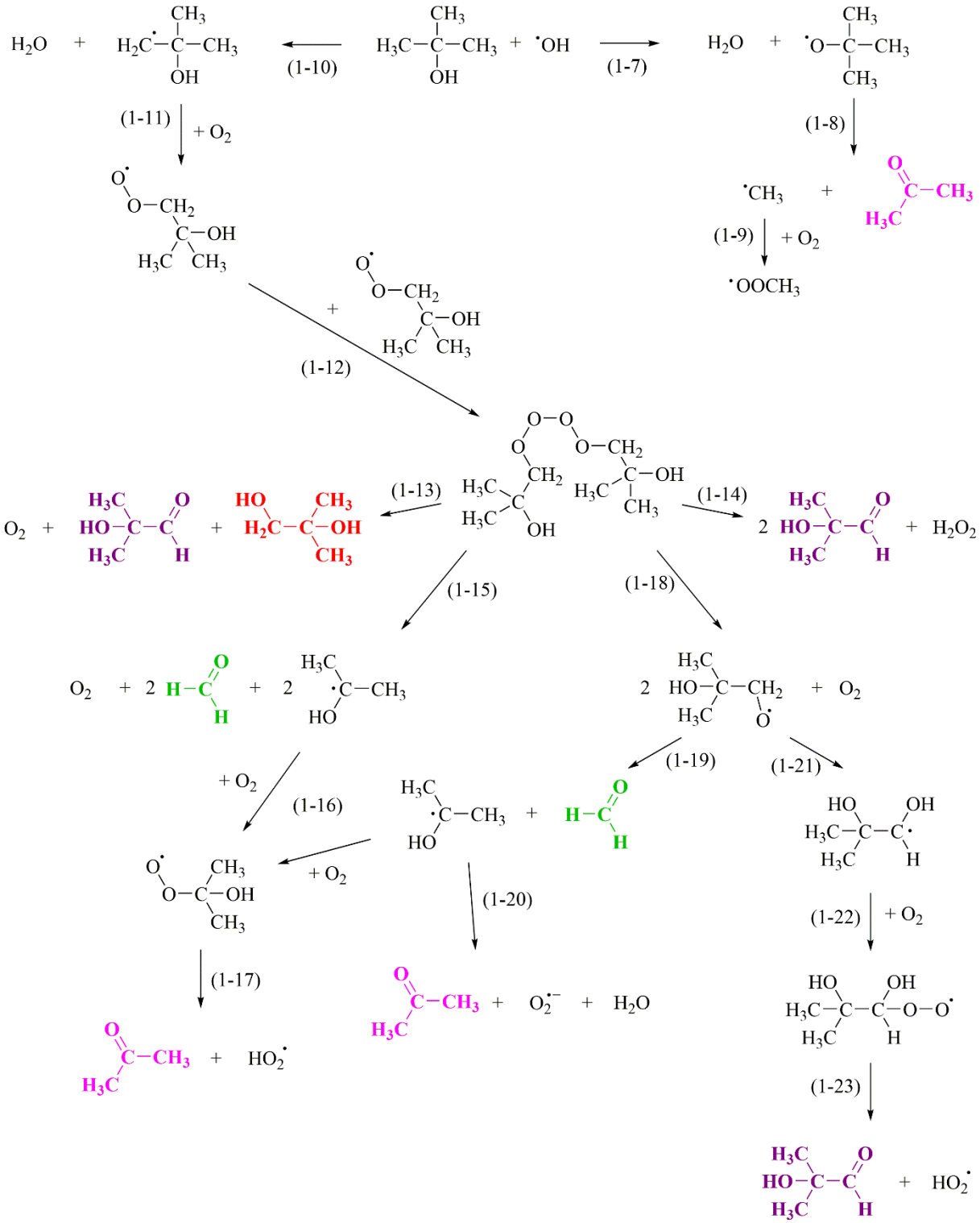

Figure 1-3: Reaction scheme for the radical chain reactions initiated by the reaction of *t*BuOH with ˙OH. The main products are indicated by following colours: acetone, formaldehyde, 2-methyl-2hydroxypropanol and 2-methyl-2hydroxypropanal

1.3.3.2 THE REACTION OF METHANOL WITH •OH

Figure 1-4 shows the reaction of •OH with methanol. •OH react with methanol by H abstraction (reaction 1-24). Its product reacts in presence of O_2 and OH^- or $H_2PO_4^{2-}$ to formaldehyde and superoxide (reactions 1-25 – 1-27). The formaldehyde yield per •OH is unity.

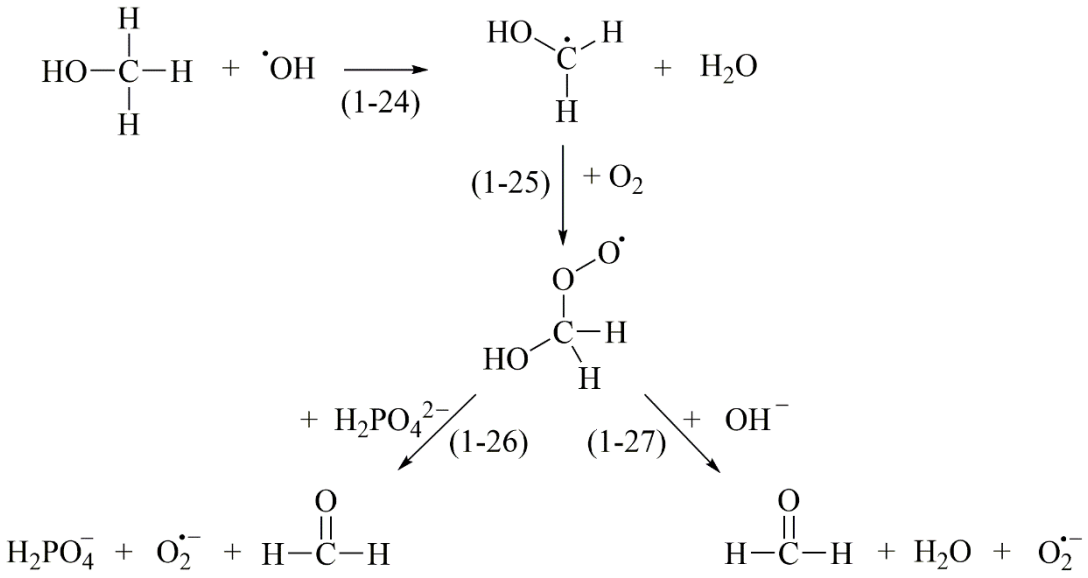

Figure 1-4: Reaction of •OH with methanol in presence of O_2, OH^- and $H_2PO_4^{2-}$

This system seems to be best suitable for systems without O_3 and H_2O_2. Superoxide formed besides formaldehyde can react with O_3 (1-28) (von Gunten, 2003a) and increase the •OH yield. H_2O_2 reacts with an intermediate (•CH_2OH/•CH_2O^-) to formaldehyde and •OH (1-29 – 1-30) (Ulanski and von Sonntag, 1999). Thus, in presence of O_3 and/or H_2O_2 formaldehyde is not only formed from the reaction with •OH. This leads to an overestimation of •OH yields.

$$O_3 + O_2^{\bullet-} \rightarrow O_3^{\bullet-} + O_2 \qquad k = 1.6 \times 10^9\ M^{-1}\ s^{-1} \qquad (1\text{-}28)$$

$$^{\bullet}CH_2OH + H_2O_2 \rightarrow CH_2O + H^+ + OH^- + {}^{\bullet}OH \qquad k = 6 \times 10^4\ M^{-1}\ s^{-1} \qquad (1\text{-}29)$$

$$^{\bullet}CH_2O^- + H_2O_2 \rightarrow CH_2O + OH^- + {}^{\bullet}OH \qquad k = 4 \times 10^5\ M^{-1}\ s^{-1} \qquad (1\text{-}30)$$

pK_a (•CH_2OH) = 10.7 (Laroff and Fessenden, 1973)

1.3.3.3 THE REACTION OF DMSO WITH •OH

•OH react fast with DMSO ($k = 7 \times 10^9\ M^{-1}\ s^{-1}$) (Buxton *et al.*, 1988) (Figure 1-5). The addition reaction (1-32) (92 %) is favored over the H-abstraction reaction (1-31) (8 %). The products of reaction (1-32) are methanesulfinic acid and a methyl radical (reactions 1-32 – 1-33). The latter

reacts with O_2 to $CH_3OO^{\bullet}$ (reaction 1-34), that oxidizes the formed methanesulfinic acid to methanesulfonic acid (reaction 1-35) (von Sonntag and von Gunten, 2012). Both acids can readily be quantified by ion chromatography and its sum represents 92 % of the present $^{\bullet}OH$ (Veltwisch *et al.*, 1980). The reaction of DMSO with O_3 is slow (k = 8.1 M^{-1} s^{-1}) (Pryor *et al.*, 1984), therefore in dependency of its concentration it can be applied in presence of O_3.

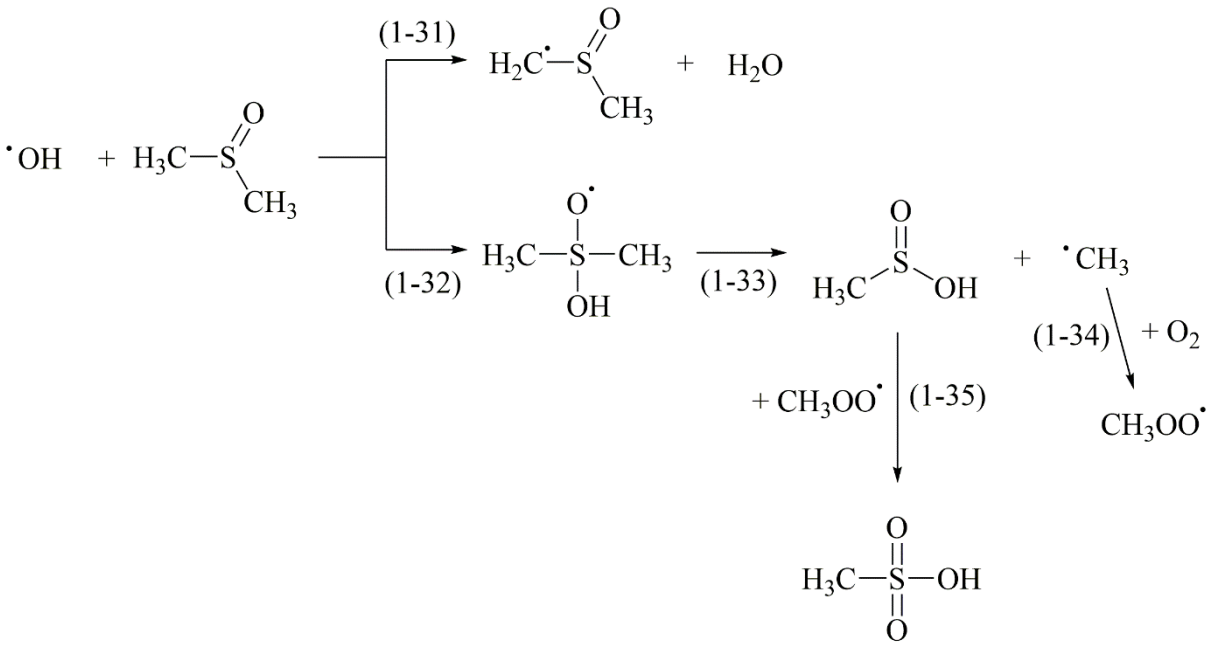

Figure 1-5: Reaction scheme for the reaction of DMSO with $^{\bullet}OH$

1.3.3.4 THE REACTION OF TEREPHTHALIC ACID WITH $^{\bullet}OH$

Another approach to quantify $^{\bullet}OH$ is the terephthalate dosimeter investigated by Fang *et al.* (1996) (Figure 1-6). Here the reaction of $^{\bullet}OH$ with terephthalic acid yields 2-hydroxyterephthalate which can be measured by fluorimetry. The yield of 2-hydroxyterephthalate is not equivalent to 100 % of the present $^{\bullet}OH$, as there is a competition in the first step (addition of OH in ipso (reaction 1-36) vs. ortho position (reaction 1-37)) and only the product of the addition in ortho position contributes to the 2-hydroxyterephthalate yield. The formed hydroxycyclohexadienyl radical has to be further oxidized. If the oxidation occurs by oxygen (reaction 1-38), the 2-hydroxyterephthalate yield is only around 35 %, as the formed intermediate may also react in competition to its decomposition to 2-hydroxyterephtalate (reaction 1-39) yielding other products (reactions 1-40 – 1-41). To achieve a higher yield a stronger oxidation agent, e.g. $IrCl_6^{2-}$ is required. In its presence, a 2-hydroxyterephthalate yield of 84 % is reached.

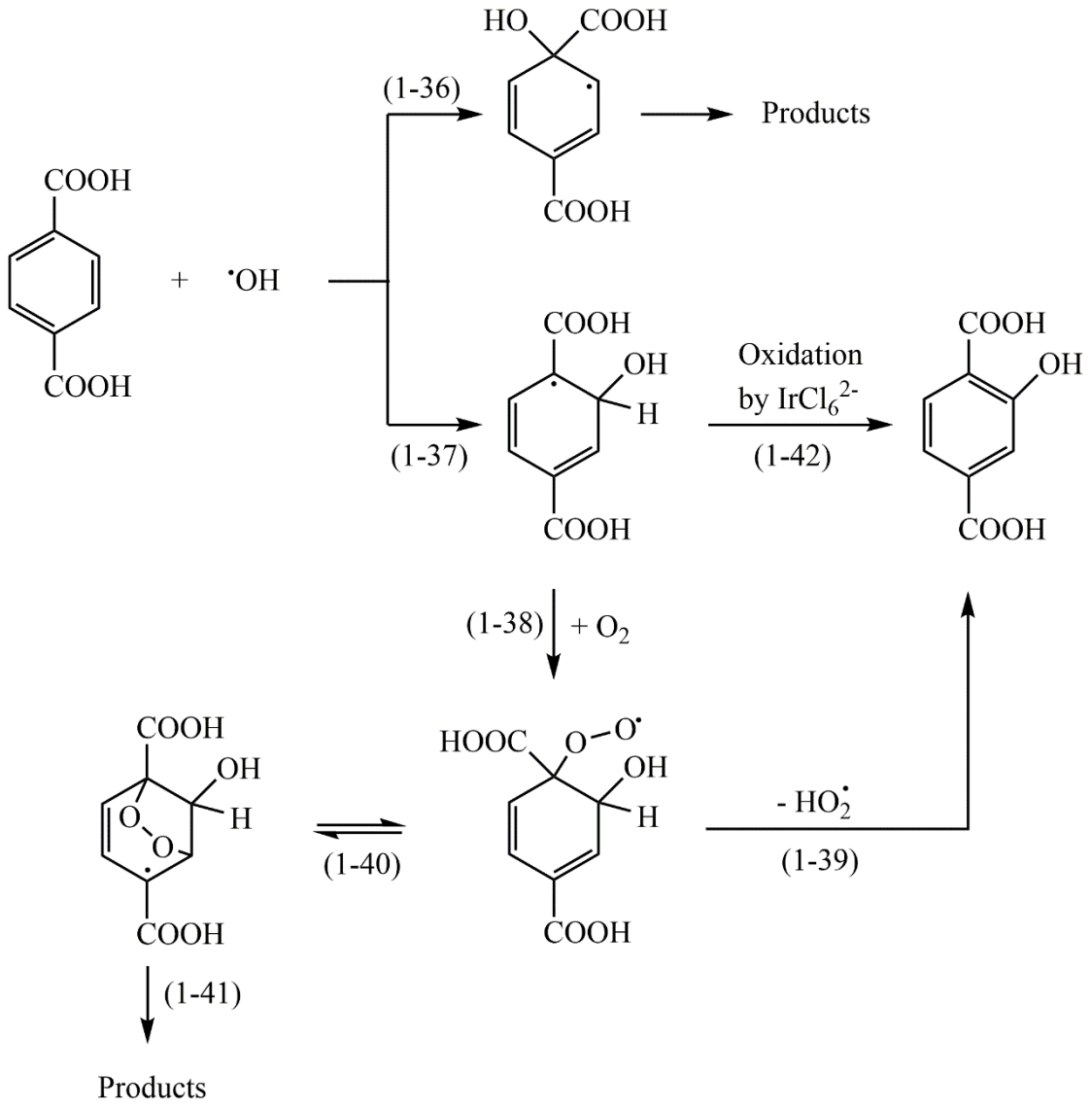

Figure 1-6: Reaction scheme for the reaction of terephthalic acid with •OH.

1.3.3.5 •OH QUANTIFICATION BY ELECTRON SPIN RESONANCE

A direct quantification of •OH by electron spin resonance (ESR) would be possible, if •OH would be present in high concentrations. Janzen (1971) described a method of spin trapping of •OH to yield a more stable radical that can be detected by ESR. The reaction of spin traps with •OH is an addition reaction. Such spin traps are 5,5'-Dimethyl-1-pyrroline-1-oxide (DMPO) and phenyl-tert-butylnitrone (PBN), which are applied to trap •OH yielding stable long lived nitroxide free radicals. DMPO reacts diffusion-controlled with •OH ($k = 2 \times 10^9$ M^{-1} s^{-1}) (von Sonntag, 2006) giving DMPO-OH with characteristic electron paramagnetic splitting pattern (reaction 1-43) (Cheng *et al.*, 2003). This method is not widespread in the field of environmental research and only barely applied in this field, but often in the field of biological systems.

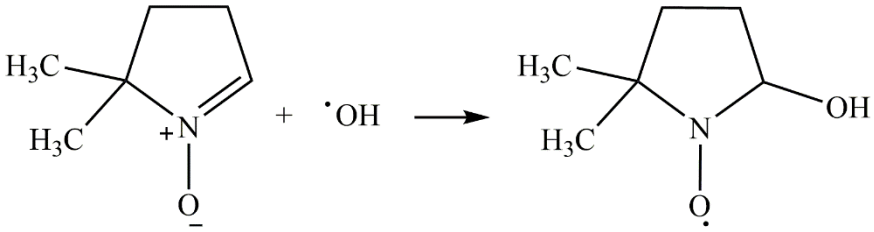

(1-43)

1.4 DETERMINATION OF •OH IN OZONE REACTIONS - O_3 AND •OH EXPOSURES: THE R_{CT} CONCEPT

The R_{ct} concept is a tool to characterize the oxidation of micropollutants in water by ozone and •OH (Elovitz and von Gunten, 1999). It can be used for the prediction/modeling of oxidation processes in ozone-based water treatment. For a characterization of these oxidation processes the concentration or exposure (integral of concentration over time) of ozone and •OH have to be known. The concentration of ozone can be easily measured by calorimetric, spectrometric and electrochemical methods. However, the determination of the •OH concentration is much more difficult, as •OH are highly reactive and their steady-state concentration is too low to be measured directly. An indirect method to determine the •OH exposure is measuring the decay of a probe compound. The prerequisites for a probe compound are a low reactivity with O_3 and a high reactivity with •OH. A typically used probe compound is *p*CBA, as it reacts very slowly with O_3 ($k_{O_3+pCBA} \leq 0.15\ M^{-1}s^{-1}$) (Neta *et al.*, 1988), but readily with •OH ($k_{\cdot OH+pCBA} = 5 \times 10^9\ M^{-1}\ s^{-1}$) (Buxton *et al.*, 1988).

The reaction of the probe compound can be described as a second order reaction. Since the probe compound does not react with O_3, just the reaction with •OH is taken into account.

$$\frac{-d[\text{probe}]}{dt} = k_{\bullet\text{OH+probe}} \times [\text{probe}][\bullet\text{OH}] \qquad (1\text{-}44)$$

Integration and rearrangement of equation (1-44) leads to equation (1-45).

$$-\ln\left(\frac{[\text{probe}]}{[\text{probe}]_0}\right) = k_{\bullet\text{OH+probe}} \times \int [\bullet\text{OH}]dt \qquad (1\text{-}45)$$

R_{ct} describes the ratio of the exposures of •OH and O_3.

$$R_{ct} = \frac{\int [\bullet\text{OH}]dt}{\int [O_3]dt} \qquad (1\text{-}46)$$

Insertion of equation (1-46) in equation (1-45) results in equation (1-47).

$$-\ln\left(\frac{[probe]}{[probe]_0}\right) = k_{\bullet OH+probe} \times R_{ct} \int [O_3]dt \qquad (1\text{-}47)$$

By plotting the decay of the probe compound ($\ln([probe]/[probe]_0)$) over ozone exposure ($\int [O_3]dt$) the R_{ct} value can be calculated from the slope, as $k_{\cdot OH+probe}$ is known. Once a certain water is "calibrated" by determination of the R_{ct}-value, the $^{\bullet}$OH-exposure can be calculated *via* equation (1-46) if the O_3 exposure is known. Since O_3 can be determined on-line over time by suitable electrodes, the $^{\bullet}$OH-exposure is available as real-time value. This enables a continuous prediction of pollutant degradation (equation 1-45), which can be used for process control.

The R_{ct} value in ozonation depends on the water quality, e.g., dissolved organic carbon (DOC) concentration, pH, alkalinity and temperature and thus, largely varies for different kinds of water sources. Typically, waters with a high ozone stability yield low R_{ct}-values. Since in conventional ozonation, O_3 is mainly scavenged by organic matter, low-DOC groundwaters have lower R_{ct}-values than rich-DOC surface waters von (Elovitz *et al.*, 2000a). Furthermore, ozone decay may reveal different kinetic stages in conventional ozonation. Figure 1-7 shows an example of the first order decay of ozone in ozone-based processes. In conventional ozonation, typically two kinetic regimes of ozone decay can be observed, i.e., a first rapid phase and a second slower phase (Figure 1-7). In the first phase fast-reacting electron rich moieties of DOC result in a rapid O_3 consumption (ca. 5 – 30 % in drinking water ozonation). These moieties are consumed within the first seconds of reaction time resulting in slower ozone decay kinetics in the second phase. This is also reflected by the R_{ct}-values which are higher in the first phase of ozone decay compared to the second phase. In the second phase of ozone decomposition, the R_{ct}-value is fairly stable over a longer period of time (often throughout the whole hydraulic retention time of full scale reactors) and thus, describes the ratio of $^{\bullet}$OH to ozone consumption at any time of the reaction (Elovitz and von Gunten, 1999, Acero and von Gunten, 2001b). However, in some cases third-order kinetics regimes can be observed, which are slower than the second-order kinetics reactions.

At high DOC concentrations (e.g., wastewater) the ozone decay and thus the R_{ct} resembles the values in the peroxone process. In the peroxone process, such stages of ozone decay kinetics are typically not observed (Figure 1-7). This is due to the fact the chemical nature of the initiator (HO_2^-) does not change during the reaction.

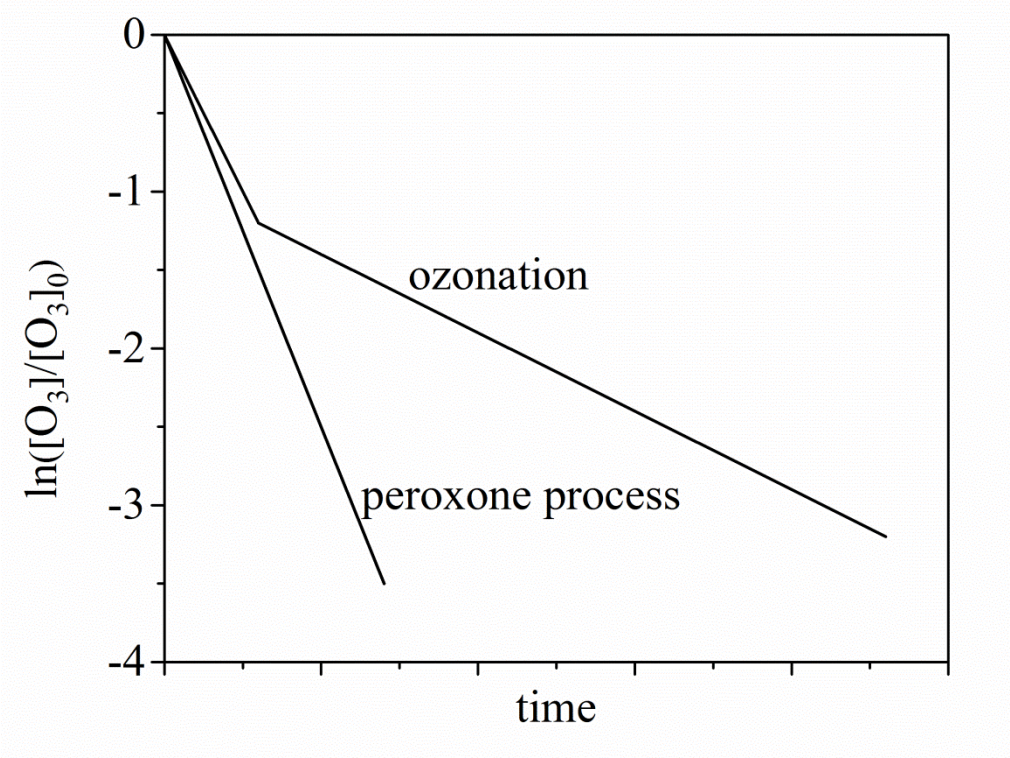

Figure 1-7: Generic representation of ozone decay in ozonation and in the peroxone process. Kinetics of ozone decay in the peroxone process is constant over time, whereas it displays two phases in ozonation only, with a first rapid phase followed by a slower phase.

During drinking water treatment a high R_{ct}-value indicates a good degradation of ozone refractive micropollutants. However, since a high R_{ct}-value is often accompanied by a low ozone exposure disinfection efficiency is weak (see section 1.5 Ozone and •OH In Disinfection). Typical values for R_{ct} in ozonation are in the range of 10^{-9}-10^{-8}, while in the peroxone process the values are up to two orders of magnitude higher.

1.5 Reaction Kinetics and Modeling of Micropollutant Degradation

The degradation of micropollutants reacting with ozone and •OH can be predicted for batch or plug-flow reactors based on their second-order reaction kinetics. The degradation of a micropollutant (MP) can be expressed as follows:

$$-\frac{d[MP]}{d} = k_{\bullet_{OH+MP}} \times [^{\bullet}OH] \times [MP] + k_{O_3+MP} \times [O_3] \times [MP] \qquad (1\text{-}48)$$

Replacing [•OH] in equation (1-48) by $R_{ct} \times [O_3]$ according to equation (1-46) gives:

$$-\frac{d[MP]}{d} = k_{\bullet_{OH+MP}} \times R_{ct} \times [O_3] \times [MP] + k_{O_3+MP} \times [O_3] \times [MP] \qquad (1\text{-}49)$$

Integrating equation (1-49) results in:

$$ln\frac{[MP]_t}{[MP]_0} = -\left(\int_0^t [O_3]\,dt\right)\left(k_{\bullet OH+MP} \times R_{ct} + k_{O_3+MP}\right) \quad (1\text{-}50)$$

After determination of R_{ct} (cf. section 1.3) and with the second-order rate constants of micropollutants (k_{O_3+MP} and $k_{\bullet OH+MP}$) at hand, it is possible to predict the oxidation of a micropollutant as a function of ozone exposure using equation (1-50). Applying different H_2O_2/O_3 ratios in raw water and determining ozone exposures and R_{ct}-values at different H_2O_2/O_3 ratios thus, allows a rough assessment of the degradation of several micropollutants without the need to measure their degradation at each H_2O_2/O_3 ratio. This is a useful tool to evaluate the optimal H_2O_2/O_3 ratio with just few experiments (Acero and von Gunten, 2001b). It has to be noted that the error in the reaction rate *k* may bias such a prediction on the degree of pollutant degradation.

It must be considered that in waters with high O_3 stability, the addition of H_2O_2 accelerates the degradation of micropollutants, but may not necessarily change the overall oxidation efficiency significantly (von Gunten, 2003b).

The fraction of ˙OH reacting with a pollutant is typically very small, since most of ˙OH are consumed by water matrix constituents. The reaction rate constants of such matrix constituents are compiled in Table 1-2. With that data at hand it is possible to calculate the actual percentage of radical reactions targeting a micropollutant (here *p*CBA) by applying equation (1-51). Equation (1-51) includes all relevant water matrix components and added chemicals (H_2O_2) that scavenge ˙OH. Thus, it gives the ratio of the rate of *p*CBA oxidation and the rate of all ˙OH scavengers (S) present in the water.

$$\%^{\bullet}OH_{pCBA} = 100\frac{k_{\bullet OH+pCBA}[pCBA]}{\{k_{\bullet OH+pCBA}[pCBA]+\sum k_{\bullet OH+S}[S]\}} \quad (1\text{-}51)$$

Matrix compounds present in natural waters that need to be considered as possible ˙OH scavengers are listed in Table 1-2. At typical water treatment conditions (1 mg/L DOC, 1 mM HCO_3^-, 10 µg/L Br^-) only a fraction of ca. 6.69 % ˙OH is reacting with *p*CBA (0.5 µM) and most radicals are consumed by DOC (66.89 %) followed by HCO_3 (22.74 %). Such calculations allow assessing which matrix constituents are the most important factors affecting the pollutant degradation efficiency.

Table 1-2: Reaction rate constants of matrix compounds in natural waters and H_2O_2 with $^{\bullet}OH$

Matrix compound	Reaction rate constant with $^{\bullet}OH$	Reference
Dissolved organic carbon	2.5×10^4 L mg^{-1} s^{-1}	(Larson and Zepp, 1988)
HCO_3^-	8.5×10^6 M^{-1} s^{-1}	(Hoigne and Bader, 1983)
CO_3^{2-}	3.9×10^8 M^{-1} s^{-1}	(Buxton *et al.*, 1988)
NO_2^-	8×10^9 M^{-1} s^{-1}	(Buxton *et al.*, 1988)
Br^-	1.1×10^{10} M^{-1} s^{-1}	(Zehavi and Rabani, 1972)
H_2O_2	2.7×10^7 M^{-1} s^{-1}	(Buxton *et al.*, 1988)

A possible scavenger for $^{\bullet}OH$ may also be O_3. However, (Rosenfeldt *et al.*, 2006) tested the approach with and without the reaction of O_3 with $^{\bullet}OH$ and observed a minimal difference in the $^{\bullet}OH$ fraction reacting with *p*CBA ($\Delta\%^{\bullet}OH_{pCBA}$) of 0.5 % between the two test scenarios. Thus, the $^{\bullet}OH$ reaction with ozone can be neglected.

It must be considered that the calculated fraction is just valid for the initial conditions of a reaction and that errors in measuring the concentrations of the matrix compounds and discrepancies in published reaction rates can significantly change the result of the $^{\bullet}OH$ fraction reacting with the target compound.

Reaction rate constants *k* are useful to evaluate the reaction of a micropollutant with an oxidant and obtain half-lives of micropollutants. Many rate constants are compiled for ozone (Hoigne and Bader, 1983, Hoigne and Bader, 1983b, von Sonntag and von Gunten, 2012) and $^{\bullet}OH$ (Buxton *et al.*, 1988, Neta *et al.*, 1988). If reaction rate constants cannot be found in literature, they can be experimentally determined by different methods (Huber, 2004) or be predicted. Quantitative structure-activity relationships (QSARs) are tools to predict rate constants for reactions of oxidants with micropollutants.

Lee and von Gunten (2012) developed QSARs for the reactions of O_3 with phenols, phenolates, benzene derivatives, olefins and amines. These QSARs are based on the correlation between Hammett σ (σ, σ^+ and σ^-) and Taft σ^* constants with reaction rate constants (some values are compiled by Hansch *et al.* (1991)) . The authors also developed cross-correlations between *k*-

values for the reaction of O_3 vs. ClO_2 and O_3 vs. HOCl. Two multiple linear regression-based standardized QSAR model equations for $k_{\cdot OH}$ and k_{O3} were introduced by Sudhakaran and Amy (2013). A plot of the predicted $k_{\cdot OH}$ vs. experimentally obtained $k_{\cdot OH}$ for haloalkanes, aromatics, alkanes and activated aromatics shows a good correlation ($r^2 = 0.9178$). The models can be applied for reactions with $^{\bullet}OH$ in a pH range of 5 – 8 and $k_{\cdot OH}$-values between 4×10^7 and 1.8×10^{10} M^{-1} s^{-1} and for O_3 reactions in a pH range of 5 – 8 and k_{O3}-values between 5×10^{-4} and 10^5 M^{-1} s^{-1}.

Li *et al.* (2013) developed a QSAR model to predict *k*-values for the reactions of O_3 with organic chemicals at different temperatures. The equation includes 13 descriptors and is suitable for the prediction of *k*-values for the reaction of O_3 with structurally diverse compounds with various functional groups (e.g., >C=C<, −C≡C−, −OH, −CHO, −O−, >C=O, −COOH, −C≡N, $-NO_2$ and −X(Cl, F).

1.6 OZONE AND $^{\bullet}$OH IN DISINFECTION

Ozonation is widely practiced for the effective inactivation of viruses, bacteria and their spores, and to a lower extent for inactivation of protozoa. Ozone targets a broad spectrum of pathogens, which makes it more effective than other common disinfectants such as chlorine dioxide, free chlorine and chloramines (von Gunten, 2003b). The kinetics for the inactivation of bacteria, spores and protozoa by ozone are analogous to the kinetics for their inactivation by UV radiation. Typically, the kinetic starts with a lag that is caused by repair mechanisms of the microorganisms, followed by a first order decay. However, in many cases the lag phase is very short and can be neglected (von Sonntag and von Gunten, 2012). In the inactivation process by O_3 and UV radiation, the DNA is the main target. The mode of action of O_3 is different than that of UV and O_3 is more effective. A single lesion of the DNA is not leading to inactivation, since the cells have repair mechanisms for their DNA. Ozone causes single base lesions, while double-strand breaks and crosslinks are of minor importance (von Sonntag and von Gunten, 2012).

As it is not feasible to monitor all possible pathogens, indicator microorganisms are monitored instead. A typical indicator microorganism in water is *E. coli* that indicates a fecal contamination of the water. This approach works well only if the inactivation of other pathogens is as efficient as the inactivation of the indicator microorganism or even better. A much more

reliable approach to assess the disinfection efficiency is the ct-concept. It can be described by Chick and Watson equation:

$$\ln\left(\frac{N}{N_0}\right) = -k \times c \times t \qquad (1\text{-}52)$$

where N and N0 are the numbers of microorganisms after a certain exposure time t (N) and the initial number of microorganisms N_0, k is the inactivation rate constant for a certain microorganism, c is the disinfectant concentration and, t is the disinfectant exposure time. The exposure (or ct-value) is calculated by integrating the disinfectant concentration over time.

The oxidant exposure during the lag phase on the inactivation curve (ctlag) is subtracted from the ct-value. The assessment of the disinfection is based on published ct-values (see Table 1-3) obtained from the measurement of the inactivation of a specific microorganism. If a ct-value is not available, it can be obtained from the determination of O_3 exposure, which can practically and theoretically be determined by different methods (Roustan et al., 1993, von Gunten et al., 1999, Do-Quang et al., 2000, Rakness et al., 2005).

Table 1-3: Kinetics of the inactivation of selected microorganisms (bacteria, spores, virus and protozoa) by ozone

Microorganism	k_{ozone} (L mg^{-1} min^{-1})	ct_{lag} (mg min L^{-1})	ct (mg min L^{-1}) for inactivation of 4-log	Temperature (°C)	Reference
E. coli	7800	-	0.001	20	(Hunt and Mariñas, 1997)
B. subtilis	4.91	2.12	4	20	(Larson and Mariñas, 2003)
spores	2.9	2.9	6.1	20	(Driedger *et al.*, 2001)
Rotavirus	76	-	0.12	5	(von Sonntag and von Gunten, 2012)
G. lamblia cysts	29	-	0.32	25	(Wickramanayake *et al.*, 1984a)
G. muris cysts	2.4	-	3.9	25	(Wickramanayake *et al.*, 1984b)
C. parvum oocysts	0.84	0.83	11.8	20	(Driedger *et al.*, 2001)

The combination of O_3 with UV improves the water disinfection, given the complementary modes of action of the two disinfection agents. In the O_3/UV AOP, the UV-C radiation inactivates the microorganisms, as it is absorbed by DNA and RNA.

Lee and von Gunten (2012) describe the bacterial disinfection in chlorotetracyline (antibiotic) containing wastewater. The disinfection was investigated by UV and ozone alone and by their combination (O_3/UV). While ozone alone lead to a < 2-log inactivation within1 h reaction time, UV resulted in a 4-log reduction within 20 min and a 5-log reduction within 40 min reaction time. The best results though were achieved by the combination of ozone and UV, which showed a synergistic effect. Here, the disinfection was enhanced, showing more than a 5-log reduction within 20 min.

Wolfe *et al.* (1989) investigated the inactivation of *E. coli*, two coliphages, (MS2 and f2) and *G. muris* by ozone and peroxone process in surface water. The applied molar H_2O_2:O_3 ratios were between 0.07 and 0.4. No significant difference between the inactivation of *E. coli* and the two coliphages in ozonation and in the peroxone process was observed. The inactivation of *G. muris* was slightly higher in the peroxone process than in ozonation alone.

Addition of H_2O_2 leads to a faster production of $^{\bullet}OH$ and a faster consumption of ozone. Thus, less ozone is available for disinfection. The role of $^{\bullet}OH$ in the disinfection of drinking water is not clear. At R_{ct} values (see section 1.3) of 10^{-8} typically found in ozonation, $^{\bullet}OH$ can be neglected as disinfectant. This is different from AOPs where the R_{ct} values are about 10^{-6} and $^{\bullet}OH$ may play a role in the inactivation of microorganisms with small k_{ozone}, e.g., *B. subtilis* spores, *G. muris* cysts and *C. parvum* oocysts (Table 1-3). One also has to consider that the main target for the inactivation of a microorganism is its DNA and that $^{\bullet}OH$ are scavenged by the cell wall or other non-critical cell constituents before reaching the DNA (von Gunten, 2003b).

1.7 WATER QUALITY IMPACT ON PROCESS PERFORMANCE AND BY-PRODUCT FORMATION

1.7.1 REACTIONS WITH WATER MATRIX COMPONENTS

In analogy to O_3 based processes the water matrix influences both the efficiency of pollutant degradation and by-product formation. In that regard the concentration of other solutes (i.e., DOC, CO_3^{2-}/HCO_3^-, and Br^-) and the pH value play a role (Figure 1-8). The effect of pH on the reaction rate of O_3 with H_2O_2 (reaction 1-53) that initiates $^{\bullet}OH$ formation is as follows. The

reaction of O_3 with H_2O_2 is very slow ($k < 0.01\ M^{-1}\ s^{-1}$), but that with its anion, HO_2^-, is several orders of magnitude faster ($k = 5.5 \times 10^6\ M^{-1}\ s^{-1}$). Hence, only the latter species is relevant for the peroxone process resulting in a strong pH dependency of the apparent reaction rate constant $k_{obs.}$ Due to the high p*K*a (H_2O_2) of 11.8, the reaction is fast only at elevated pH values. The k_{obs}–values for pH 6, 7 and 8 were calculated to be 8.72 $M^{-1}\ s^{-1}$, 87.2 $M^{-1}\ s^{-1}$ and 872 $M^{-1}\ s^{-1}$, respectively. At a low $k_{obs}(O_3 + H_2O_2)$ the fraction of O_3 reactions with DOC (reaction 1-54) increases, turning the peroxone process into conventional ozonation. This can be compensated by increasing the H_2O_2 dosage. However, with increasing concentrations of H_2O_2 the reaction of $^{\bullet}OH$ with H_2O_2 becomes important (reaction 1-56). $^{\bullet}OH$ react with H_2O_2 *via* H-abstraction yielding $HO_2^{\bullet}$ (k ($^{\bullet}OH + H_2O_2 = 2.7 \times 10^7\ M^{-1}\ s^{-1}$ (Buxton *et al.*, 1988)) giving rise to superoxide ($O_2^{\bullet-}$) (Christensen *et al.*, 1982) upon $HO_2^{\bullet}$ deprotonation (p*K*a = 4.8 (Bielski *et al.*, 1985)). $O_2^{\bullet-}$ reacts fast with O_3 yielding $^{\bullet}OH$, resulting in a catalyzed O_3 decomposition. This deteriorates both the disinfection strength and the pollutant degradation. However, the reaction of O_3 with electron rich moieties of DOC (i.e., phenolic moieties and deprotonated amines) also initiates $^{\bullet}OH$ formation (von Sonntag and von Gunten, 2012) with yields comparable to the peroxone process in DOC rich waters (von Gunten, 2003a). DOC, carbonate and bicarbonate consume $^{\bullet}OH$ (reaction 1-55 and 1-57) (k($^{\bullet}OH$ + DOC) = $2.5 \times 10^4\ L\ mg^{-1}\ s^{-1}$ (von Sonntag and von Gunten, 2012), k($^{\bullet}OH + HCO_3^-$) = $8.5 \times 10^6\ M^{-1}\ s^{-1}$, k ($^{\bullet}OH + CO_3^{2-}$) = $3.9 \times 10^8\ M^{-1}\ s^{-1}$) (Buxton *et al.*, 1988). This leads to a loss of oxidation strength in the peroxone process which in particular targets the degradation of O_3 recalcitrant pollutants *via* the $^{\bullet}OH$ pathway. The reaction of $^{\bullet}OH$ with organic compounds typically yields carbon centered radicals ($R^{\bullet}$), which rapidly add oxygen ($k(O_2 + R^{\bullet}) \approx 10^9\ M^{-1}\ s^{-1}$ (von Sonntag and Schuchmann, 1997)) (von Sonntag and von Gunten, 2012). The ensuing peroxyl radical ($ROO^{\bullet}$) may cleave to superoxide ($O_2^{\bullet-}$) (reaction 1-58) which contributes in the turnover of O_3 into $^{\bullet}OH$ (reaction 1-59) and thus, increase the rate of pollutant degradation. Reactions accelerating $^{\bullet}OH$ formation are called propagation reactions (von Gunten, 2003a).

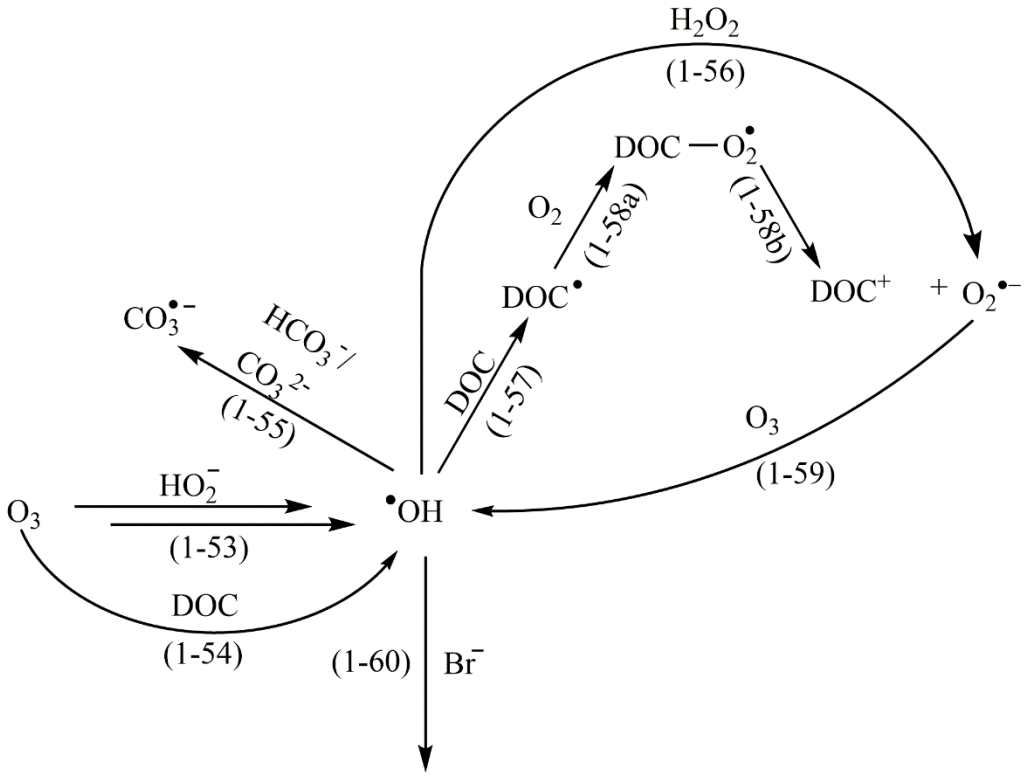

Figure 1-8: Relevant reactions of •OH with water matrix constituents influencing the peroxone process

The reaction of •OH with HCO_3^- and CO_3^{2-} (reaction 1-55) yields carbonate radicals ($CO_3^{\bullet-}$), which do neither significantly contribute in pollutant degradation nor react with O_3. Such kind of reactions which exclusively consume •OH are called scavenging reactions (von Gunten, 2003a). Waters with a high alkalinity and a low DOC concentration (e.g., ground waters) typically have a high scavenging and a low radical initiation/propagation capacity. This dramatically lowers the degradation efficiency of O_3 recalcitrant pollutants in ozonation and the degradation of such pollutants can substantially be improved by addition of the initiator H_2O_2 (von Gunten, 2003a).

It is noteworthy that H_2O_2 may affect the oxidation of reduced manganese species. Colloidal MnO_2 is rapidly reduced by H_2O_2, which may hamper the O_3 based removal of reduced Mn species. The oxidation of reduced Mn and Fe species in conventional ozonation is mainly driven by O_3, since the reaction is fast ($k(O_3 + Fe^{2+}) \approx 8 \times 10^5\ M^{-1}\ s^{-1}$; $k(O_3 + Mn^{2+}) \approx 10^3\ M^{-1}\ s^{-1}$) (von Sonntag and von Gunten, 2012) and O_3 concentrations are typically several orders of magnitude higher than •OH concentration (Elovitz *et al.*, 2000a). Hence, destabilization of O_3 by addition of H_2O_2 is counterproductive regarding the removal of these metal species. Indeed,

all treatment targets, which rely on reactions of O_3, may be hampered by addition of H_2O_2. Hence, the peroxone process is a tradeoff of bromate control and degradation of O_3 recalcitrant compounds with a loss of most other treatment aims of conventional ozonation such as micro-flocculation, disinfection, enhanced biodegradation and removal of reduced metal species (see above).

1.7.2 BROMATE FORMATION AND MITIGATION STRATEGIES

Bromate is a by-product formed in ozonation processes. As it is considered to be carcinogenic, the drinking water standard is 10 µg/L. Bromate formation is a multi-step process (Haag and Hoigné, 1983, von Gunten and Hoigné, 1994), that was recently revised in the last step (BrO_2^- + O_3) (reaction 1-72) (Fischbacher *et al.*, 2015). The formation of bromate and possible mitigation strategies are presented in Figure 1-9.

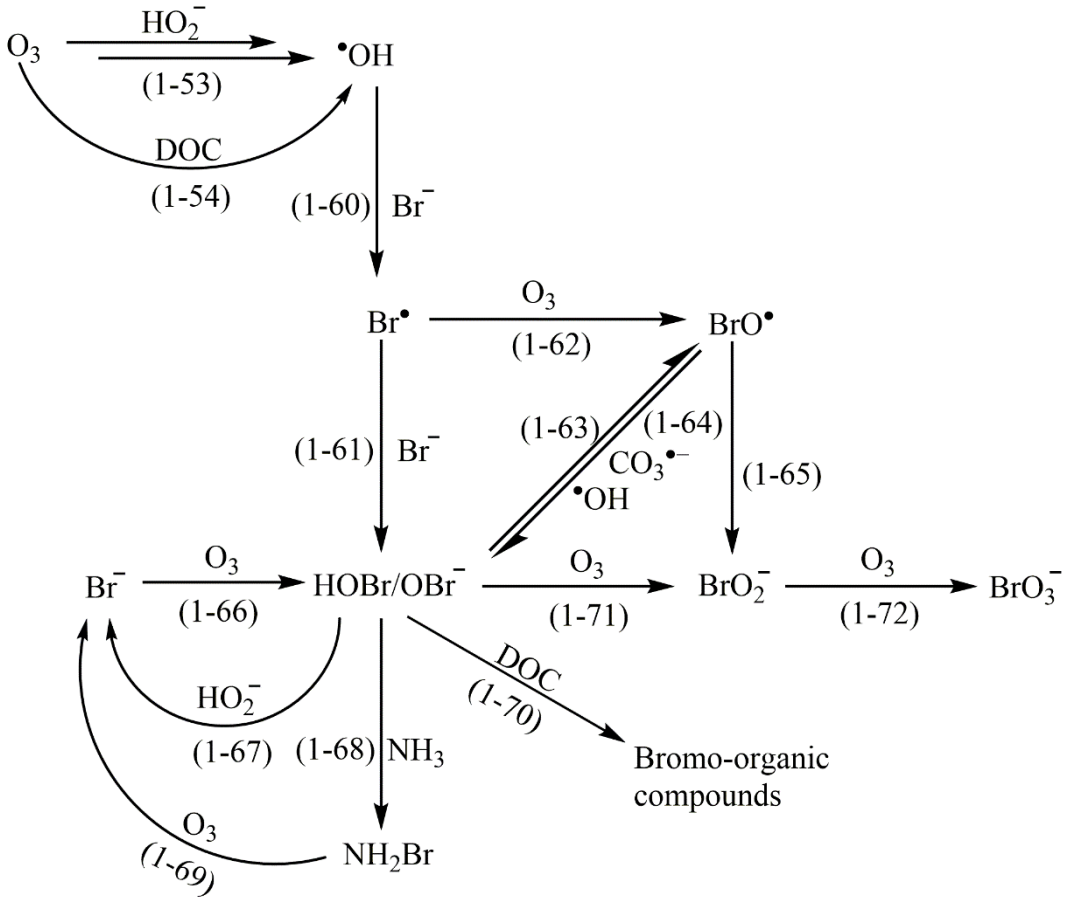

Figure 1-9: Bromate formation in ozone based processes and mitigation strategies

Mitigation of bromate formation is an important aim in the peroxone process. The bromate minimizing effect is based on interception of an intermediate in bromate formation (i.e., hypobromous acid ($HOBr/OBr^-$), formed in reactions (1-61) and (1-66) by H_2O_2 (reaction 1-

67). This reaction reveals a distinctive pH-dependency (von Gunten and Oliveras, 1997). The rate of this reaction increases with increasing pH up to a maximum at pH 10.2, which corresponds to the average of the pK_a values of H_2O_2 (≈11.8) and HOBr (≈8.5) (von Gunten and Oliveras, 1997). This behavior was explained by a reaction of a free acid and an anion and it was proposed that the mechanism is a nucleophilic substitution (von Gunten and Oliveras, 1997). Since HO_2^- is a stronger nucleophile than H_2O_2 and HOBr a stronger electrophile than OBr^- reaction (1-73) was proposed to happen (von Gunten and Oliveras, 1997).

$$HO_2^- + HOBr \rightarrow Br^- + H_2O + O_2 \qquad k = 7.1 \times 10^5\ M^{-1}\ s^{-1} \qquad (1\text{-}73)$$

The pH-dependency of reaction (1-73) is very important regarding the efficiency of H_2O_2 to control bromate formation. At pH ≤ 7 the reaction becomes so slow ($k_{app} \leq 25\ M^{-1}\ s^{-1}$) (von Gunten and Oliveras, 1997), that H_2O_2 may have to be added in excess over O_3 to compete against oxidation of HOBr (reactions 1-63 and 1-71). This however, can result in the ozone decomposing loop of reactions (1-56) and (1-59) and thus, largely lower the efficiency of pollutant degradation and disinfection.

The presence of NH_3/NH_4^+ and DOC also contributes to scavenging the intermediate $HOBr/OBr^-$ (reactions 1-68 and 1-69). HOBr readily brominates NH_3/NH_4^+ and the ensuing bromamines are oxidized by O_3 yielding nitrate and bromide (Pinkernell and von Gunten, 2001, von Sonntag and von Gunten, 2012). In case of DOC as $HOBr/OBr^-$ scavenger, electron rich phenolic moieties of DOC react with HOBr. Remarkably, incorporation of bromine into DOC *via* electrophilic substitution is of minor importance in this reaction (≈ 20 – 30 % yield with respect to HOBr consumed) (Criquet *et al.*, 2015). Instead, a large yield of bromide was observed which was explained with an electron transfer reaction (Criquet *et al.*, 2015). The presence of DOC and ammonia principally lower the yield of bromate, which may reduce the required H_2O_2 doses for bromate control. However, HCO_3/CO_3^{2-} possibly enhance formation of bromate, since $CO_3^{\bullet-}$ from reaction (1-55) may contribute in oxidation of HOBr (reaction 1-63) (von Sonntag and von Gunten, 2012).

The interception of $Br^\bullet$ in reaction (1-62) opens a pathway of bromate formation without $HOBr/OBr^-$ as intermediate via reaction (1-65) (dismutation of $BrO^\bullet$). Hence, bromate formation cannot completely be controlled by addition of H_2O_2 albeit reaction (1-62) is disfavored in the peroxone process due to destabilization of O_3.

(Acero *et al.*, 2001) could show that the addition of H_2O_2 to ozone leads to a reduction of the bromate formation by approximately a factor of two. Three different natural waters were

investigated at pH 7 and 8. All water samples were spiked with bromide to achieve an initial concentration of 50 µg/L. The molar ratio of H_2O_2 and O_3 was 0.5 (0.34 mg H_2O_2 per mg O_3). The bromate concentrations in all water samples exceeded the drinking water standard (10 µg/L) when treated with ozone alone ([BrO_3^-] = 12 and 20.7 µg/L). The concentration of bromate formed in the peroxone process varied between 4.2 and 12.5 µg/L at an ozone dose of 2 mg/L.

In the peroxone process BrO^- can be reduced by hydrogen peroxide to bromide. In the O_3/UV process even bromate can be reduced by UV to bromite, then to hypobromous acid and finally to bromide (reaction 1-74 – 1-76) (Siddiqui *et al.*, 1996).

$$2\ BrO_3^- + h\nu \rightarrow 2\ BrO_2^- + O_2 \qquad (1\text{-}74)$$

$$2\ BrO_2^- + h\nu \rightarrow 2\ BrO^- + O_2 \qquad (1\text{-}75)$$

$$2\ BrO^- + h\nu \rightarrow 2\ Br^- + O_2 \qquad (1\text{-}76)$$

Siddiqui *et al.* (1996) examined bromate photolysis under different UV exposure and water quality conditions. Four different UV light sources were used, namely VUV (184.9 nm)/UV(253.7 nm) LP-, UV(253.7 nm) LP-, and (200-400 nm) MP Hg-arc lamps, and a pulse electric arc discharge source (VUV-UV range). Of note, both LP lamps emitted both the 184.9 nm and 253.7 nm radiation, but the operating power and the quartz sleeves were different for the two LP lamps, which allowed the isolation of 253.7 nm radiation from one of the lamps. As bromate has an absorption maximum at 195 nm, the VUV (184.9 nm)/UV(253.7 nm) LP-Hg was the most effective at bromate conversion to bromide among the investigated UV radiation sources. Dissolved organic carbon and nitrate affected the removal yield at 184.9 nm due to the competition for photons with BrO_3^-, but did not change the overall performance of VUV light source relative to the other UV light sources. The decrease in temperature lowered the removal yields, whereas pH did not have any measurable effect. The study provides UV dose data for specific bromate removal yields, but it is unclear how the UV radiation field was monitored at the reactor wall and whether the fluid dynamics were incorporated in the UV dose calculations.

Zhao *et al.* (2013) investigated the bromate formation and humic acid removal in water treatment by O_3/UV. The used LP Hg-lamp emitted light at 254 nm and 185 nm, but due to experimental setup light at 185 nm was absorbed by the quartz sleeves and the oxygen in the quartz sleeves. Ozone dose was 2 mg/L. At 100 µg/L bromide, a reaction time of 60 minutes

and without adding humic acids to the water, bromate concentrations were higher in O_3/UV (17.1 – 77.6 µg/L) than for ozone alone (8 – 33.8 µg/L). The authors explained this high bromate formation with the fact that there was no DOC present to scavenge O_3 and $^{\bullet}OH$. After a reaction time of 60 minutes (first stage) UV irradiation was applied for 30 min without further addition of ozone (second stage). In this stage bromate was reduced by UV light by about 20 %. When humic acid was added to the water bromate formation in the O_3/UV process was lower than in ozonation. However, the bromate concentration in the O_3/UV process exceeded the 10 µg/L drinking water standard at high ozone dose and low humic acid concentrations.

1.7.3 Formation of Assimilable Organic Carbon

A further important by-product formed in drinking water treatment is the assimilable organic carbon (AOC). AOC is defined as the amount of substrate (organic carbon) utilized by microorganisms. As most bacteria in drinking water distribution systems are heterotrophic, carbon is essential for their growth. AOC is a small fraction of total organic carbon that tends to be composed of small molecular weight compounds and thus, can readily be degraded by microorganisms. Water is defined as biological stable, if AOC is present in concentrations below 50 µg/L. (Kaplan *et al.*, 1993). In contrast to bromate AOC can be decreased by applying biological filters after the oxidation step. (Hacker *et al.*, 1994) investigated the AOC formation in ozonation and the peroxone process. They could show that the addition of hydrogen peroxide resulted in a higher AOC formation. However, they could not show a clear relationship between higher H_2O_2/O_3 ratios and higher AOC formation. Filtration of ozone- and peroxone process-treated water by a dual-media filtration (biologically active anthracite/sand filters) resulted in an AOC reduction by 75 – 90 % which corresponded to an AOC concentration that was equal or even lower than the AOC concentration in the raw waters.

1.7.4 *N*-Nitrosodimethylamine Formation

NDMA is a human carcinogen and there have been growing concerns about NDMA contamination, as trace levels were found in surface and drinking waters (WHO, 2006). It is a secondary pollutant produced in water from nitrogeneous precursors. It was found to be formed during water disinfection with chloramines (Najm and Trussell, 2001, Mitch and Sedlak, 2002). If dimethylamine is present in water it reacts with monochloramine to 1,1-dimethylhydrazine, that is oxidized to NDMA. Recently, it was shown that NDMA can also be formed in ozonation, if *N*,*N*-dimethylsulfamide (DMS), a degradation product of the fungicide tolyfluanide is present (Lee *et al.*, 2007). (von Gunten *et al.*, 2010) found that the direct reactions of DMS with O_3 and

•OH do not lead to NDMA. NDMA is only formed, if Br^- is present. Br^- is oxidized by O_3 and •OH to HOBr which reacts with the primary amine of DMS yielding a Br-DMS species. This Br-DMS species reacts then with O_3 to NDMA.

(Lee *et al.*, 2007) studied the NDMA degradation in conventional ozonation and O_3/H_2O_2 in two different lake waters (Lake Zurich: DOC = 1.2 mg/L, HCO_3^- = 2.6 mM, pH 7.9; Lake Greifensee: DOC = 3.9 mg/L, HCO_3^- = 4.1 mM, pH 8.1). They showed that applying O_3/H_2O_2 results in a higher degradation of NDMA than in conventional ozonation. It was degraded in conventional ozonation (160 µM O_3) by 25 % in Lake Zurich water, and by 9 % in Lake Greifensee water. During the peroxone process at same O_3 doses and a H_2O_2:O_3 ratio of 0.5, NDMA was oxidized by 55 % in Lake Zurich and 28 % in Lake Greifensee water. In Lake Greifensee water more •OH were scavenged by HCO_3^-, which resulted in a lower NDMA degradation in both processes. As in conventional ozonation O_3 was not completely consumed, the NDMA oxidation per mol of consumed O_3 was the same in ozonation and peroxone process. Higher O_3 doses would result in an increase of NDMA degradation, but also in an increase of bromate formation. Thus, bromate formation may be the limiting factor for NDMA oxidation.

(Lee *et al.*, 2007) investigated the abatement of NDMA by several AOPs and their combinations in wastewaters. As the reaction rate constant for the reaction of NDMA with •OH is low ($k_{\bullet OH + NDMA} = 4 \times 10^8\ M^{-1}\ s^{-1}$), O_3/H_2O_2 is not suitable to degrade NDMA in wastewater. However, direct photolysis contributes almost 100 % to the abatement of NDMA and a UV-based process should be applied, if NDMA degradation is the treatment goal. In addition the formation of NDMA in ozonation and O_3/H_2O_2 from the reaction of NDMA precursors with O_3 was studied. In three of seven investigated wastewaters significant concentrations of NDMA were formed in ozonation. The application of O_3/H_2O_2 in comparison led to an only slight reduction in NDMA formation (-4 % – 14 %). As the reaction of NDMA precursors with O_3 is fast it is difficult to avoid NDMA formation in ozonation and the peroxone process. The authors could show that O_3/H_2O_2 is a suitable treatment process for micropollutant degradation in wastewater, as a high abatement of several micropollutants, except NDMA, could be achieved and ambient and formed NDMA is mainly attenuated by UV-based processes.

1.8 PROCESS ECONOMICS AND LIMITATIONS

One important factor for comparing and assessing the efficiency of water treatment processes is the electrical energy demand for achieving a certain pollutant treatment goal. Bolton *et al.*

(2001) introduced two figures of merit for electrical energy-driven-systems i.e., electrical energy per mass (E_{EM}) and electrical energy per order (E_{EO}).

E_{EM} is defined as the electric energy in kWh required to degrade a contaminant by a mass unit (e.g., 1 kg). It is used when the contaminant concentration is high, as its degradation rate is directly proportional to the electric energy rate (zero-order kinetics). As such conditions were not found in water treatment, since the concentration of pollutants is typically small, E_{EM} is not further explained here.

The second approach is E_{EO}. It is defined as the electrical energy in kWh required to degrade a contaminant by one order of magnitude (90 %) in 1 m^3 water. E_{EO} is used for situations where the contaminant concentration is low and the required energy is independent of the contaminant concentration (first-order kinetics). This means that it takes the same amount of electric energy to degrade 10 mg/L to 1 mg/L of a contaminant as it would take to degrade 10 µg/L to 1 µg/L. The energy demand can be calculated for batch reactors (eq. 1-77) and flow-through operation (eq. 1-78).

$$E_{EO} = \frac{P \times t \times 1000}{V \times \log\left(\frac{c_i}{c_f}\right)} \quad (1\text{-}77)$$

$$E_{EO} = \frac{P}{F \times \log\left(\frac{c_i}{c_f}\right)} \quad (1\text{-}78)$$

P is the rated power in kW of the system, t the treatment time in h, V the treated volume of water in L, F the flow rate of water in m^3/h, M the molar mass of the contaminant in g/mol, c_i and c_f are the initial or influent and final or effluent concentration of the contaminant in mol/L, respectively.

As a rule of thumb the required energy to produce 1 kg of ozone is assumed to be around 15 kWh. The production of H_2O_2 is estimated to be 10 kWh/kg (Rosenfeldt *et al.*, 2006).

For processes using a UV-light source the energy of the lamp can be calculated using the following equation:

$$ER_{lamp} = \frac{H_\lambda(90\%)}{I^{avg} \times \eta_{UV}} \times \frac{kWh}{3.6 \times 10^6\ J}, \quad (1\text{-}79)$$

UV/ H_2O_2 in a batch reactor in various waters, Lake Zurich (DOC: 1.3 mg/L, carbobate-alkalinity: 2.6 mM), Lake Jonsvatnet (DOC: 3 mg/L, carbonate-alkalinity: 0.4 mM), Lake Greifensee (DOC: 3.1 mg/L, carbonate-alkalinity: 4.0 mM) and wastewater Dübendorf (DOC:

3.9 mg/L, carbonate-alkalinity: 6.5 mM). It could be shown that the peroxone process has a slightly higher energy demand than ozonation, and the UV/H_2O_2 process requires around one order of magnitude more energy for the lake waters and around four times more energy for the *p*CBA removal in wastewater (Table 1-4).

Table 1-4: Energy demand for the removal of 90 % *p*CBA in various water matrices by O_3/H_2O_2 (H_2O_2:O_3 molar ratio of 0.5), O_3, and UV/H_2O_2 (5 cm path length and 0.2 mM H_2O_2) (Katsoyiannis *et al.*, 2011)

Process	Energy (kWh/m^3)			
	Lake Zurich	Lake Jonsvatnet	Lake Greifensee	Wastewater Dübendorf
O_3/H_2O_2	0.043	~0.043*	~0.08*	~0.25*
O_3	0.035	0.035	0.065	0.2
UV/H_2O_2	0.23	0.45	0.61	0.82

* Estimated values

Lekkerkerker-Teunissen *et al.* (2012) calculated the E_{EO} data for 14 micropollutants treated with peroxone process and the serial AOPs, as investigated in the pilot work at Dunea WTP (see section 4.3.2). The 14 contaminants have different structural characteristics, such that some of them react moderately to well with O_3, others are prone to •OH degradation (moderate to high reactivity), and one (metformin) reacts poorly with both O_3 and •OH. The E_{EO} values reflect such reactivities in both peroxone and serial AOP treatment. For example, the E_{EO} for bromacil treatment with peroxone was within 0.01 – 0.02 kWh/m^3/order for all used oxidant ratios, and increased for the serial AOP treatment to 0.13 – 0.17 kWh/m^3/order. This trend reflects the high reactivity towards O_3, with very little benefit from additional •OH-based treatment via the UV/H_2O_2 process. Similar examples are diglyme, ibuprofen, carbamazepine, trimethoprim, and diclofenac. On the contrary, atrazine is not well treated with O_3, has a moderate rate constant for •OH reaction, and exhibits a moderate direct photolysis at 253.7 nm. As a result, the E_{EO} for atrazine treatment with peroxone process ranged from 0.11 to 0.18 kWh/m^3/order, depending on the oxidant ratios, and increased for serial AOP treatment to 0.43 – 0.79 kWh/m^3/order, depending on the O_3/H_2O_2 ratio and applied UV dose. Metformin would require the higher electrical energy for 90 % removal with both O_3/H_2O_2 (0.21 – 0.39 kWh/m^3) and serial AOP (0.90 – 2.45 kWh/m^3). The pilot data showed that 8 out of 14 compounds were

removed by >90 % by O_3(1.5 mg/L)/H_2O_2 (6 mg/L) process with $E_{EO} \leq 0.027$ kWh/m^3/order. Atrazine treatment goal set by Dunea was of 80 %. The 80 % removal yield was achieved with an electrical energy consumption of 0.52 kWh/m^3 in the serial AOP treatment, which is much lower than that required by the LP UV/H_2O_2 process alone (0.73 kWh/m^3).

Scheideler and Bosmith (2014) provided cost analysis for metaldehyde treatment by O_3-AOP, UV-AOP, and their sequential application based on the pilot testing conducted at one of the Anglian Water (UK) water treatment plants (see section 1.8.1). The costs included were for chemicals (H_2O_2 and liquid oxygen), energy, maintenance, and CAPEX, and assumed certain prices. Investment costs and costs for parts including spare UV lamps and electronic ballasts driving the lamps were not included. Under the assumed flow rate of 800 m^3/h and a 10-year depreciation period, the costs associated with the treatment for 0.5 log metaldehyde removal by peroxone and UV-AOP individual processes were approx. 0.048 and 0.064 €/m^3, respectively. The treatment costs to achieve 90 % removal of metaldehyde were estimated at 0.091 and 0.085 €/m^3, for the UV-AOP and the O_3-AOP followed by UV/AOP, respectively. The authors concluded that the serial AOP is the treatment option when high reduction in metaldehyde concentration is needed (e.g. 1-log), as significant cost savings can be realized (~77,000 €/annum). On the other hand, the combined AOPs offer a robust barrier against micropollutants with various molecular structures, with different reactivity towards O_3, $^{\bullet}OH$, and UV radiation.

Lee *et al.* (2016) presented calculated data on the abatement of several micropollutants by four different AOPs (O_3 followed by UV, O_3/H_2O_2 followed by UV/H_2O_2, UV/H_2O_2 and O_3/H_2O_2,) in wastewater (Table 1-5). Although the calculated energy demand for O_3/H_2O_2 is lower than for all other processes, O_3/H_2O_2 is not sufficient to degrade *N*-Nitrosodimethylamine (NDMA) or its precursors from wastewaters. The highest degrees of micropollutant degradation are predicted to be achieved by the combination of O_3/H_2O_2 followed by UV/H_2O_2. The high energy demand for this combined process can be reduced by optimized conditions, which makes the process combination more economically feasible.

Table 1-5: Calculated abatement of different micropollutants (bisphenol A, atrazine, ibuprofen and NDMA) by different AOPs (UV/H_2O_2, O_3/H_2O_2, O_3 followed by UV and O_3/H_2O_2 followed by UV/H_2O_2) and the required energy (Lee *et al.*, 2016).

	Micropollutant abatement [%] at required energy			
	UV/H_2O_2	O_3/H_2O_2	O_3 + UV	O_3/H_2O_2 + UV/H_2O_2
Micropollutant	0.158 kWh/m^3	0.095 kWh/m^3	0.126 kWh/m^3	0.176 kWh/m^3
Bisphenol A	33	94	94	96
Atrazine	30	44	57	62
Ibuprofen	27	60	62	71
NDMA	80	0	80	80

1.9 APPLICATION OF THE PEROXONE PROCESS IN PILOT- AND FULL-SCALE

1.9.1 PILOT-SCALE STUDIES

As the results on the oxidation of micropollutants in water obtained from lab-scale studies cannot be often transferred to full-scale applications, there is a necessity for pilot testing. In a pilot study for the Metropolitan Water District of Southern California, Ferguson *et al.* (1990) compared the peroxone process with ozonation for the degradation of taste and odor-causing compounds in two different waters: the Colorado River water (moderate DOC and alkalinity, low Br^- level (0.03 – 0.07 mg/L)) and state project water (moderate DOC and alkalinity, high Br^- level (0.33 – 0.48 mg/L)). The pilot plant included four ozone contactors with a capacity of 2.73 m^3/h and simulated a full-scale treatment train including pre-oxidation (peroxone or ozone) with a contact time of 12 min, followed by coagulation-flocculation, sedimentation and filtration. The oxidation of 2-MIB and geosmin in Colorado River water was more effective with the peroxone process than with ozone alone. For the degradation of 90 % 2-MIB by ozone alone 4 mg/L ozone was required, while only 2 mg/L ozone was necessary to degrade 90 % 2-MIB in the peroxone process (molar H_2O_2:O_3 ratio 0.3). In state project water ~80 % 2-MIB degradation was achieved at an O_3 dose of 4 mg/L in ozonation and an O_3 dose of 1 mg/L in the

peroxone process. It was concluded that the optimal H_2O_2:O_3 ratio for the oxidation of taste and odor compounds is 0.15 to 0.3 (state project water with lower alkalinity) and 0.4 or higher (Colorado River water with higher alkalinity). The different optimal ratios for both waters were caused by the difference in water quality.

Duguet *et al.* (1990) investigated the application of O_3/H_2O_2 for the removal of chloronitrobenzenes from groundwater (pH 6.7, DOC: 1.9 mg/L, alkalinity: 225 mg/L $CaCO_3$). The main contaminant of the groundwater was o-chloronitrobenzene (up to 1,828 µg/L). The pilot plant was operated at 450 L/h, and was equipped with two ozone contactors, an ozone generator (up to 10 g/h), a dosage system for hydrogen peroxide and two parallel-running filters (sand and GAC). Under optimized conditions, removal of 99 % of aromatic compounds was achieved. The applied O_3 and H_2O_2 concentrations were 8 and 3 mg/L, respectively, with a 0.5 H_2O_2:O_3 molar ratio, and 20 min contact time. Ozonation alone with 16 mg/L O_3 and 40 min contact time resulted in 88 % degradation of chloronitrobenzene ($k_{pCNB+O3}$ = 1.6 M^{-1} s^{-1}, (Shen *et al.*, 2008)).

Wu and Englehardt (2015) applied O_3/H_2O_2 for the reduction of chemical oxygen demand (COD) in wastewater. The collected wastewater with an initial COD of 10 – 16.5 mg/L was treated biologically followed by an iron mediated aeration, flocculation, low-pressure vacuum ultrafiltration and O_3/H_2O_2. The pilot-scale experiments were conducted in a 3785 L tank. 2300 – 3030 L wastewater was recirculated at a flow of 151 L/min. To reduce 90 % COD 60 h of treatment were required at 2.3 mg/L/h O_3 (O_3:H_2O_2 mass ratio: 3.4) and less than 5 h at an O_3 dose of 18.83 mg/L/h (O_3:H_2O_2 mass ratio: 3.61). The specific O_3 consumption per COD was determined to be between 7.4 and 13.15 mg O_3/mg COD. The energy demand was calculated to be 1.73 – 2.49 kWh/m^3/order. The authors show that O_3/H_2O_2 is an attractive method for the mineralization of compounds contributing to COD, as required for water reuse and reclamation.

Lake Huron is one of the Great Lakes and is used as a drinking water source in Canada and USA. It was shown that this lake water is contaminated with pharmaceuticals and personal care products (PPCPs) and EDCs. Thus, a pilot-scale treatment plant operated in two trains at a total flow of 12.4 L/min was installed at the Walkerton Clean Water Centre, Canada (Uslu *et al.*, 2012). Both trains include a coagulation-flocculation chamber (hydraulic retention time: 90 min), a clarifier (hydraulic retention time: 20 min) followed by dual media filtration. While train 1 consists of just these units, in train 2 O_3/H_2O_2 is additionally applied prior to coagulation. O_3 is dosed at a concentration of 2 – 2.3 mg/L and H_2O_2 at 0.2 mg/L. Raw water concentrations for alkalinity ($CaCO_3$) and DOC range between 80 – 106 mg/L and 1.5 – 1.9 mg/L, respectively.

The raw water was spiked with nine micropollutants (PPCPs and EDCs). Samples were taken after the entire processes at the end of train 1, train 2 and from train 2 after passing the AOP reactor (before coagulation). The micropollutant removal in train 1 was for all compounds less than 15 %. The results for the samples of train 2 and after the AOP reactor did not significantly differ from each other. A complete removal of five (bisphenol A, naproxen, gemfibrozil, diclofenac and atrovastatin) of nine target compounds was achieved after the AOP reactor, and thus at the end of train 2 as the AOP reactor is a part of train 2. O_3-refractery compounds (e.g., atrazine and ibuprofen) were removed insufficiently. The authors concluded that this could be due to the low molar H_2O_2:O_3 ratio (0.14).

Dunea Duin & Water Company, The Netherlands, uses Meuse River water as a source for drinking water production for The Hague and surrounding areas. Organic micropollutants, among which pesticides, EDCs, PPCPs, were found in surface waters at levels ranging from ng/L to a few µg/L. Dunea provides a multi-barrier treatment of River Meuse water, through a complex infrastructure and various treatment steps. After collection in a "dead end side stream", the river water goes through conventional treatment such as coagulation, sedimentation, and micro-sieve filtration in combination with aeration. After pre-treatment, the water is pumped over 27 km to Bergambacht for additional pre-treatment (dual media filtration), prior to transportation and infiltration into the dunes (managed aquifer recharge, MAR) via two pipelines. After an average residence time of ~120 days, the dune-filtered water is pumped to three different locations for multiple step-treatment (softening, activated carbon filtration, cascade aeration, rapid sand filtration, and slow-sand filtration) prior to be distributed to the consumers (Lekkerkerker *et al.,* 2009). Dunea Water Company conducted extensive research in collaboration with WEDECO, a Xylem Inc. brand company, on advanced oxidation processes for organic micropollutant (OMP) removal, as part of Dunea's strategy to preventing any undesired compounds from being present in their treated water. A WEDECO AOP pilot system was installed onsite at the pre-treatment location Bergambacht, and used to examine the effectiveness of O_3/H_2O_2, UV/H_2O_2, and their combination for the removal of fourteen selected OMP (pesticides, pharmaceuticals, x-ray contrast agents) under various treatment conditions. Given the concern over bromate formation from bromide present in the water, bromate was a key parameter monitored in the treated water. The pilot plant research outcomes are available in the published literature (Lekkerkerker *et al.*, 2009, Scheideler *et al.*, 2011, Lekkerkerker-Teunissen *et al.*, 2012, Lekkerkerker-Teunissen *et al.*, 2013, Knol *et al.*, 2015). (Lekkerkerker-Teunissen *et al.*, 2012) reported data for both peroxone process alone and serial AOP (O_3/H_2O_2/LP-UV/H_2O_2) under selected process conditions, i.e., 5 m^3/h flow rate, 0.7 – 2 g/m^3

O_3, 0, 6 and 10 mg/L H_2O_2, and 700 and 950 mJ/cm^2 UV (253.7 nm) dose. The pre-treated water influent to either O_3/H_2O_2 or serial AOP has a relatively high DOC concentration (3 – 5 mg/L), low transmittance (73 – 83 % $T_{254nm, 1cm}$), and an average bromide concentration of 120 µg/L. At 1.5 mg/L O_3 and 6 mg/L H_2O_2, the O_3/H_2O_2 AOP achieved more than 90 % removal of bromacil, phenazone, bentazone, carbamazepine, diclofenac, furosemide, isoproturon, and trimethoprim, while keeping the bromate level below the reporting limit of 0.5 µg/L. Lower removal yields were observed for metoprolol and ibuprofen (70 – 90 %) and diglyme, iopromide, atrazine, and metformin (20 – 70 %). The treatment yields were about 10 % lower in wintertime than in summertime for most compounds. As the treatment goal set by Dunea of 80 % atrazine removal was not met by the peroxone process, a serial AOP was investigated. Sequential treatment by O_3(1.5 mg/L)/H_2O_2(6 mg/L) – LP-UV(0.73 kWh/m^3)/H_2O_2(5.5 mg/L residual from peroxone process) achieved 80 % removal of atrazine, and substantially increased conversion yields of all other contaminants, and demonstrated a synergistic effect relative to treatments observed in the two individual AOPs. Metformin, a refractory pollutant, was removed by 37 % in the serial AOP treatment. Concomitantly, the water transmittance increased by up to 5 %, and DOC was removed by approx. 0.2 mg/L. The authors indicated that distributing the UV dose across three reactors rather than one-time UV dose in a single reactor would increase the treatment efficiency of serial AOP (5 – 15 % higher removal yields) due to the increase of water %*T* across the three reactors. In 2014, Dunea Duin & Water Company decided to implement the serial AOP full-scale system at their water facility of Bergambacht. Following the tender process open to all AOP technology providers, in 2015 Dunea awarded the full-scale system implementation to WEDECO, Xylem Inc.

In a recently published study based on the extensive pilot work at Dunea, Knol *et al.* (2015) described the efficacy of O_3/H_2O_2 process at the removal of the 14 model compounds mentioned above, and emphasized the role of water quality parameters, i.e. bicarbonate, DOC, and temperature on the removal yields. The bromate formation from bromide contained in the pilot water (104 – 136 µg/L) during the peroxone treatment was monitored from August 2011 through March 2012. The ozone-loop reactor (WEDECO, Xylem Inc.) with sequential ozone dosing injection ports and reaction/degassing chamber, and the source and water quality for the pilot plant were similar to those used in the study described above. The micropollutants (1.8 – 31.5 µg/L) and H_2O_2 were dosed to the influent water (flowrate of 5 m^3/h), whereas ozone was applied at 1 m-spaced four dosing points followed by static mixers (Figure 1-10). The authors reported at least 70 % removal of micropollutants when dosing 6 mg/L H_2O_2 and 1.5 mg/L O_3 (5.65 H_2O_2:O_3 molar ratio), while keeping bromate well below the set limit of 0.5 µg/L. The

degradation rate of micropollutants increased with increasing water temperature and decreasing DOC and HCO_3^- concentrations, except for metformin which was the most poorly treated compound (~20 % irrespective the water quality conditions). Varying the H_2O_2 concentration had minimal effect on the micropollutant degradation yields, but limited the bromate formation. Bromate formation yield increased with the temperature and bromide concentration, and decreased with increasing alkalinity and pH. From these studies, Knol *et al.* (2015) concluded that the degradation of micropollutants and the bromate formation can be controlled by adjusting the ozone and H_2O_2 doses to the water temperature, and the DOC and bicarbonate concentrations. Thus, in wintertime the degradation of micropollutants can be increased by increasing the ozone dose without exceeding the bromate limit. In summertime, the bromate formation can be controlled by increasing the H_2O_2 concentration, which does not influence noticeably the degradation of micropollutants.

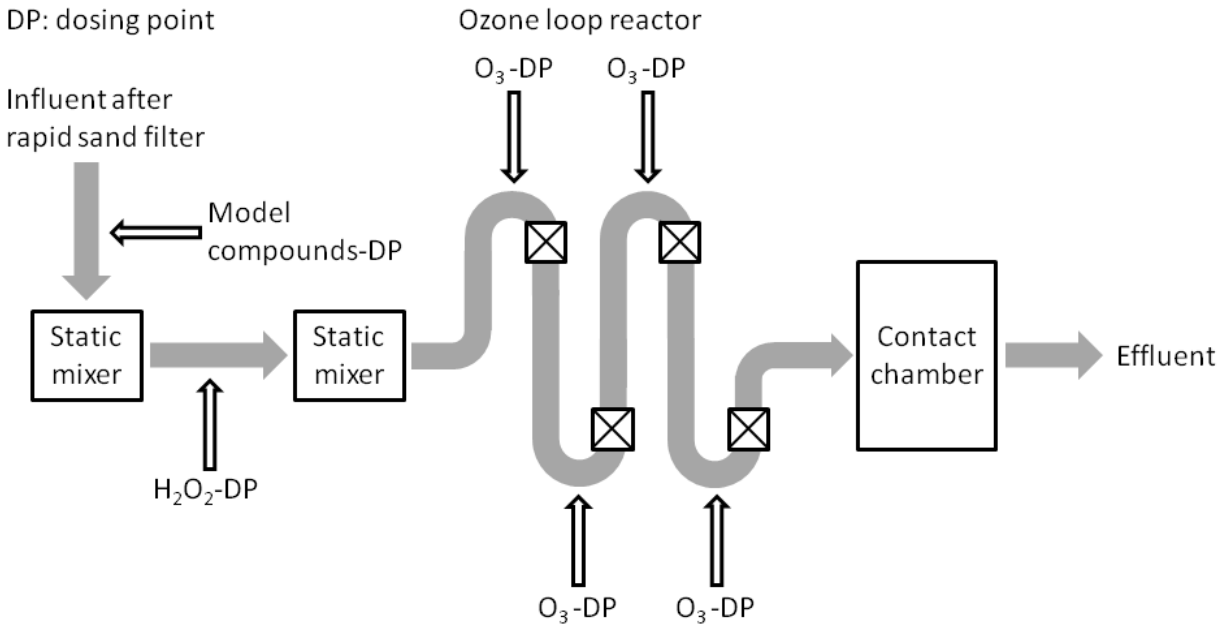

Figure 1-10: Schematic view of the pilot plant in Bergambracht, Netherlands. Adapted from Knol *et al.* (2015).

Metaldehyde is commonly used as a molluscicide in horticulture and agriculture. It contaminates groundwater and surface waters, and its maximum permissible level in drinking water in the EU countries is set to 0.1µg/L. Metaldehyde is refractory to conventional treatment processes, does not photolyze, and is not removed by ozone. It reacts with the $^{\bullet}OH$ with a reaction rate constant of $k = 1.3\times10^9\ M^{-1}\ s^{-1}$ (Autin *et al.*, 2012). (Scheideler and Bosmith, 2014) reported the metaldehyde treatment data for peroxone, UV (253.7 nm)/H_2O_2, and their combination obtained during a 8-month pilot testing at a water utility operated by Anglian

Water Services (UK). The pre-treated surface water quality used in the pilot plant was characterized by ~80 µg/L bromide, <5 µg/L bromate, ~5 mg/L DOC, ~207 mg/L hardness as $CaCO_3$, pH 8, and 88 % $T_{254nm,1cm}$. The main components of the O_3-AOP equipment (WEDECO's PRO_3MIX) consisted of ozone generator (from liquid O_2), H_2O_2 dosing, reaction chamber, the degassing and catalytic destruction of residual O_3, measuring devices. The O_3-loop reactor had five O_3 dosing ports followed by static mixers. The water flow rate varied from 30 to 40 m^3/h, H_2O_2 (up to 24 g/m^3) was dosed at the inlet, whereas O_3 (up to 16 g/m^3) was incrementally dosed across the loop reactor to minimize the bromate formation. Metaldeyde treatment goal set by Anglian Water was 0.5 log removal. The O_3/H_2O_2 study showed that 0.4-0.5 log metaldehyde reduction can be achieved with 8 g/m^3 O_3 and a O_3/H_2O_2 mass ratio of 2 – 2.5, while bromate level was kept below 3 µg/L. In order to achieve a consistent 0.5 log metaldehyde removal, one needs to increase the O_3 dose. Lower peroxide doses achieved better degradation yields, given the lower $^{\bullet}OH$ consumption by H_2O_2. The UV-AOP pilot (3×80 W low-pressure lamp reactor) data showed that in order to obtain 0.5 log removal of metaldehyde, a UV dose of 1300 mJ/cm^2 and 20 mg/L H_2O_2 would be required.

The combined AOPs indicated that for the H_2O_2 resdual from the peroxone process, the yield of metaldehyde destruction increased with increasing UV dose. The pilot data provided by Scheideler and Bosmith (2014) indicates that 0.5 log metaldehyde removal can be achieved with 8 mg/L O_3/(16 – 22 mg/L H_2O_2) followed by less than 500 mJ/cm^2 UV dose, which is much lower than the UV dose required for the UV-AOP alone. This observation suggests a synergistic effect of the combined AOPs. Should 90 % (1.0 log) removal of metaldehyde be targeted, a post-O_3-AOP UV dose of 1200 mJ/cm^2 would suffice (as compared to 2600 mJ/cm^2 for the UV-AOP alone). Bromate standard was not exceeded under any of the pilot conditions used in this work.

1.9.2 FULL-SCALE APPLICATIONS IN WATER TREATMENT

Sung-Nam Water Treatment Plant (WTP), South Korea (http://www.xylem.com/treatment/nz/case-studies).

The Sung-Nam Metro City WTP is operated by K-Water and produces tap drinking water for more than 3 million people and clean water for a beverage industry filling around 45,000 drinking water bottles per day. The treated water originates from the Han-River. During the seasonal algae blooming, taste and odor-causing compounds (e.g., geosmin and 2-MIB) are released into the water, affecting the aesthetics of drinking water delivered to the consumers. These compounds are effectively treated with hydroxyl radical-based AOPs. In order to provide

high quality water to the customers, K-Water selected the peroxone advanced oxidation process combined with activated carbon filtration. The taste and odor compounds are removed using the WEDECO MiPRO^{TM} eco$_3$ AOP system. The AOP system is designed to achieve 0.5 log (70 %) removal of 2-MIB. It consists of three ozone generators (WEDECO PDO 1000, Xylem) with a total capacity of 51 kg O_3/h. Ozone is generated from liquid oxygen, and is injected into the water at a dose of 2 g/m^3. The ozone feed is combined with H_2O_2 (0.5 mg/L) at a H_2O_2:O_3 molar ratio of 0.35, to generate efficiently hydroxyl radicals for the oxidation of the T&O compounds. The 34,390 m^3 water/h flows through two ozone injection lines, then into two separate concrete contact tanks for reaction and degassing. The equipment includes also the hydrogen peroxide storage and the H_2O_2 delivery system, which ensures an efficient mixing of the two oxidants and their uniform distribution into the water streams. The O_3-AOP is in use at Sung-Nam WTP since 2012.

Moosbrunn Waterworks, Austria.

Vienna Waterworks supplies its customers with drinking water from pristine sources. The demand of 400,000 m^3/d is covered by 32 springs allocated to two water supply mains. These were installed in the 1870s and have been operated since then without any reconstruction. In case of reconstruction of one of the two mains or increased water demand during hot and dry summer time, the Vienna Waterworks decided to provide a further water source as back-up. The new source, two horizontal groundwater wells (Moosbrunn Waterworks), has been in operation since 2006 (Werderitsch, 2013). This groundwater is contaminated with tetrachloroethene (PCE) and trichloroethene (TCE). The contaminant concentrations were monitored over several years (1989 - 2005). A rising contamination trend has been observed in both wells and in 2005 the concentrations of the chlorinated hydrocarbons in well 1 and 2 were in the range of 25 – 30 µg/L and 7 – 10 µg/L, respectively. The total chlorinated hydrocarbon (TCE and PCE) drinking water standard of 10 µg/L was exceeded. After a half-year pilot testing (864 m^3/d), the Vienna Waterworks decided to install an AOP treatment step. H_2O_2 is injected to the raw water followed by O_3 injection. The water is mixed in a static mixer, and then pumped into the O_3/H_2O_2-reaction chamber. The treated water is stored in a reservoir and disinfected with ClO_2 before being discharged. Optimal process conditions were defined during the pilot plant work as 2.5 g/m^3 O_3, 1.75 g/m^3 H_2O_2 (H_2O_2:O_3 molar ratio of 0.98), and a minimum 10 min-hydraulic residence time in the reaction tank in order to achieve at least 90 % degradation of both TCE and PCE, and to mitigate the bromate formation. However, due to increased chlorine dioxide demand caused by residual H_2O_2, the H_2O_2 dose was decreased; therefore, the H_2O_2/O_3 molar ratio decreased from 1 to 0.7 without significantly influencing the degradation

rate of the chlorinated hydrocarbons. The throughput of the full-scale treatment plant is 64,000 m^3/d. Bromate formation was mitigated by the optimized dosing of oxidants and a short hydraulic retention time (≤10 min).

Andalucia, Spain. (http://www.mcilvainecompany.com/Decision_Tree/subscriber/articles/ITT_Water_and_Wastewater_Case_Studies.pdf).

In order to comply with the EU drinking water regulations on trihalomethanes (100 µg/L) and pesticides (0.1 µg/L each pesticide, maximum level of total pesticides and their metabolites of 0.5 µg/L), GIAHSA, one of the water suppliers in Andalucia, Spain, decided to implement pre-ozonation, intermediate ozonation coupled with H_2O_2 (O_3-AOP), and granular activated carbon filtration at the drinking water treatment plants of Aljaraque, Tinto, and Lepe. The WTPs are equipped with ozonation stations which provide O_3 gas for pre- and intermediate ozonation steps. The station has two WEDECO SMO 700 O_3 generators with automatic O_3 dose control and O_3 analyzer, gas flowmeters, gas diffusion systems, catalytic O_3 destruction, and SCADA. Each O_3 unit has a max. capacity of 9300 g/h at 10 % (by weight) from liquid O_2 and a water cooling temperature of 20 ºC. The O_3 design dose for each ozonation step is 1 – 4 mg/L, and the minimum and maximum water flow rate at the plants are 2160 and 4320 m^3/h, respectively. The project was funded by The Public Administration of Andalusia, and the O_3 units were installed in 2007.

1.9.3 FULL-SCALE APPLICATIONS IN GROUNDWATER REMEDIATION

ATPwater (Sacramento, CA, USA) systems are used for remediation of contaminated water. There are two different operating systems offered, namely, in situ chemical oxidation (PulseOx®) and a continuous in-line system (HiPOx®). The PulseOx® process is based on the peroxone process for the remediation of contaminated soil and groundwater. A sequence of pressurized pulses of ozone, hydrogen peroxide, oxygen and air are injected directly into the subsurface. The oxidation occurs in situ. The PulseOx® process was/is operated among others at following sites:

Active Gas Station, Bridgeport, CA, USA (http://www.wateronline.com/doc/pulseox-in-well-reactor-iwr-case-study-0002)

A release at an active gasoline service station in 1993 caused a contamination of soil and groundwater with BTEX, MTBE and TPH-g. In 2007 the concentration of benzene, BTEX, MTBE and TPH-g were 56 µg/L, 243 µg/L, 9 µg/L and 660 mg/L, respectively. Hence, in 2008 two in-well reactors (IWR) were installed in two existing monitoring wells. The IWRs were operated for six weeks. Ozone and hydrogen peroxide were injected at a dose of 0.45 kg/d and

3.8 L/d in each IWR, respectively at a recirculation rate of 3.8 – 19 L/min. After six weeks of operation the contaminant concentrations were reduced below regulatory detection limits.

Cooper Drum Superfund Site, CA, USA (http://www.wateronline.com/doc/pulseox-case-study-cooper-drum-superfund-0001)

Since 1941, the site (an area of about 15,000 m^2) was used by Cooper Drum Co. and several other companies to recondition used steel drums. The drum process waste was collected in open concrete trenches. This waste collection resulted in leaching of contaminants (e.g., 1,4-dioxane and volatile organic compounds (VOCs)) into the soil and groundwater beneath the site. From 1996 to 2001 the United States Environmental Protection Agency (U.S. EPA) conducted remedial investigation experiments on this site and added it to the National Priority List of hazardous waste sites requiring remedial action. The contaminated site is located close to drinking water wells (the nearest well is located within less than 1 km of the site) supplying 335,000 people. The contaminant plume is 250 m long, 75 m wide and 12 – 25 m below the ground. Ozone and hydrogen peroxide doses were 0.9 kg/d and 90 L/d, respectively. The pilot plant operation period was from July 2005 to June 2006. 1,4-Dioxane was degraded by 88 % in one of the test points and ≥ 49 % in all other points. After successful piloting, U.S. EPA indicate that it will suggest full-scale implementation of PulseOx process for *in situ* removal of 1,4-dioxane at Cooper Drum Company site.

HiPOx is a continuous in-line system using the peroxone process for water treatment with patented injection and mixing techniques. The HiPOx® process was/is operated at following sites:

US Air Force Plant 44, AZ, USA (http://www.wateronline.com/doc/hipox-case-study-us-air-force-plant-44-0002)

The US Air Force Plant 44 facility is located on the Tucson International Airport superfund site. Since the 1950's it was used for manufacturing missile and aircraft components. The process waste was disposed of in open ponds. A leaching into soil and groundwater results in contamination with 1,4-dioxane and trichloroethene (TCE). The contaminant plume impacted the drinking water supply for the City of Tucson. In the 1980's a remediation of groundwater and soil started. The water was treated by air-stripping followed by activated carbon adsorption and the soil by a soil vapor extraction system. In 2002 1,4-dioxane was identified in influent and effluent of the treatment system. As it is not very volatile and does not adsorb on the activated carbon, it was passing the treatment system. To eliminate 1,4-dioxane besides TCE the HiPOx® AOP system was installed in 2009 and replaced the 20+ year equipment at the US

Air Force site. The plant has a capacity of 13.1 million L/d and the applied ozone dosage is 27 kg/d. Groundwater is pumped to the plant and re-injected after treatment at the site. The new system successfully degrades TCE and 1,4-dioxane and reduces water losses caused by evaporation by over 121 million L per year.

Polyester Manufacturing Facility, South Korea (http://aptwater.com/hipox/case-studies/hipox-case-study-polyester-aop-water-treatment-south-korea/)

A polyester manufacturer in South Korea produces wastewater with high concentrations of 1,4 –dioxane (up to 65 mg/L) and other surfactants resulting in a COD of about 200 mg/L. 1,4-Dioxane passed through the treatment plant (anaerobic treatment process) and was discharged to a river. To improve the river water quality industries are required by the Ministry of the Environment to remove contaminants, e.g. 1,4-dioxane from their wastewater prior to discharging. The HiPOx® system was installed in 2005. The system is operated with a flow of 0.5 – 0.75 m^3/min and an ozone dosing capacity of 90 kg/d. The reduction of 1,4-dioxane to below the regulatory limit of 10 mg/L could be achieved. The plant was operated for over 48,000 hours and treated more than 34 million L of water with only minimal maintenance.

Keefe Environmental Services Superfund Site, NH, USA (http://www.wateronline.com/doc/hipox-case-study-keefe-environmental-0001)

In 2003, the U.S. EPA detected 1,4-dioxane in the groundwater in Epping at the Keefe Environmental Services superfund site. The site was operated as hazardous waste storage from 1978 – 1981. 1,4-dioxane was detected in the water treatment (metal removal and air-stripping remediation systems) effluent. A bench testing in October 2004 showed a good degradation of 1,4-dioxane from 270 µg/L to below the project regulatory limit of 3 µg/L. Based on these results a full-scale plant installation was completed in 2005. The HiPOx® system is operated at a flow of 100 L/min and an ozone dosage of 1.6 kg/d.

Nebraska Ordnance Plant, Mead, NE, USA (http://www.wateronline.com/doc/hipox-case-study-nebraska-ordnance-plant-0002)

During the World War II and the Korean War bombs, shells and rockets were assembled at the Nebraska Ordnance Plant site. These site activities resulted in a contamination of the groundwater with chlorinated solvents, e.g., TCE. In 2002, the U.S. Army Corps of Engineers started a remediation project at the site. The treatment facility consisted of air-stripping and vapor-phase carbon adsorption. Due to very high TCE contaminations of 5.8 mg/L, the treatment facility could not economically meet remediation goals. In 2008, a HiPOx® system was installed operated at a flow of 2.3 m^3/min and dosages for O_3 and H_2O_2 of 45 kg/d and 57

L/d, respectively. A contaminant removal of about >99.8 % was achieved and thus the treated water meets the public health requirements with a TCE concentration of less than 10 µg/L. In the first six months 540,000 m^3 water were treated and 770 kg of TCE degraded. The treatment costs decreased by 71 % ($ 164,000/yr) compared to the existing air-stripping system.

South Lake Tahoe, CA, USA (http://aptwater.com/hipox/case-studies/hipox-case-study-in-south-lake-tahoe-ca/)

In 1998, the City of South Lake Tahoe discovered a contamination in 13 of 34 drinking water supply wells with MTBE and its degradation product *t*BuOH. These contaminated wells had to be closed. In order to restore the wells, the City of South Lake Tahoe installed one HiPOx® systems in 2002 (flow: 3 m^3/min) and a second one in 2004 (flow: 5.7 m^3/min) at a different well. The MTBE and *t*BuOH concentrations in the second well were 6 and 8 µg/L, respectively. A degradation of both contaminants below the detection limits could be achieved (for MTBE <0.2 µg/L). The ozone capacity of both systems is 27 kg/day.

Wichita Aquifer Storage Recovery (ASR), KS, USA (http://aptwater.com/hipox/case-studies/wichita-asr-project-ks-bromate-control/)

This application regards seasonal (spring and fall) treatment of storm water from Little Arkansas River for groundwater recharge. The initial design of the 1.1×10^5 m^3/d surface water treatment for aquifer recharge consisted of river water intake, sedimentation, ultrafiltration, and chlorination. Concerns over contamination with atrazine from the agricultural runoff, pathogens including viruses, high TOC levels, and turbidity led City of Wichita to examine potential treatment processes for storm water. Powdered or granular activated carbon required additional chemicals, operations and maintenance- and on-site waste handling high costs, UV technology is not applicable in high-turbidity water, and O_3 alone is not effective at atrazine removal and generates bromate. In 2008 and 2009, a series of bench- and pilot-scale tests using the ATPwater HiPOx® system were conducted under a variety of experimental conditions. The pilot test results demonstrated that HiPOx® technology could achieve atrazine removal below the drinking water maximum contaminant level of 3 µg/L, control the bromate formation below the regulatory limit of 10 µg/L, while providing 4 to 5 log inactivation of poliovirus. The City of Wichita and CDM recommended implementation of HiPOx® technology for storm water treatment for Aquifer Storage Recovery project at the 1.1×10^5 m^3/d plant, approved in September 2009 by the Kansas Department of Health and Environment, and installed in 2011.

1.10 REFERENCES

Acero, J. L., Haderlein, S. B., Schmidt, T. C., Suter, M. J. F. and von Gunten, U. (2001). MTBE oxidation by conventional ozonation and the combination ozone/hydrogen peroxide: efficiency of the processes and bromate formation. Environmental Science & Technology, **35**(21), 4252-4259.

Acero, J. L. and von Gunten, U. (2001b). Characterization of oxidation processes: ozonation and the AOP O_3/H_2O_2. Journal American Water Works Association, **93**(10), 90-100.

Asmus, K. D., Mockel, H. and Henglein, A. (1973). Pulse radiolytic study of the site of hydroxyl radical attack on aliphatic alcohols in aqueous solution. Journal of Physical Chemistry, **77**(10), 1218-1221.

Atkins, P. W. (1998). Physical chemistry. Oxford University Press, Oxford.

Autin, O., Hart, J., Jarvis, P., MacAdam, J., Parsons, S. A. and Jefferson, B. (2012). Comparison of UV/H_2O_2 and UV/TiO_2 for the degradation of metaldehyde: kinetics and the impact of background organics. Water Research, **46**(17), 5655-5662.

Bielski, B. H. J., Cabelli, D. E., Arudi, R. L. and Ross, A. B. (1985). Reactivity of HO_2/O_2^- radicals in aqueous solution. Journal of Physical and Chemical Reference Data, **14**(4), 1041-1100.

Bolton, J. R., Bircher, K. G., Tumas, W. and Tolman, C. A. (2001). Figures-of-merit for the technical development and application of advanced oxidation technologies for both electric- and solar-driven systems - (IUPAC technical report). Pure and Applied Chemistry, **73**(4), 627-637.

Buxton, G. V., Greenstock, C. L., Helman, W. P. and Ross, A. B. (1988). Critical review of rate constants for reactions of hydrated electrons, hydrogen atoms and hydroxyl radicals ($^{\cdot}OH/^{\cdot}O^-$) in aqueous solution. Journal of Physical and Chemical Reference Data, **17**(2), 513-886.

Cheng, S.-A., Fung, W.-K., Chan, K.-Y. and Shen, P. K. (2003). Optimizing electron spin resonance detection of hydroxyl radical in water. Chemosphere, **52**(10), 1797-1805.

Christensen, H., Sehested, K. and Corfitzen, H. (1982). Reactions of hydroxyl radicals with hydrogen peroxide at ambient and elevated temperatures. Journal of Physical Chemistry, **86**(9), 1588-1590.

Criquet, J., Rodriguez, E. M., Allard, S., Wellauer, S., Salhi, E., Joll, C. A. and von Gunten, U. (2015). Reaction of bromine and chlorine with phenolic compounds and natural organic matter extracts - Electrophilic aromatic substitution and oxidation. Water Research, **85**, 476-486.

Czapski, G. and Bielski, B. H. J. (1993). Absorption spectra of the OH and O- radicals in aqueous solutions. Radiation Physics and Chemistry, **41**(3), 503-505.

Do-Quang, Z., Roustan, M. and Duguet, J. P. (2000). Mathematical modeling of theoretical cryptosporidium inactivation in full-scale ozonation reactors. Ozone-Science & Engineering, **22**(1), 99-111.

Driedger, A., Staub, E., Pinkernell, U., Mariñas, B., Köster, W. and von Gunten, U. (2001). Inactivation of bacillus subtilis spores and formation of bromate during ozonation. Water Research, **35**(12), 2950-2960.

Duguet, J. P., Anselme, C., Mazounie, P. and Mallevialle, J. (1990). Application of combined ozone-hydrogen peroxide for the removal of aromatic-compounds from a groundwater. Ozone-Science & Engineering, **12**(3), 281-294.

Elovitz, M. S. and von Gunten, U. (1999). Hydroxyl radical/ozone ratios during ozonation processes. I. The R_{ct} concept. Ozone-Science & Engineering, **21**(3), 239-260.

Elovitz, M. S., von Gunten, U. and Kaiser, H. P. (2000a). The influence of dissolved organic matter character on ozone decomposition rates and R_{ct}. In: Natural organic matter and disinfection by-products (ed.), 761, American Chemical Society, pp. 248-269.

Fang, X. W., Mark, G. and von Sonntag, C. (1996). OH radical formation by ultrasound in aqueous solutions. Part I: the chemistry underlying the terephthalate dosimeter. Ultrasonics Sonochemistry, **3**(1), 57-63.

Ferguson, D. W., McGuire, M. J., Koch, B., Wolfe, R. L. and Aieta, E. M. (1990). Comparing peroxone and ozone for controlling taste and odor compounds, disinfection by-products, and microorganisms. Journal American Water Works Association, **82**(4), 181-191.

Fischbacher, A., Löppenberg, K., von Sonntag, C. and Schmidt, T. C. (2015). A new reaction pathway for bromite to bromate in the ozonation of bromide. Environmental Science & Technology, **49**(19), 11714-11720.

Flyunt, R., Leitzke, A., Mark, G., Mvula, E., Reisz, E., Schick, R. and von Sonntag, C. (2003). Determination of ·OH, O_2^{-}·, and hydroperoxide yields in ozone reactions in aqueous solution. Journal of Physical Chemistry B, **107**(30), 7242-7253.

Glaze, W. H., Kang, J. W. and Chapin, D. H. (1987). The chemistry of water treatment processes involving ozone, hydrogen peroxide and ultraviolet radiation. Ozone-Science & Engineering, **9**(4), 335-352.

Haag, W. R. and Hoigné, J. (1983). Ozonation of bromide-containing waters: kinetics of formation of hypobromous acid and bromate. Environmental Science & Technology, **17**(5), 261-267.

Hacker, P. A., Paszko-Kolva, C., Stewart, M. H., Wolfe, R. L. and Means, E. G. (1994). Production and removal of assimilable organic carbon under pilot-plant conditions through the use of ozone and peroxone. Ozone: Science & Engineering, **16**(3), 197-212.

Hansch, C., Leo, A. and Taft, R. W. (1991). A survey of hammett substituent constants and resonance and field parameters. Chemical Reviews, **91**(2), 165-195.

Hoigne, J. and Bader, H. (1983). Rate constants of reactions of ozone with organic and inorganic compounds in water - I non-dissociating organic compounds. Water Research, **17**(2), 173-183.

Hoigne, J. and Bader, H. (1983b). Rate constants of reactions of ozone with organic and inorganic compounds in water - II dissociating organic compounds. Water Research, **17**(2), 185-194.

Holton, O. T. and Stevenson, J. W. (2013). The role of platinum in proton exchange membrane fuel cells. Platinum Metals Review, **57**(4), 259-271.

Huber, M. M. (2004). Elimination of pharmaceuticals during oxidative treatment of drinking water and wastewater: application of ozone and chlorine dioxide. PhD thesis, ETH Zurich, Switzerland

Hunt, N. K. and Mariñas, B. J. (1997). Kinetics of Escherichia coli inactivation with ozone. Water Research, **31**(6), 1355-1362.

Janzen, E. G. (1971). Spin trapping. Accounts of Chemical Research, **4**(1), 31-40.

Kaplan, L. A., Bott, T. L. and Reasoner, D. J. (1993). Evaluation and simplification of the assimilable organic carbon nutrient bioassay for bacteria growth in drinking water. Applied and Environmental Microbiology, **59**(5), 1532-1539.

Katsoyiannis, I. A., Canonica, S. and von Gunten, U. (2011). Efficiency and energy requirements for the transformation of organic micropollutants by ozone, O_3/H_2O_2 and UV/H_2O_2. Water Research, **45**(13), 3811-3822.

Knol, A. H., Lekkerkerker-Teunissen, K., Houtman, C. J., Scheideler, J., Ried, A. and van Dijk, J. C. (2015). Conversion of organic micropollutants with limited bromate formation during the peroxone process in drinking water treatment. Drinking Water Engineering and Science, **8**(2), 25-34.

Laroff, G. P. and Fessenden, R. W. (1973). Equilibrium and kinetics of the acid dissociation of several hydroxyalkyl radicals. Journal of Physical Chemistry, **77**(10), 1283-1288.

Larson, M. A. and Mariñas, B. J. (2003). Inactivation of Bacillus subtilis spores with ozone and monochloramine. Water Research, **37**(4), 833-844.

Larson, R. A. and Zepp, R. G. (1988). Environmental chemistry. Reactivity of the carbonate radical with aniline derivatives. Environmental Toxicology and Chemistry, **7**(4), 265-274.

Lee, C., Yoon, J. and von Gunten, U. (2007). Oxidative degradation of N-nitrosodimethylamine by conventional ozonation and the advanced oxidation process ozone/hydrogen peroxide. Water Research, **41**(3), 581-590.

Lee, Y., Gerrity, D., Lee, M., Gamage, S., Pisarenko, A., Trenholm, R. A., Canonica, S., Snyder, S. A. and von Gunten, U. (2016). Organic contaminant abatement in reclaimed water by UV/H_2O_2 and a combined process consisting of O_3/H_2O_2 followed by UV/H_2O_2: prediction of abatement efficiency, energy consumption, and byproduct formation. Environmental Science & Technology, **50**(7), 3809-3819.

Lee, Y. and von Gunten, U. (2012). Quantitative structure–activity relationships (QSARs) for the transformation of organic micropollutants during oxidative water treatment. Water Research, **46**(19), 6177-6195.

Lekkerkerker-Teunissen, K., Knol, A. H., Derks, J. G., Heringa, M. B., Houtman, C. J., Hofman-Caris, C. H. M., Beerendonk, E. F., Reus, A., Verberk, J. Q. J. C. and van Dijk, J. C.

(2013). Pilot plant results with three different types of UV lamps for advanced oxidation. Ozone-Science & Engineering, **35**(1), 38-48.

Lekkerkerker-Teunissen, K., Knol, A. H., van Altena, L. P., Houtman, C. J., Verberk, J. Q. J. C. and van Dijk, J. C. (2012). Serial ozone/peroxide/low pressure UV treatment for synergistic and effective organic micropollutant conversion. Separation and Purification Technology, **100**, 22-29.

Lekkerkerker, K., Scheideler, J., Maeng, S. K., Ried, A., Verberk, J. Q. J. C., Knol, A. H., Amy, G. and van Dijk, J. C. (2009). Advanced oxidation and artificial recharge: a synergistic hybrid system for removal of organic micropollutants. Water Science and Technology: Water Supply, **9**(6), 643-651.

Li, X., Zhao, W., Li, J., Jiang, J., Chen, J. and Chen, J. (2013). Development of a model for predicting reaction rate constants of organic chemicals with ozone at different temperatures. Chemosphere, **92**(8), 1029-1034.

Luo, Y.-R. (2007). Comprehensive handbook of chemical bond energies. CRC Press Taylor & Francis Group, Boca Raton.

Mitch, W. A. and Sedlak, D. L. (2002). Formation of N-nitrosodimethylamine (NDMA) from dimethylamine during chlorination. Environmental Science and Technology, **36**(4), 588-595.

Najm, I. and Trussell, R. R. (2001). NDMA formation in water and wastewater. Journal / American Water Works Association, **93**(2), 92-99.

Neta, P., Huie, R. E. and Ross, A. B. (1988). Rate constants for reactions of inorganic radicals in aqueous solution. Journal of Physical and Chemical Reference Data, **17**(3), 1027-1284.

Pinkernell, U. and von Gunten, U. (2001). Bromate minimization during ozonation: mechanistic considerations. Environmental Science & Technology, **35**(12), 2525-2531.

Prasse, C., Stalter, D., Schulte-Oehlmann, U., Oehlmann, J. and Ternes, T. A. (2015). Spoilt for choice: a critical review on the chemical and biological assessment of current wastewater treatment technologies. Water Research, **87**(Supplement C), 237-270.

Pryor, W. A., Giamalva, D. H. and Church, D. F. (1984). Kinetics of ozonation. 2. amino acids and model compounds in water and comparisons to rates in nonpolar solvents. Journal of the American Chemical Society, **106**(23), 7094-7100.

Rakness, K. L., Najm, I., Elovitz, M., Rexing, D. and Via, S. (2005). Cryptosporidium log-inactivation with ozone using effluent CT_{10}, geometric mean CT_{10}, extended integrated CT_{10} and extended CSTR calculations. Ozone-Science & Engineering, **27**(5), 335-350.

Rosenfeldt, E. J., Linden, K. G., Canonica, S. and von Gunten, U. (2006). Comparison of the efficiency of OH radical formation during ozonation and the advanced oxidation processes O_3/H_2O_2 and UV/H_2O_2. Water Research, **40**(20), 3695-3704.

Roustan, M., Beck, C., Wable, O., Duguet, J. P. and Mallevialle, J. (1993). Modeling hydraulics of ozone contactors. Ozone-Science & Engineering, **15**(3), 213-226.

Scheideler, J. and Bosmith, A. (2014). AOP für den Abbau von Metaldehyd: Weitergehende Oxidationprozesse gegen Pestizid im Oberflächenwasser. Aqua & Gas, **94**(3), 52-57.

Scheideler, J., Lekkerkerker-Teunissen, K., Knol, T., Ried, A., Verberk, J. and van Dijk, H. (2011). Combination of O_3/H_2O_2 and UV for multiple barrier micropollutant treatment and bromate formation control - an economic attractive option. Water Practice and Technology, **6**(4).

Schuchmann, M. N. and von Sonntag, C. (1979). Hydroxyl radical-induced oxidation of 2-methyl-2-propanol in oxygenated aqueous solution. A product and pulse radiolysis study. Journal of Physical Chemistry, **83**(7), 780-784.

Shen, J. M., Chen, Z. L., Xu, Z. Z., Li, X. Y., Xu, B. B. and Qi, F. (2008). Kinetics and mechanism of degradation of p-chloronitrobenzene in water by ozonation. Journal of Hazardous Materials, **152**(3), 1325-1331.

Siddiqui, M. S., Amy, G. L. and McCollum, L. J. (1996). Bromate destruction by UV irradiation and electric arc discharge. Ozone: Science and Engineering, **18**(3), 271-290.

Sudhakaran, S. and Amy, G. L. (2013). QSAR models for oxidation of organic micropollutants in water based on ozone and hydroxyl radical rate constants and their chemical classification. Water Research, **47**(3), 1111-1122.

Ulanski, P. and von Sonntag, C. (1999). The OH radical-induced chain reactions of methanol with hydrogen peroxide and with peroxodisulfate. Journal of the Chemical Society-Perkin Transactions 2(2), 165-168.

Uslu, M. O., Rahman, M. F., Jasim, S. Y., Yanful, E. K. and Biswas, N. (2012). Evaluation of the reactivity of organic pollutants during O_3/H_2O_2 process. Water, Air, & Soil Pollution, **223**(6), 3173-3180.

Veltwisch, D., Janata, E. and Asmus, K. D. (1980). Primary processes in the reaction of OH-radicals with sulphoxides. Journal of the Chemical Society-Perkin Transactions 2(1), 146-153.

von Gunten, U. (2003a). Ozonation of drinking water: part I. Oxidation kinetics and product formation. Water Research, **37**(7), 1443-1467.

von Gunten, U. (2003b). Ozonation of drinking water: part II. Disinfection and by-product formation in presence of bromide, iodide or chlorine. Water Research, **37**(7), 1469-1487.

von Gunten, U., Elovitz, M. and Kaiser, H. P. (1999). Calibration of full-scale ozonation systems with conservative and reactive tracers. Journal of Water Supply Research and Technology-Aqua, **48**(6), 250-256.

von Gunten, U. and Hoigné, J. (1994). Bromate formation during ozonation of bromide-containing waters: interaction of ozone and hydroxyl radical reactions. Environmental Science & Technology, **28**(7), 1234-1242.

von Gunten, U. and Oliveras, Y. (1997). Kinetics of the reaction between hydrogen peroxide and hypobromous acid: implication on water treatment and natural systems. Water Research, **31**(4), 900-906.

von Gunten, U., Salhi, E., Schmidt, C. K. and Arnold, W. A. (2010). Kinetics and mechanisms of N-nitrosodimethylamine formation upon ozonation of N,N-dimethylsulfamide-containing waters: bromide catalysis. Environmental Science & Technology, **44**(15), 5762-5768.

von Sonntag, C. (2006). Free-radical-induced DNA damage and its repair: a chemical perspective. Springer Verlag, Berlin, Heidelberg.

von Sonntag, C. and Schuchmann, H.-P., Eds. (1997). Peroxyl radicals in aqueous solution. Peroxyl radicals (The chemistry of free radicals). Chichester, Wiley.

von Sonntag, C. and von Gunten, U. (2012). Chemistry of ozone in water and wastewater treatment - from basic principles to applications. IWA Publishing, London.

Werderitsch, M. (2013). Planning, construction and operation of a full scale advanced oxidation treatment plant for drinking water. AOT-Conference, San Diego.

WHO (2006). N-Nitrosodimethylamine in drinking-water. Background document for development of WHO guidelines for drinking-water quality, http://www.who.int/water_sanitation_health/dwq/chemicals/ndma2ndadd.pdf.

Wickramanayake, G. B., Rubin, A. J. and Sproul, O. J. (1984a). Inactivation of Giardia lamblia cysts with ozone. Applied and Environmental Microbiology, **48**(3), 671-672.

Wickramanayake, G. B., Rubin, A. J. and Sproul, O. J. (1984b). Inactivation of Naegleria and Giardia cysts in water by ozonation. Journal Water Pollution Control Federation, **56**(8), 983-988.

Wolfe, R. L., Stewart, M. H., Scott, K. N. and McGuire, M. J. (1989). Inactivation of Giardia muris and indicator organisms seeded in surface water supplies by peroxone and ozone. Environmental Science & Technology, **23**(6), 744-745.

Wu, T. and Englehardt, J. D. (2015). Peroxone mineralization of chemical oxygen demand for direct potable water reuse: kinetics and process control. Water Research, **73**, 362-372.

Zehavi, D. and Rabani, J. (1972). Oxidation of aqueous bromide ions by hydroxyl radicals. A pulse radiolytic investigation. Journal of Physical Chemistry, **76**(3), 312-319.

Zhao, G., Lu, X., Zhou, Y. and Gu, Q. (2013). Simultaneous humic acid removal and bromate control by O_3 and UV/O_3 processes. Chemical Engineering Journal, **232**, 74-80.

Chapter 2

SCOPE

The research described in the Introduction (Chapter 1) shows a great interest in •OH that are generated as reactive species in applications in water treatment processes. These processes are called AOPs. Chapter 3 and 4 deal with the formation of •OH in AOPs. One of the AOPs, the Fenton process, was first described in 1894. However, the mechanism is hitherto not completely understood. Nevertheless, the Fenton process is applied for water treatment, e.g. industrial wastewater and may be used more efficiently if all factors influencing the •OH formation in the Fenton process are well defined. The aim of Chapter 3 is to investigate the influence of the pH, Fe(II):H_2O_2 ratio and presence of selected ligands on the •OH yield in the Fenton process.

Another AOP is the peroxone process, a reaction of O_3 with H_2O_2. It is often applied for drinking water production and remediation of groundwater. It was assumed that in the peroxone process the •OH yield is unity with respect to O_3. In Chapter 4 the •OH yield of the peroxone process is determined using different approaches to clarify the •OH yield per consumed O_3. For comparison some of the experiments are also conducted with authentic •OH generated by γ-radiolysis.

Since bromate is one of the most important by-products in ozonation of bromide-containing waters, the reaction of bromate formation is of great interest. The postulated mechanism includes O-transfer reactions of O_3 with Br-species. An electron transfer reaction, that may be possible in the last step, the reaction of bromite with O_3, would lead to the formation of •OH that may contribute to the bromate formation increasing the bromate concentration. The goal of Chapter 5 is the mechanistic investigation of the reaction of bromide with O_3, especially in the last step, by measuring the •OH yield in the system and the influence of the formed •OH on the by-product formation and if necessary update the postulated mechanism.

As direct quantification of •OH is nearly impossible there are a few indirect methods for the •OH quantification described. One of these methods is the analysis of products formed in the reaction of *t*BuOH with •OH. These products are formaldehyde, acetone, 2-methyl-2-hydroxylpropanol and 2-methyl-2-hydroxypropanal. The two latter are not commercially available and therefore, their quantification is not possible. The quantification of •OH is hitherto just based on formaldehyde. The formaldehyde yield represents ~ 30% of •OH. In presence of O_3 the factor changes and the formaldehyde yield represents 50% of •OH. The availability of all products would allow a more precise quantification of •OH. Chapter 6 deals with the synthesis of the both commercially unavailable products from the reaction of •OH with *t*BuOH, 2-methyl-2-hydroxypropanol and 2-methyl-2-hydroxypropanal to gain all four products.

Figure 2-1 shows the structure of the present thesis and briefly summarizes the relationship of the individual Chapters.

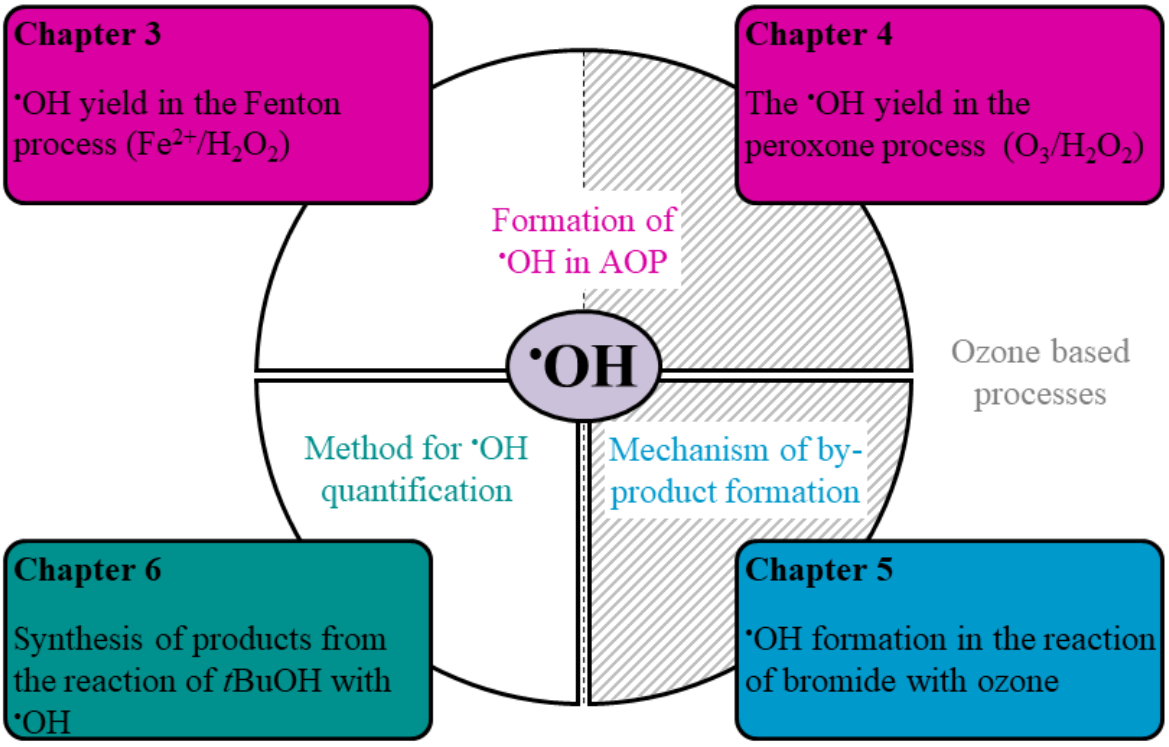

Figure 2-1: Visualization of the scope and the structure of this thesis

Chapter 3

THE HYDROXYL RADICAL YIELD IN THE FENTON REACTION ($Fe^{2+} + H_2O_2$)

Redrafted from "Fischbacher, A; von Sonntag, C.; Schmidt, T. C., Hydroxyl radical yields in the Fenton process under various pH, ligand concentrations and hydrogen peroxide/Fe(II) ratios. *Chemosphere*, **2017**, *182*, pp 738–744.", DOI: 10.1016/j.chemosphere.2017.05.039,

3.1 ABSTRACT

The Fenton process, one of several advanced oxidation processes, describes the reaction of Fe(II) with hydrogen peroxide. Fe(II) is oxidized to Fe(III) that reacts with hydrogen peroxide to Fe(II) and again initiates the Fenton reaction. In the course of the reactions reactive species, e.g. hydroxyl radicals, are formed. Conditions such as pH, ligand concentrations and the hydrogen peroxide/Fe(II) ratio may influence the OH radical yield. It could be shown that at pH < 2.7 and > 3.5 the OH radical yield decreases significantly. Two ligands were investigated, pyrophosphate and sulfate. It was found that pyrophosphate forms a complex with Fe(III) that does not react with hydrogen peroxide and thus, the Fenton reaction is terminated and the OH radical yields do not further increase. The influence of sulfate is not as strong as that of pyrophosphate. The OH radical yield is decreased when sulfate is added but even at higher concentrations the Fenton reaction is not terminated.

3.2 INTRODUCTION

The Fenton reaction is named after Henry J. H. Fenton and describes the reaction of Fe^{2+} with H_2O_2, as in 1894, Fenton reported that H_2O_2 oxidizes tartaric acid in the presence of Fe(II) salts (Fenton, 1894). Several decades later it was proposed that the oxidative species generated by the Fenton reaction is the hydroxyl radical ($^{\bullet}OH$) (Haber and Weiss, 1934). The formed $^{\bullet}OH$, one of the most powerful oxidants ($E° = 2.73$ V), are nonselective and fast reacting with organic and inorganic compounds. Fe(II) reacts with H_2O_2 to Fe(III) and $^{\bullet}OH$ (reaction 3-1). The Fenton reaction is conducted under acidic conditions (Barb *et al.*, 1951).

$$Fe(II) + H_2O_2 \rightarrow Fe(III) + OH^- + {}^{\bullet}OH \qquad (3\text{-}1)$$

Fe(III) formed in reaction (3-1) can be reduced by H_2O_2 to Fe(II) (reaction 3-2) and again initialize reaction (3-1). Reported reaction rate constants for reaction (3-1) vary from 40 to 80 $M^{-1}\ s^{-1}$ while reaction (3-2) was found to be several orders of magnitude slower (Pignatello *et al.*, 2006).

$$Fe(III) + H_2O_2 \rightarrow Fe(II) + HO_2^{\bullet} + H^+ \qquad (3\text{-}2)$$

Reactions (3-1) and (3-2) summarize the overall Fenton reactions. In more detail it is assumed that in the first step H_2O_2 adds to Fe^{2+} giving a hydroperoxy complex (reaction 3-3) that decomposes yielding $^{\bullet}OH$ and Fe(III) (reaction 3-4) (von Sonntag, 2008).

$$Fe^{2+} + H_2O_2 \rightleftarrows FeOOH^+ + H^+ \qquad (3\text{-}3)$$

$$FeOOH^{+} + H^{+} \rightleftarrows FeOH^{2+} + {}^{\bullet}OH \qquad (3\text{-}4)$$

It is expected, that the hydroperoxy complex could also decompose yielding Fe(IV) and OH^{-} (reaction 3-5) (von Sonntag, 2008). Fe(IV) has been suggested as a second reactive species besides $^{\bullet}OH$ (Hug and Leupin, 2003) in particular at higher pH when no $^{\bullet}OH$ are formed.

$$FeOOH^{+} \rightleftarrows FeO^{2+} + OH^{-} \qquad (3\text{-}5)$$

Fe(III) that is formed in reaction (3-4) forms a hydroperoxy complex with H_2O_2 that decomposes unimolecularly to yield Fe(II) and $HO_2^{\bullet}$ (reactions 3-6 – 3-9) (De Laat and Le, 2005).

$$Fe^{3+} + H_2O_2 \rightleftarrows Fe^{III}(HO_2)^{2+} + H^{+} \qquad K = 3.1 \times 10^{-3} \qquad (3\text{-}6)$$

$$FeOH^{2+} + H_2O_2 \rightleftarrows Fe^{III}(OH)(HO_2)^{+} + H^{+} \qquad K = 2 \times 10^{-4} \qquad (3\text{-}7)$$

$$Fe^{III}(HO_2)^{2+} \rightarrow Fe^{2+} + HO_2^{\bullet} \qquad k = 2.7 \times 10^{-3}\ s^{-1} \qquad (3\text{-}8)$$

$$Fe^{III}(OH)(HO_2)^{2+} \rightarrow Fe^{2+} + HO_2^{\bullet} + OH^{-} \qquad k = 2.7 \times 10^{-3}\ s^{-1} \qquad (3\text{-}9)$$

According to reactions (3-10 – 3-12) $HO_2^{\bullet}$ can recombine yielding H_2O_2 which can contribute to the Fenton reaction (Bielski *et al.*, 1985).

$$O_2^{\bullet-} + H^{+} \rightleftarrows HO_2^{\bullet} \qquad (3\text{-}10)$$

$$O_2^{\bullet-} + HO_2^{\bullet} + H_2O \rightarrow H_2O_2 + O_2 + OH^{-} \qquad k = 9.7 \times 10^{7}\ M^{-1}\ s^{-1} \qquad (3\text{-}11)$$

$$2\ HO_2^{\bullet} \rightarrow H_2O_2 + O_2 \qquad k = 8.3 \times 10^{5}\ M^{-1}\ s^{-1} \qquad (3\text{-}12)$$

Besides the reaction of Fe(II) with H_2O_2 Fe(II) can also be oxidized to Fe(III) by oxygen present in the solution without yielding $^{\bullet}OH$. The reaction rates of these autoxidation reactions depend on the iron species (reactions 3-13 – 3-15). The more OH^{-} are bound to the Fe(II), the faster the reaction (King, 1998).

$$Fe^{2+} + O_2 \rightarrow Fe^{3+} + O_2^{\bullet-} \qquad k = 9.2 \times 10^{-7}\ M^{-1}\ s^{-1} \qquad (3\text{-}13)$$

$$Fe(OH)^{+} + O_2 \rightarrow Fe(OH)^{2+} + O_2^{\bullet-} \qquad k = 6.95\ M^{-1}\ s^{-1} \qquad (3\text{-}14)$$

$$Fe(OH)_2 + O_2 \rightarrow Fe(OH)_2^{+} + O_2^{\bullet-} \qquad k = 8.75 \times 10^{5}\ M^{-1}\ s^{-1} \qquad (3\text{-}15)$$

Besides Fe(III) superoxide is formed in the autoxidation reactions (3-13 – 3-15) that can recombine to hydrogen peroxide (reactions 3-10 – 3-12) and contribute to the Fenton reaction.

Figure 3-1 shows the fractions of Fe(II) present in aqueous solution at different pH. At pH below 9 the predominant species is Fe^{2+}, which indicates that at acidic and neutral pH autoxidation (reaction 3-13) is very slow and can be neglected, if no ions that accelerate the reaction, e.g. CO_3^{2-}/HCO_3^-, are present. At higher pH (> 9) autoxidation becomes more relevant as the predominant species is $Fe(OH)_2$ which reacts faster with O_2 (reaction 3-15). As the Fenton reaction is not conducted at such high pH, the reaction of $Fe(OH)_2$ with O_2 can be neglected.

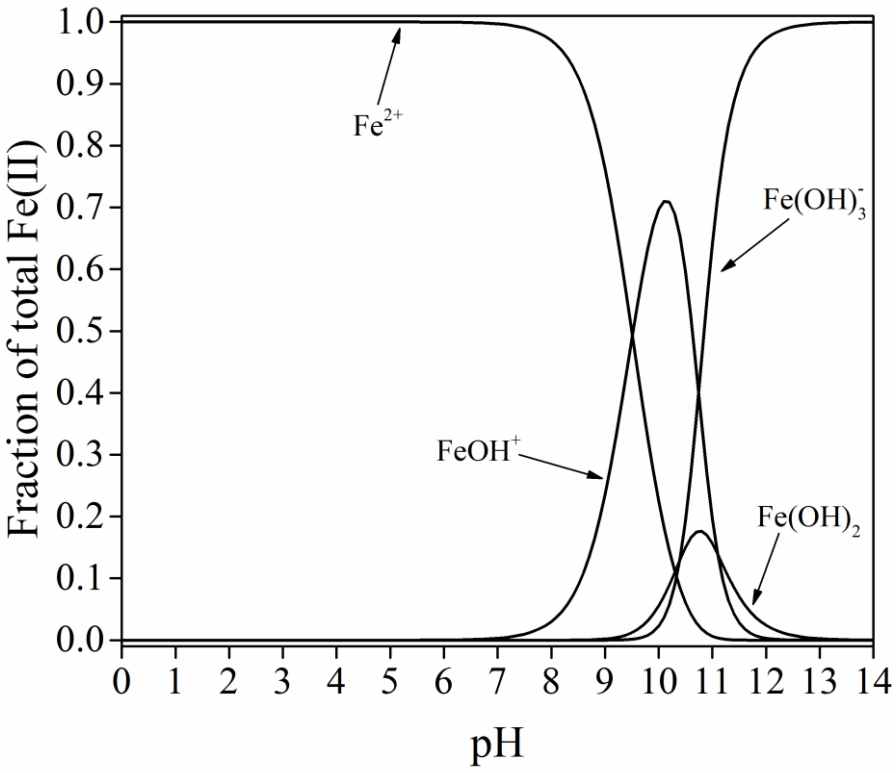

Figure 3-1: Iron(II) speciation diagram in aqueous solution as a function of pH at 25°C and ionic strength of 1 M based on data from (Turner *et al.*, 1981)

As the Fenton process describes a reaction that generates •OH (reaction 3-1) it is assigned to the advanced oxidation processes (AOPs). The reaction takes place under acidic conditions. Therefore, the Fenton reaction is not often applied as most of the treated waters are in a neutral to slightly basic pH range. The only efficient field of application are acidic industrial wastewaters because no pH shift is needed and the used chemicals are easy to handle compared to other advanced oxidation processes.

If other transition metals than Fe(II) are present (e.g. Cu(I), Fe(III)) the reaction is called Fenton-type or Fenton-like. There are several other Fenton-based reactions known, e.g. photo-Fenton, electro-Fenton and sono-Fenton reactions (Wang, 2012).

The Fenton process is a very complex and not fully understood sequence of reactions. When inorganic ions are present in the solution it becomes even more complex. Some inorganic ions, e.g. Cl^- and Br^- can act as $^{\bullet}OH$ scavenger, as they are very reactive towards $^{\bullet}OH$ ($k_{Cl^- + {}^{\bullet}OH} = 3 \times 10^9$ M^{-1} s^{-1} (Grigorev *et al.*, 1987) and $k_{Br^- + {}^{\bullet}OH} = 1.1 \times 10^{10}$ M^{-1} s^{-1} (Zehavi and Rabani, 1972)). They can be present in high concentration in waters to be treated suppressing the reaction of $^{\bullet}OH$ with contaminants. The reaction of chloride with $^{\bullet}OH$ yields $Cl_2^{\bullet-}$ that reacts more selectively than $^{\bullet}OH$ and decreases the oxidation rate. Besides scavenging of $^{\bullet}OH$ chloride can form complexes with Fe(III). These Fe(III)-chlorocomplexes are less reactive towards H_2O_2 and decrease the $^{\bullet}OH$ yield as reaction (3-2) is suppressed (De Laat and Le, 2006). However, due to the high reaction rate constant of chloride with $^{\bullet}OH$ the scavenging effect is much more important than the inhibition caused by the complexation. Other inorganic ions, e.g. phosphate form complexes with Fe(III) which are less reactive towards H_2O_2 (Lu *et al.*, 1997). In this case the catalytic cycle of the Fenton reaction is disrupted as there is no reduction of Fe(III) to Fe(II) possible. The Fenton reaction can also be affected by other ligands in the contrary way. Wells and Salam observed that increasing the concentration of some halides, sulfate and tripolyphosphate accelerates the reaction of Fe(II) with H_2O_2 (Wells and Salam, 1967, Wells and Salam, 1968). Also some chelating ligands, e.g. EDTA and oxalate, can accelerate the reaction of Fe(II) with H_2O_2 when forming Fe(II) complexes that are more reactive towards H_2O_2 ($k_{Fe(II)\text{-}C_2O_4^{2-}} = 1 \times 10^4$ M^{-1} s^{-1} (Park *et al.*, 1997) and $k_{Fe(II)\text{-EDTA}} = 1.75 \times 10^4$ M^{-1} s^{-1} (Rush and Koppenol, 1986)). The reaction of the Fe(II)-EDTA complex with H_2O_2 is supposed not to yield $^{\bullet}OH$, as the product does not undergo reactions that are characteristic for $^{\bullet}OH$, but behaves more like a FeO(II)-EDTA complex (Rush and Koppenol, 1986). Stability constants relevant for this study are compiled in Table 3-1.

Table 3-1: Stability constants (log β) at 25°C for Fe^{2+} and Fe^{3+} and ligands (L) in aqueous solution

Ligand	Complex	Stability constant log β for L with Fe^{2+}	Reference	Complex	Stability constant log β for L with Fe^{3+}	Reference
SO_4^{2-}	FeHL	0.29	(Sillén and Martell, 1964)	FeL	3.92	(Benjamin, 2002)
	FeL	2.25	(Benjamin, 2002)	FeL_2	5.42	(Benjamin, 2002)
PO_4^{3-}	FeHL	7.34 (30°C)	(Sillén and Martell, 1964)	FeHL	17.78	(Benjamin, 2002)
	FeH_2L	22.25	(Benjamin, 2002)	Fe_2HL	11.14	(Sillén and Martell, 1964)
$P_2O_7^{4-}$	not available			FeH_2L	6.97	(Sillén and Martell, 1964)
				FeH_3L	5.58	(Sillén and Martell, 1964)
				Fe_2L	23.3 or 23.5	(Sillén and Martell, 1964)

The •OH yield in the Fenton process depends on the pH value, the H_2O_2/Fe^{2+} ratio and possible ligands present in the solution. It can be affected by dissolved organic matter that acts as •OH scavenger and inorganic or chelating compounds that can act as ligands and influence the reaction leading to a decrease or increase of the •OH yield. Many authors deal with conditions for the Fenton reaction maximizing •OH yield, which are summarized by (Pignatello *et al.*, 2006). However, knowledge on conditions and compounds acting as ligands influencing the generation of •OH in the Fenton process is not only important in water treatment. Sometimes, the Fenton reaction and •OH formation is undesired, for example in fuel cells. Here, •OH destroy the membrane located in a fuel cell and minimize its lifetime (Holton and Stevenson, 2013).

Nowadays, it is assumed that •OH could be just one of several oxidative species formed in the Fenton reaction. Although the reaction was first described over 100 years ago and the process is applied in full-scale, the reactive species are still not fully identified and the mechanism is still not clarified.

The aims of this study are to quantify the •OH yield at different H_2O_2/Fe^{2+} ratios in a pH range of 1.5 – 5 and to characterize the influence of pyrophosphate and sulfate that act as ligands and may influence the •OH yield.

3.3 MATERIAL AND METHODS

3.3.1 CHEMICALS

Following chemicals were used as received without any further purification: dimethyl sulfoxide (99.9 %) VWR, ethanol (99.8 %) Sigma-Aldrich, iron(II) sulfate heptahydrate (≥ 99 %) Riedel-de Haën, hydrogen peroxide (30 %) Merck, perchloric acid (70 %) Fluka, sulfuric acid (≥ 98 %) VWR, phosphoric acid (85 %) Merck, methanesulfonic acid (> 99 %) Merck, manganese(II) sulfate monohydrate (99 – 101 %) Fluka, sodium methanesulfinate (95 %) Alfa Aesar, sodium carbonate (≥ 99.8 %) Riedel-de Haën, sodium sulfite (≥ 98 %) Sigma-Aldrich, sodium pyrophosphate decahydrate (≥ 99 %) Sigma Aldrich, sodium sulfate (≥ 99.0 %) Fluka, sodium hydrogencarbonate (≥ 99.7 %) Fluka, sodium hydroxide (50 %) Sigma Aldrich, oxalic acid (≥ 99 %) Sigma Aldrich, pure water (Millipore, 18 MΩ cm)

3.3.2 EXPERIMENTAL PROCEDURE

3.3.2.1 CONDITION VARIATIONS

All experiments were carried out in a pH range of 1.5 – 5. To adjust the chosen pH all stock solutions were prepared in pure water that was adjusted to the respective pH with $HClO_4$ before its use. The Fe(II) concentration was kept constant at 0.2 mM. To obtain different molar H_2O_2/Fe^{2+} ratios the H_2O_2 concentration was varied between 2 mM and 0.2 M. In all experiments H_2O_2 was added in excess over Fe(II). The applied H_2O_2/Fe^{2+} ratios were 1000:1, 100:1, 50:1, 25:1 and 10:1 resulting in H_2O_2 concentrations of 0.2, 0.02, 0.01, 0.005 and 0.002 M, respectively. When pyrophosphate was added as ligand, it was added in a molar ratio to Fe^{2+} of 0:1, 0.5:1, 1:1 and 2:1 giving a pyrophosphate concentration of 0, 0.1, 0.2 and 0.4 mM. When sulfate was added as ligand it has to be taken into account that sulfate is already present in the solution in the same concentration than iron, as the Fe(II) solution was prepared from $FeSO_4$. The sulfate concentrations that were additionally added were 0, 0.4, 1, 2 and 4 mM leading to SO_4^{2-} concentrations present in the solution of 0.2, 0.6, 1.2, 2.2 and 4.4 mM at the SO_4^{2-}/Fe^{2+} ratios of 1:1, 3:1, 6:1, 11:1 and 21:1, respectively.

As H_2O_2 was added in excess over Fe^{2+} and the pH range was 1.5 – 5 autoxidation (reactions 3-13 – 3-15) could be neglected for all experiments.

DMSO was used to determine the $^{\bullet}OH$ yield (details see below). To ensure that all $^{\bullet}OH$ were scavenged by DMSO it was added to the solutions in excess over all other compounds reacting with $^{\bullet}OH$. DMSO concentration in the solution was always 0.1 M. The fraction of $^{\bullet}OH$ reacting

with DMSO was calculated using concentrations and reaction rate constants of all compounds (see Table 3-2) present in the solution. It was calculated to be at least 99.2 % at highest H_2O_2 (0.2 M) and pyrophosphate (4 mM) concentrations (at H_2O_2/Fe^{2+} ratio of 1000:1) and 99.9 % at a H_2O_2 concentration of 0.02 M (at H_2O_2/Fe^{2+} ratio of 100:1).

Table 3-2: Relevant reactions with •OH and their reaction rate constants for the calculation of the fraction of •OH reacting with DMSO

Reaction	k / M^{-1} s^{-1}	Reference
H_2O_2 + •OH	2.7×10^7	(Buxton *et al.*, 1988)
DMSO + •OH	7×10^9	(Veltwisch *et al.*, 1980)
Fe^{2+} + •OH	$3.2\ 10^8$	(Stuglik and Zagorski, 1981)
$P_2O_7^{4-}$ + •OH	2.2×10^5	(Melton and Bielski, 1990)

The reaction times were 3 and 24 h, respectively. During this time, the solutions were stored in a dark place at room temperature. Stopping the reaction after a certain time is challenging as the reaction is proceeding as long as the reacting compounds are still in the solution. A good method to stop the reaction is to oxidize H_2O_2 by catalase (Liu *et al.*, 2003). However, this was tested prior to the experiments and did not work well at acidic conditions. Another method is the reduction of H_2O_2 by SO_3^{2-}. This approach worked well, but there was also a loss of products that were measured to determine the •OH yield. For these reasons, a third more inconvenient method was chosen to quench the Fenton reaction. To stop the reaction at a certain time the pH was adjusted with NaOH to 11 leading to precipitation of Fe(III), which interrupts the catalytic cycle in the Fenton process. To avoid that further •OH formed from the Fe(II) that was still present in solution reacted with DMSO ethanol (1.6 M) was added in excess to DMSO to scavenge all •OH ($k_{C2H5OH+•OH} = 1.9 \times 10^9$ M^{-1} s^{-1} (Buxton *et al.*, 1988)).

3.3.2.2 DETERMINATION OF THE FE(II) CONCENTRATION

As Fe(II) can be oxidized by oxygen present in the aqueous solution (Sung and Morgan, 1980), the Fe(II) stock solution must be prepared freshly before every use. The ferrous iron concentration is determined by titration with $KMnO_4$. As $KMnO_4$ is also not stable over time, it has to be standardized prior to the titration of the Fe(II) solution by determining its exact concentration. The exact $KMnO_4$ concentration is determined by titration of a stable solution,

e.g. oxalic acid. Around 50 mg oxalic acid is dissolved in 100 mL pure water. After adding 10 mL of 2.5 M sulfuric acid and one drop of an aqueous 1 M Mn^{2+} solution the whole solution is heated to 80°C, as oxalate reacts very slowly with MnO_4^- at room temperature. According to the standard procedure described by McBride (1912) the hot oxalic acid is titrated with the $KMnO_4$ solution until the appearance of a faint pink color and the $KMnO_4$ concentration is calculated according to the ratio obtained from reaction (3-16). This solution is then used as standard oxidizing solution for the determination of the Fe(II) concentration.

$$2\ MnO_4^- + 5\ C_2O_4^{2-} + 16\ H^+ \rightleftarrows 2\ Mn^{2+} + 10\ CO_2 + 8\ H_2O \qquad (3\text{-}16)$$

For the determination of the Fe(II) concentration present in the Fe(II) stock solution it was titrated with the standardized $KMnO_4$ solution (see above). To 50 mL Fe(II) solution 10 mL 2.5 M H_2SO_4 and 10 mL Reinhardt-Zimmermann-solution (100 mL H_3PO_4 (85 %) + 60 mL H_2O + 40 mL H_2SO_4 (≥98 %) + 20 g $MnSO_4$ x 7 H_2O in 100 mL) (Müller, 1987) were added and filled up to 100 mL with pure water. According to reaction (3-17) 1 mol MnO_4^- oxidizes 5 mol of Fe^{2+}. The 1:5 ratio provides the basis for the calculation of the Fe(II) concentration.

$$MnO_4^- + 5\ Fe^{2+} + 8\ H^+ \rightleftarrows Mn^{2+} + 5\ Fe^{3+} + 4\ H_2O \qquad (3\text{-}17)$$

3.3.2.3 $^{\bullet}OH$ QUANTIFICATION

As $^{\bullet}OH$ are fast reacting, a direct measurement is not possible. Scavenging of $^{\bullet}OH$ with a suitable compound is a good indirect method for $^{\bullet}OH$ quantification. Here, $^{\bullet}OH$ were scavenged by DMSO. Its fast reaction (k = 7 x 10^9 M^{-1} s^{-1}) with $^{\bullet}OH$ is well known (reaction 3-18).

$$(CH_3)_2SO + {}^{\bullet}OH \rightarrow {}^{\bullet}CH_2CH_3SO + CH_3SOOH \qquad (3\text{-}18)$$

DMSO is oxidized by $^{\bullet}OH$ to methanesulfinic acid (Veltwisch *et al.*, 1980), which can be further oxidized to methanesulfonic acid (Flyunt *et al.*, 2001). The sum of both acids gives 92 % of the $^{\bullet}OH$ yield (Veltwisch *et al.*, 1980). Methanesulfonic acid and methanesulfinic acid were measured by ion chromatography (Dionex, ICS 900 Starter Line IC System) using the following column: IONPAC AS14A 4 × 250 mm equipped with a pre-column AG14A 4 × 50 mm. The eluent consisted of 0.17 mM $NaHCO_3$ and 0.18 mM Na_2CO_3. The measurements were conducted at a flow of 1 mL/min. Retention times of methanesulfinic acid and methanesulfonic acid were 5.9 and 6.9 minutes, respectively.

3.4 RESULTS AND DISCUSSION

3.4.1 PYROPHOSPHATE ACTING AS LIGAND

•OH yields were determined after 3 and 24 h of reaction. Figure 3-2a shows that at pH 2.8 after 3 h of reaction there is a difference in the •OH yield depending on pyrophosphate addition just for the H_2O_2/Fe^{2+} ratio of 1000:1. For all other ratios the difference is not significant within this reaction time. As in the first hours only reaction (3-1) seems to proceed and at smaller H_2O_2/Fe^{2+} ratios there is no difference in the •OH yields of solutions with and without pyrophosphate, even if pyrophosphate accelerates the reaction of Fe(II) with H_2O_2 (Rachmilovich-Calis *et al.*, 2011) it seems that it does not influence the •OH yield of the reaction. In case of the high hydrogen peroxide concentration (H_2O_2/Fe^{2+} ratio of 1000:1) reaction (3-2) also occurred within the first 3 h because of its higher observed reaction rate causing a difference in the •OH yields of the solutions with and without pyrophosphate. This is a first indication that pyrophosphate affects the reaction of Fe(III) with H_2O_2.

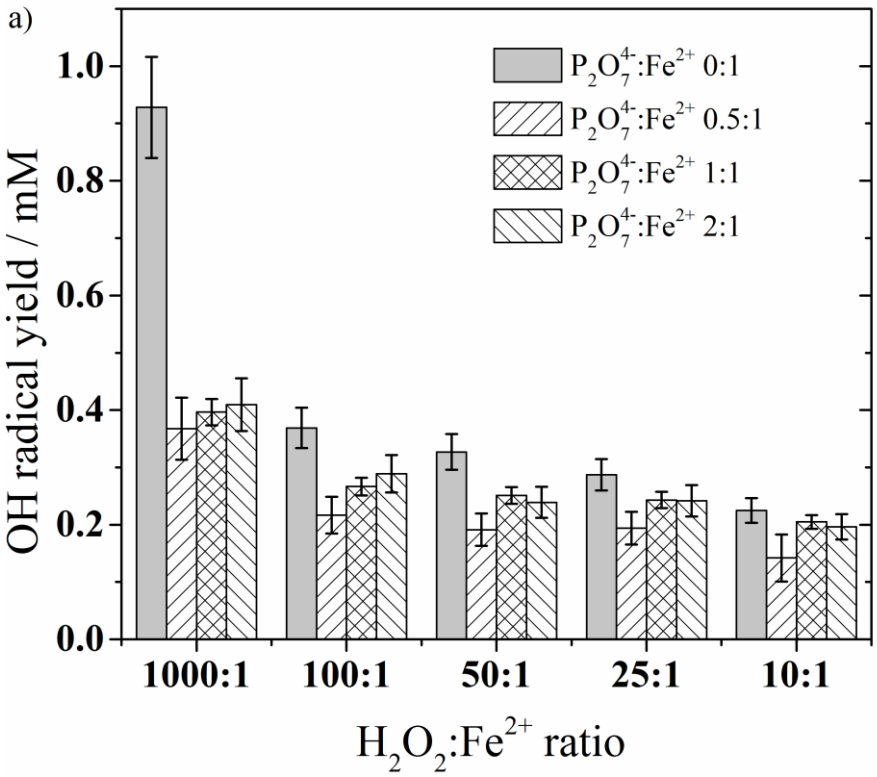

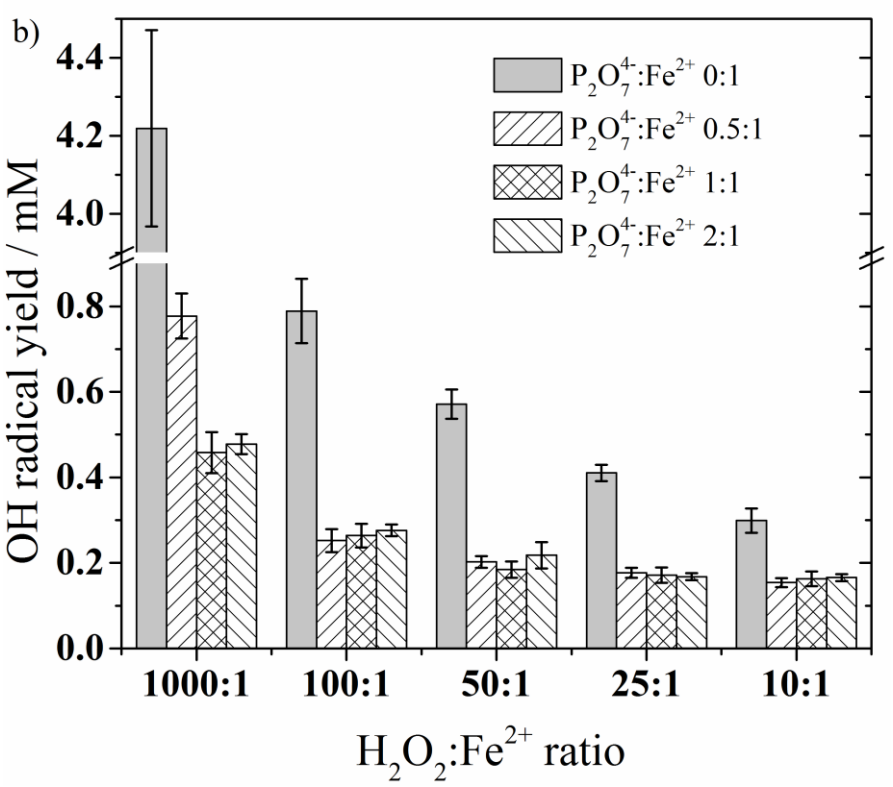

Figure 3-2: ˙OH yields calculated from the product analysis of the reaction of ˙OH with DMSO at different molar H_2O_2/Fe^{2+} ratios with addition of different pyrophosphate concentrations at pH 2.8, a) quenched after 3 h and b) after 24h.

As shown in Figure 3-2b the difference in the ˙OH yields changed after 24 h of reaction. Even at smaller H_2O_2/Fe^{2+} ratios there is a significant difference in the ˙OH yields between solutions with and without pyrophosphate addition. It can be observed that the higher the excess of H_2O_2 over Fe(II) the bigger the difference in the ˙OH yield if no pyrophosphate is added. As H_2O_2 is in all cases in excess over Fe(II) it can be assumed that all Fe(II) is oxidized to Fe(III). After 24 h of reaction one can assume that besides reaction (3-1) also reaction (3-2) occurred. The difference in the ˙OH yields with and without pyrophosphate can be explained as follows. Once Fe(III) is formed it could be complexed by pyrophosphate analogous to the complexation reaction of Fe(III) with phosphate (Lu *et al.*, 1997). Lu *et al.* (1997) described that if phosphate is present in the solution it forms a stable complex with Fe(III), that is not reactive towards H_2O_2. The comparison of the stability constants for phosphate and pyrophosphate (see Table 3-1) shows an even higher constant for pyrophosphate with Fe(III), indicating that a stable $Fe_2H_xP_2O_7^{(2+x)+}$ complex is formed. Although other complexes of Fe(III) with pyrophosphate are possible (see Table 3-1) the latter seems to be the most stable which is corroborated by the fact that all Fe(III) is complexed by pyrophosphate even at a $P_2O_7^{4-}/Fe^{2+}$ ratio of 0.5:1. The speciation of the pyrophosphate has no influence on the complex formation, as Fe(III)

preferably binds to the P=O double bonds that allow π backbonding according to the Dewar-Chatt-Duncanson model (Dewar, 1951, Chatt and Duncanson, 1953) and not to pyrophosphate's O^- or OH. As the •OH yield did not increase much with time when pyrophosphate is present, the formed complex seems to be not reactive towards H_2O_2, analogous to the complex with phosphate.

At a H_2O_2/Fe^{2+} ratio of 1000:1 the •OH yield increased within 24 h of reaction when pyrophosphate was added in a ratio to Fe^{2+} of 0.5:1. This can be explained by the high excess of H_2O_2. Here, not all formed Fe(III) is complexed by pyrophosphate as it is formed in situ and in competition to the complexation also reacts with H_2O_2 to Fe(II) and yields further •OH.

Due to the low reactivity of •OH towards $P_2O_7^{4-}$ (Table 3-2) (Melton and Bielski, 1990) scavenging of •OH by $P_2O_7^{4-}$ decreasing the •OH yield can be neglected.

Figure 3-3 shows •OH yields of solutions with and without pyrophosphate at an H_2O_2/Fe^{2+} ratio of 100:1 in the pH range of 1.5 – 5. After 3 hours of reaction at all of the investigated pH values there are just minor differences in the •OH yields between solutions with and without pyrophosphate. This changes after 24 h of reaction in the pH range of 2.5 – 3.5. It shows that pyrophosphate acts as ligand and decreases the overall •OH yield in the Fenton reaction which corroborates the assumption that the reaction of Fe(III) with H_2O_2 is inhibited due to the complexation of Fe(III) with pyrophosphate.

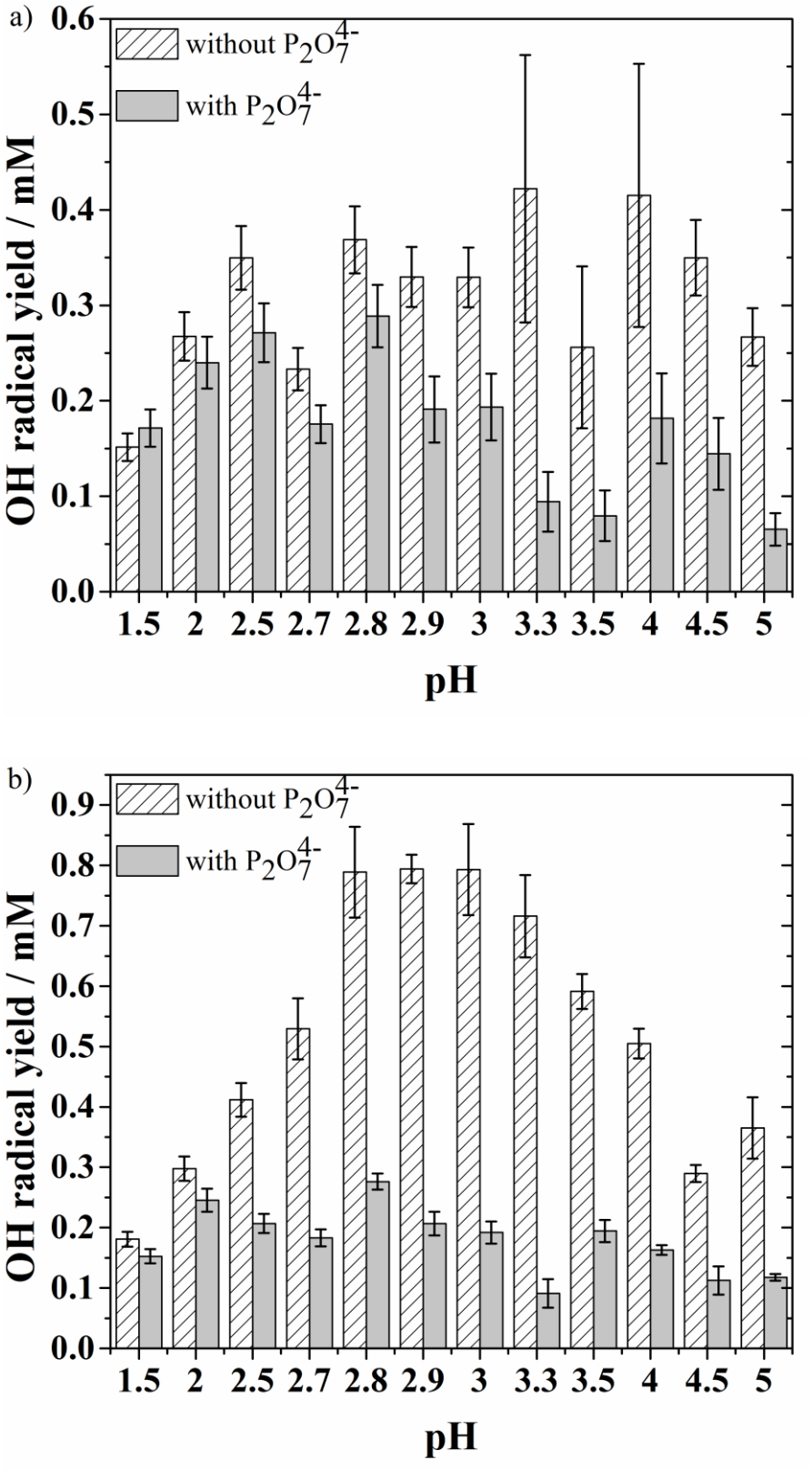

Figure 3-3: •OH yields calculated from the product analysis of the reaction of •OH with DMSO at a molar H_2O_2/Fe^{2+} ratio of 100:1 without and with the addition of pyrophosphate (molar $P_2O_7^{4-}/Fe^{2+}$ ratio 0:1 and 2:1); a) quenched after 3 h reaction time and b) after 24 h.

Comparing the •OH yields in a system without any addition of pyrophosphate after a reaction time of 3 and 24 h shows that without the addition of pyrophosphate there is a significant difference in the •OH yield between a reaction time of 3 and 24 h in the pH range of 2.7 – 3.5 (Figure S3-1). Hence, a longer reaction time leads to a higher •OH yield. In the pH range of 1.5 – 2.5 and 4 – 5 the difference is not significant and thus, no further •OH are generated in the reaction. The decrease of the •OH yields at higher pH and the small difference of the •OH yields after 3 and 24 h of reaction can be explained by the precipitation of Fe(III) and thus termination of the reaction between Fe(III) and H_2O_2. At pH ≥ 3.1 $Fe(OH)_3$ precipitates as its concentration exceeds its solubility. As higher pH leads to decreasing $Fe(OH)_3$ solubility and thus to precipitation, the reaction rate of the reaction of Fe(III) with H_2O_2 decreases.

This changes completely when adding pyrophosphate in a molar ratio to Fe^{2+} of 2:1. In a pH range of 1.5 – 5 no significant difference in the •OH yield determined after 3 and 24 h of reaction can be observed (except the yield at pH 3.5 that seems to be an outlier due to an experimental error). An addition of pyrophosphate to the solution leads to a termination of the Fenton reaction, as all Fe(II) seems to be completely oxidized within 3 h and due to the complexation of Fe(III) with pyrophosphate no Fe(III) can be reduced to Fe(II) and lead to further •OH formation.

3.4.2 SULFATE ACTING AS LIGAND

After 3 h of reaction sulfate has no influence on the •OH yields at H_2O_2/Fe^{2+} ratios of 100:1, 50:1, 25:1 and 10:1. The •OH yields for all SO_4^{2-}/Fe^{2+} ratios and H_2O_2/Fe^{2+} ratios except 1000:1 are equal (Figure 3-4). The only difference can be observed for an H_2O_2/Fe^{2+} ratio of 1000:1. Here, in contrast to the results obtained with pyrophosphate the higher sulfate concentration inhibits the Fenton reaction more than smaller concentrations. Sulfate seems to have no influence on the •OH yield in the reaction of Fe(II) with H_2O_2 even if it accelerates this reaction (De Laat *et al.*, 2004). The difference in the •OH yields at an H_2O_2/Fe^{2+} ratio of 1000:1 can be explained as for pyrophosphate (see above). Comparing the results of sulfate with the results of pyrophosphate it is obvious that the influence of sulfate on the •OH yield is not as strong as the influence of pyrophosphate, even if the applied SO_4^{2-}/Fe^{2+} ratios are considerably higher. The fact that higher sulfate concentrations have a stronger influence on the •OH yields than lower sulfate concentrations indicates that the complex with Fe(III) is not as strong as the complex of pyrophosphate with Fe(III), which is in agreement with the small stability constant for Fe(III) with sulfate (see Table 3-1). The speciation of sulfate seems to have a negligible influence on

the complex formation since the experimental data do not indicate any difference due to speciation.

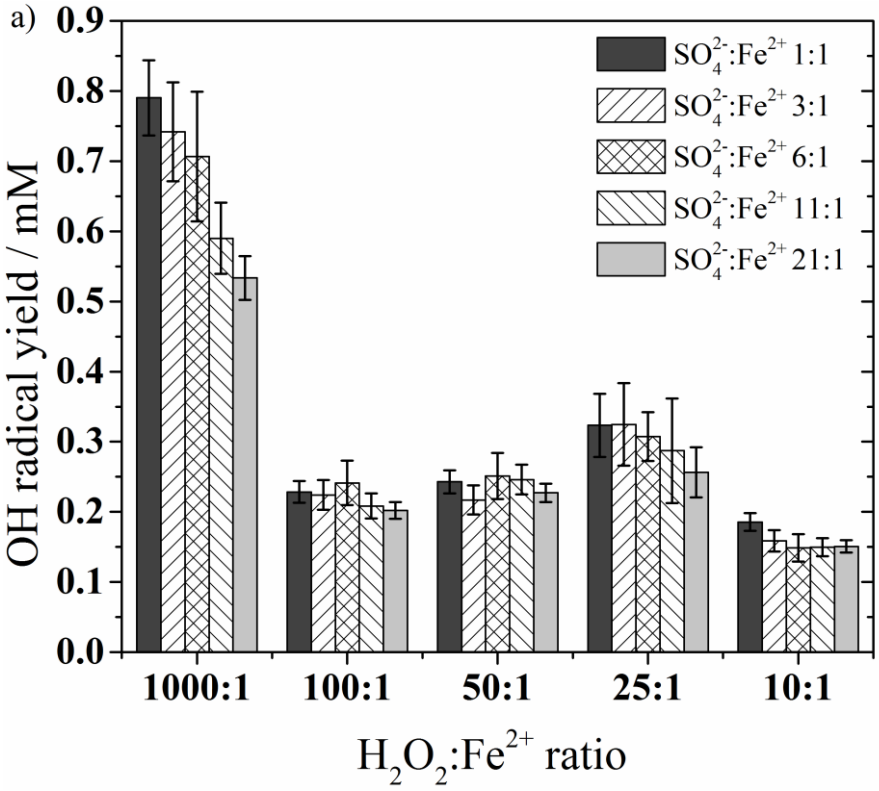

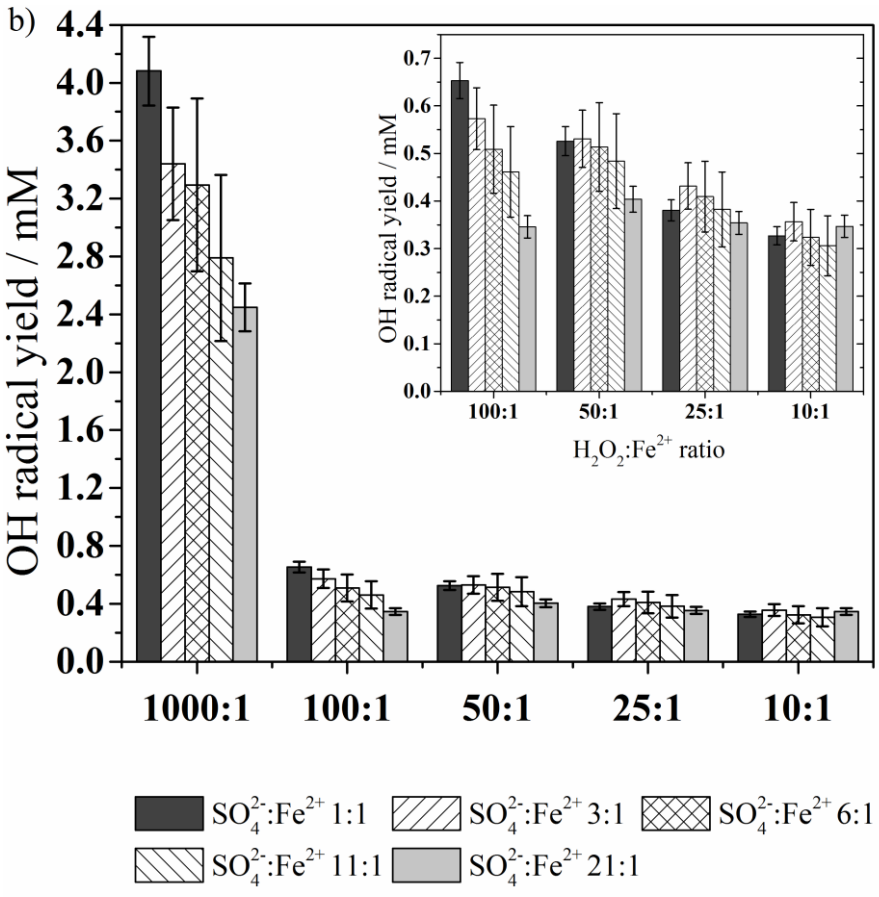

Figure 3-4: •OH yields calculated from the product analysis of the reaction of •OH with DMSO at different molar H_2O_2/Fe^{2+} ratios with addition of different sulfate concentrations at pH 2.8; a) quenched after 3 h and b) 24 h.

As shown in Figure 3-4b the difference in the •OH yields after 24 h of reaction between the solutions with and without additional sulfate are much smaller than in case of pyrophosphate. This corroborates the assumption that sulfate is not such a strong complexing agent than pyrophosphate. De Laat and Le (2005) described that the Fe(III)-SO_4^{2-} complexes ($FeSO_4^+$ and $Fe(SO_4)_2^-$) are non-reactive towards H_2O_2, terminating the Fenton reaction. According to De Laat and Le (2005) a much higher sulfate concentration 0.1 – 1 M would be sufficient to observe significant influence on the Fenton reaction. Thus, at low concentrations the inhibiting effect of sulfate can be neglected.

There is no significant difference in the •OH yields after 3 h of reaction (Figure S3-2). After 24 h of reaction a very slight difference in the •OH yields in the pH range 2.7 – 3.3 can be observed. At lower and higher pH there is no significant difference. This means that the influence of sulfate is very low at present conditions even after a reaction time of 24 h.

Figure 3-5a shows the difference in the •OH yields *without* sulfate after 3 and 24 h reaction time and Figure 3-5b shows the difference in the •OH yields *with* sulfate after 3 and 24 h reaction time. In both cases there is an apparent difference observed. In contrast to the results obtained with pyrophosphate it is obvious that if sulfate is added the Fenton reaction is not terminated after 3 h. Figure 3-3b that corresponds to Figure 3-5b shows no difference in the •OH yields at any pH after 3 and 24 h if pyrophosphate is present, while in Figure 3-5b a difference can be observed for pH ≥ 2.7. The weak complex of Fe(III) with sulfate leads to reduced •OH yields but not to a complete termination of the reaction.

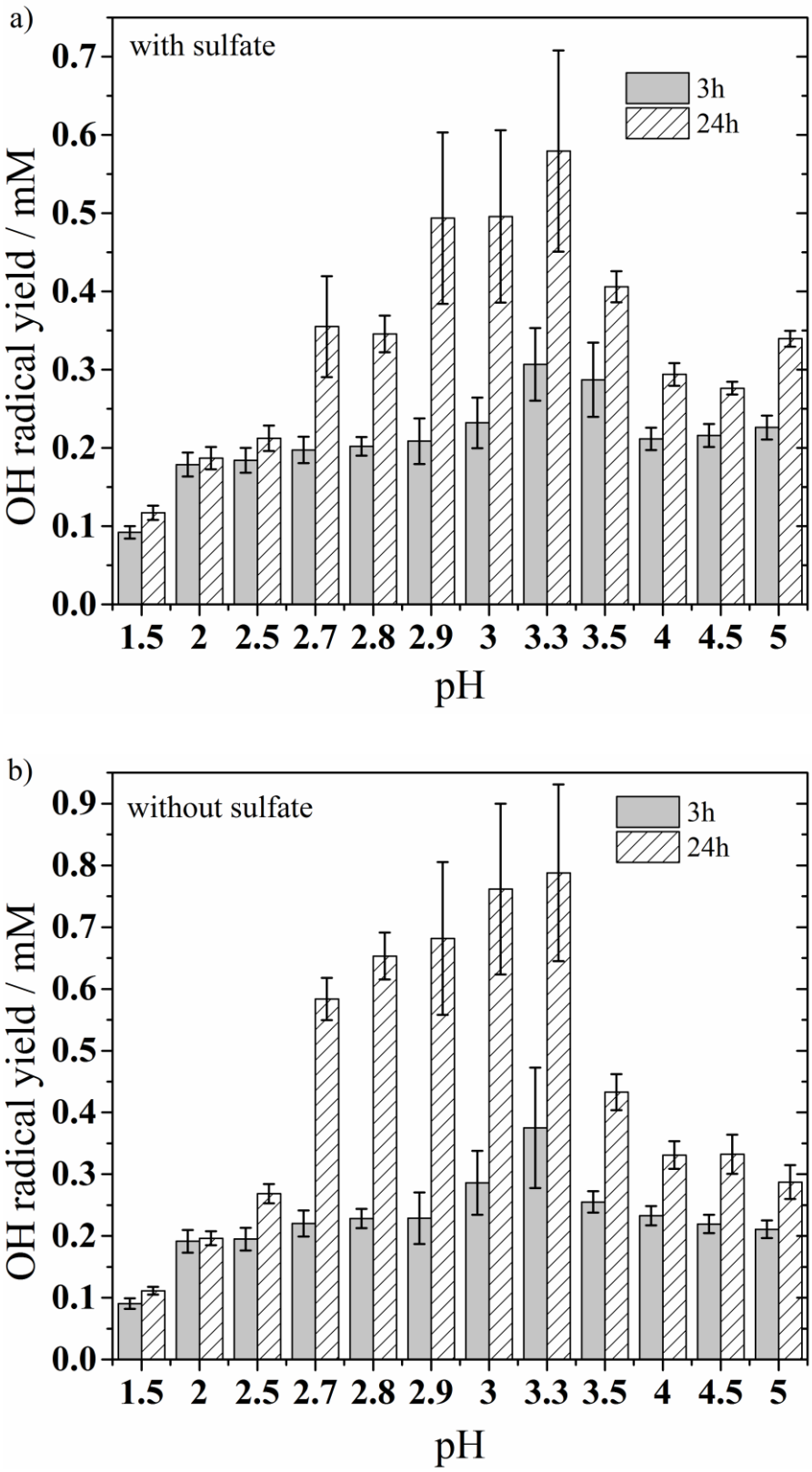

Figure 3-5: ˙OH yields calculated from the product analysis of the reaction of ˙OH with DMSO at a molar H_2O_2/Fe^{2+} ratio of 100:1 a) without any further addition of sulfate (molar SO_4^{2-}/Fe^{2+} ratio 1:1) and b) with addition of sulfate (molar SO_4^{2-}/Fe^{2+} ratio 21:1); quenched after 3 and 24 h reaction time.

3.5 PRACTICAL IMPLICATIONS

The present paper shows that ligands, e.g. pyrophosphate can influence the Fenton reaction and the •OH yield. In case of pyrophosphate the •OH yield is decreased as pyrophosphate adds to Fe(III) forming a complex that terminates the Fenton reaction, as Fe(III) is not available for the back-reaction with H_2O_2. Sulfate also influences the Fenton reaction but not to the same extent than pyrophosphate. In case of sulfate the complex with Fe(III) seems to be less reactive towards H_2O_2 than uncomplexed Fe(III) and even at higher sulfate than pyrophosphate concentrations it influences the reaction not that much. It is necessary to know all conditions that enhance or inhibit the Fenton reaction to be able to predict reactions that are involved in the Fenton reaction yielding •OH or other reactive species. This present study is just a first step in a better understanding of constraints of the Fenton reaction needed for such a prediction. If industrial wastewater treated with the Fenton process contains compounds acting as ligands and inhibiting the •OH generation, one could consider another AOP for the treatment of such a water to make the process more efficient. In cases where the Fenton reaction occurs unintentionally ligands can be added to avoid the undesired •OH formation. The better conditions leading to •OH are understood the better the reaction can be controlled.

3.6 REFERENCES

Barb, W. G., Baxendale, J. H., George, P. and Hargrave, K. R. (1951). Reactions of ferrous and ferric ions with hydrogen peroxide. Part II. - The ferric ion reaction. Transactions of the Faraday Society, **47**, 591-616.

Benjamin, M. M. (2002). Water chemistry. McGraw-Hill, New York.

Bielski, B. H. J., Cabelli, D. E., Arudi, R. L. and Ross, A. B. (1985). Reactivity of HO_2/O_2^- radicals in aqueous solution. Journal of Physical and Chemical Reference Data, **14**(4), 1041-1100.

Buxton, G. V., Greenstock, C. L., Helman, W. P. and Ross, A. B. (1988). Critical review of rate constants for reactions of hydrated electrons, hydrogen atoms and hydroxyl radicals ($\cdot OH/\cdot O^-$) in aqueous solution. Journal of Physical and Chemical Reference Data, **17**(2), 513-886.

Chatt, J. and Duncanson, L. A. (1953). Olefin co-ordination compounds. Part III. Infra-red spectra and structure: attempted preparation of acetylene complexes. Journal of the Chemical Society(OCT), 2939-2947.

De Laat, J. and Le, T. G. (2005). Kinetics and modeling of the Fe(III)/H_2O_2 system in the presence of sulfate in acidic aqueous solutions. Environmental Science and Technology, **39**(6), 1811-1818.

De Laat, J. and Le, T. G. (2006). Effects of chloride ions on the iron(III)-catalyzed decomposition of hydrogen peroxide and on the efficiency of the Fenton-like oxidation process. Applied Catalysis B: Environmental, **66**(1–2), 137-146.

De Laat, J., Truong Le, G. and Legube, B. (2004). A comparative study of the effects of chloride, sulfate and nitrate ions on the rates of decomposition of H_2O_2 and organic compounds by Fe(II)/H_2O_2 and Fe(III)/H_2O_2. Chemosphere, **55**(5), 715-723.

Dewar, J. S. (1951). A review of the Pi-complex theory. Bulletin De La Societe Chimique De France, **18**(3-4), C71-C79.

Fenton, H. J. H. (1894). Oxidation of tartaric acid in presence of iron. Journal of the Chemical Society, Transactions, **65**, 899-910.

Flyunt, R., Makogon, O., Schuchmann, M. N., Asmus, K. D. and von Sonntag, C. (2001). OH-radical-induced oxidation of methanesulfinic acid. The reactions of the methanesulfonyl radical in the absence and presence of dioxygen. Journal of the Chemical Society, Perkin Transactions 2(5), 787-792.

Grigorev, A. E., Makarov, I. E. and Pikaev, A. K. (1987). Formation of $Cl_2^{\bullet-}$ in the bulk solution during the radiolysis of concentrated aqueous solutions of chlorides. High Energy Chemistry, **21**(2), 99-102.

Haber, F. and Weiss, J. (1934). The catalytic decomposition of hydrogen peroxide by iron salts. Proceedings of the Royal Society of London A: Mathematical, Physical and Engineering Sciences, **147**(861), 332-351.

Holton, O. T. and Stevenson, J. W. (2013). The role of platinum in proton exchange membrane fuel cells. Platinum Metals Review, **57**(4), 259-271.

Hug, S. J. and Leupin, O. (2003). Iron-catalyzed oxidation of arsenic(III) by oxygen and by hydrogen peroxide: pH-dependent formation of oxidants in the fenton reaction. Environmental Science & Technology, **37**(12), 2734-2742.

King, D. W. (1998). Role of carbonate speciation on the oxidation rate of Fe(II) in aquatic systems. Environmental Science & Technology, **32**(19), 2997-3003.

Liu, W. J., Andrews, S. A., Stefan, M. I. and Bolton, J. R. (2003). Optimal methods for quenching H_2O_2 residuals prior to UFC testing. Water Research, **37**(15), 3697-3703.

Lu, M. C., Chen, J. N. and Chang, C. P. (1997). Effect of inorganic ions on the oxidation of dichlorvos insecticide with Fenton's reagent. Chemosphere, **35**(10), 2285-2293.

McBride, R. S. (1912). The standardization of potassium permanganate solution by sodium oxalate. Journal of the American Chemical Society, **34**(4), 393-416.

Melton, J. D. and Bielski, B. H. J. (1990). Studies of the kinetic, spectral and chemical properties of Fe(IV) pyrophosphate by pulse radiolysis Radiation Physics and Chemistry, **36**(6), 725-733.

Müller, G.-O. (1987). Lehrbuch der angewandten Chemie. Band 3: Quantitativ anorganisches Praktikum. S. Hirzel Verlag, Leipzig.

Park, J. S. B., Wood, P. M., Davies, M. J., Gilbert, B. C. and Whitwood, A. C. (1997). A kinetic and ESR investigation of iron(II) oxalate oxidation by hydrogen peroxide and dioxygen as a source of hydroxyl radicals. Free Radical Research, **27**(5), 447-458.

Pignatello, J. J., Oliveros, E. and MacKay, A. (2006). Advanced oxidation processes for organic contaminant destruction based on the Fenton reaction and related chemistry. Critical Reviews in Environmental Science and Technology, **36**(1), 1-84.

Rachmilovich-Calis, S., Masarwa, A., Meyerstein, N. and Meyerstein, D. (2011). The effect of pyrophosphate, tripolyphosphate and ATP on the rate of the Fenton reaction. Journal of Inorganic Biochemistry, **105**(5), 669-674.

Rush, J. D. and Koppenol, W. H. (1986). Oxidizing intermediates in the reaction of ferrous EDTA with hydrogen peroxide. Reactions with organic molecules and ferrocytochrome c. Journal of Biological Chemistry, **261**(15), 6730-6733.

Sillén, L. G. and Martell, A. E. (1964). Stability constants of metal-ion complexes. The Chemical Society, London.

Stuglik, Z. and Zagorski, Z. P. (1981). Pulse radiolysis of neutral iron(II) solutions: oxidation of ferrous ions by OH radicals. Radiation Physics and Chemistry, **17**(4), 229-233.

Sung, W. and Morgan, J. J. (1980). Kinetics and products of ferrous iron oxygenation in aqueous systems. Environmental Science & Technology, **14**(5), 561-568.

Turner, D. R., Whitfield, M. and Dickson, A. G. (1981). The equilibrium speciation of dissolved components in freshwater and seawater at 25 degrees C and 1 atm pressure. Geochimica & Cosmochimica Acta, **45**(6), 855-881.

Veltwisch, D., Janata, E. and Asmus, K. D. (1980). Primary processes in the reaction of OH-radicals with sulphoxides. Journal of the Chemical Society-Perkin Transactions 2(1), 146-153.

von Sonntag, C. (2008). Advanced oxidation processes: mechanistic aspects. Water Science and Technology, **58**(5), 1015-1021.

Wang, J. L. X., L. J. (2012). Advanced oxidation processes for wastewater treatment: formation of hydroxyl radical and application. Critical Reviews in Environmental Science and Technology, **42**(3), 251-325.

Wells, C. F. and Salam, M. A. (1967). Complex formation between Fe(II) and inorganic anions. Part 1. - Effect of simple and complex halide ions on the Fe(II)+H_2O_2 reaction. Transactions of the Faraday Society, **63**(0), 620-629.

Wells, C. F. and Salam, M. A. (1968). Complex formation between iron(II) and inorganic anions. Part 2. The effect of oxyanions on the reaction of iron(II) with hydrogen peroxide. Journal of the Chemical Society A: Inorganic, Physical, Theoretical(0), 308-315.

Zehavi, D. and Rabani, J. (1972). Oxidation of aqueous bromide ions by hydroxyl radicals. A pulse radiolytic investigation. Journal of Physical Chemistry, **76**(3), 312-319.

3.7 SUPPORTING INFORMATIONS

3.7.1 PYROPHOSPHATE ACTING AS LIGAND

Figure S3-1 shows the •OH yields in a system with and without the addition of pyrophosphate after a reaction time of 3 and 24 h. It shows that without the addition of pyrophosphate there is a significant difference in the •OH yield between a reaction time of 3 and 24 h in the pH range of 2.7 – 3.5. The •OH yield increases with time. In the pH range of 1.5 – 2.5 and 4 – 5 the difference is not significant and thus, no further •OH are generated in the reaction. Comparing both reaction times (3 and 24 h) when pyrophosphate was added in a molar ratio to Fe^{2+} of 2:1 shows that there is no significant difference in the •OH yield at any pH (except an outlier at pH 3.5 due to experimental error).

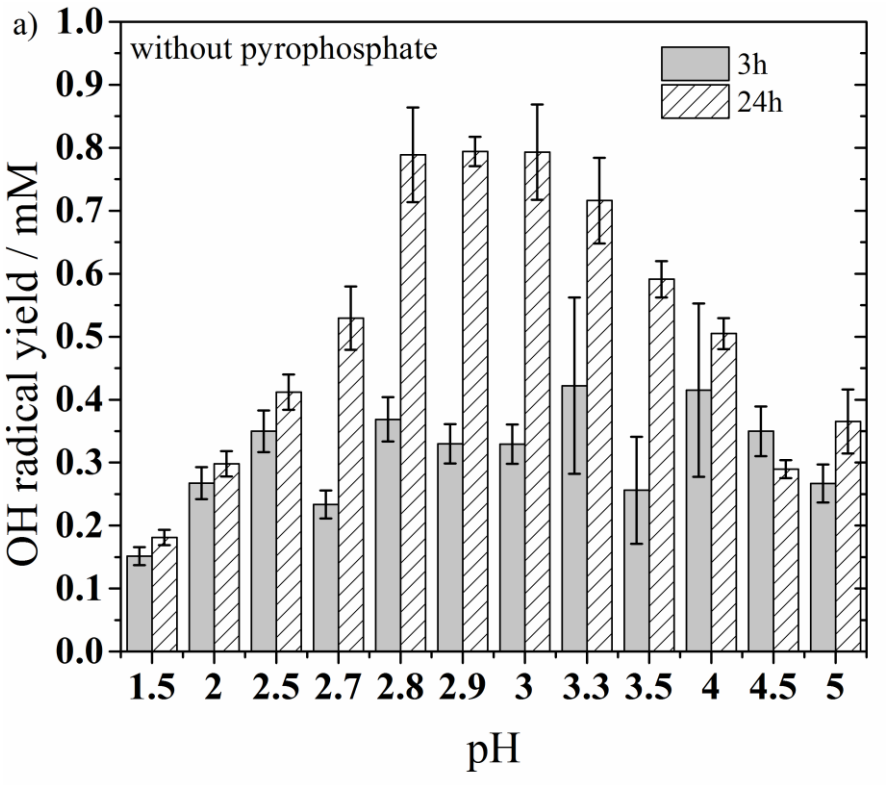

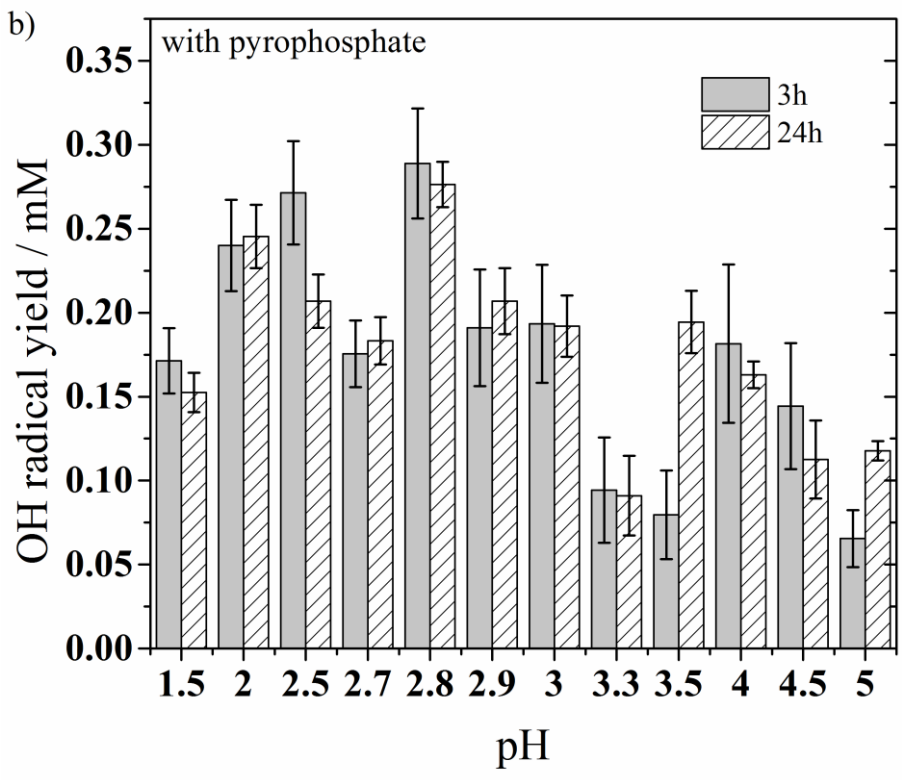

Figure S3-1: ˙OH yields calculated from the product analysis of the reaction of ˙OH with DMSO at a molar H_2O_2/Fe^{2+} ratio of 100:1 a) without addition of pyrophosphate and b) with addition of pyrophosphate (molar $P_2O_7^{4-}/Fe^{2+}$ ratio 2:1); quenched after 3 and 24 h reaction time.

3.7.2 SULFATE ACTING AS LIGAND

Figure S3-2 shows ˙OH yields obtained with and without the addition of sulfate after 3 h and 24 h. There is no significant difference in the ˙OH yields after 3 h of reaction (Figure S3-2). After 24 h of reaction a very slight difference in the ˙OH yields in the pH range 2.7 – 3.3 can be observed. At lower and higher pH there is no significant difference. This means that the influence of sulfate is very low at present conditions even after a reaction time of 24 h.

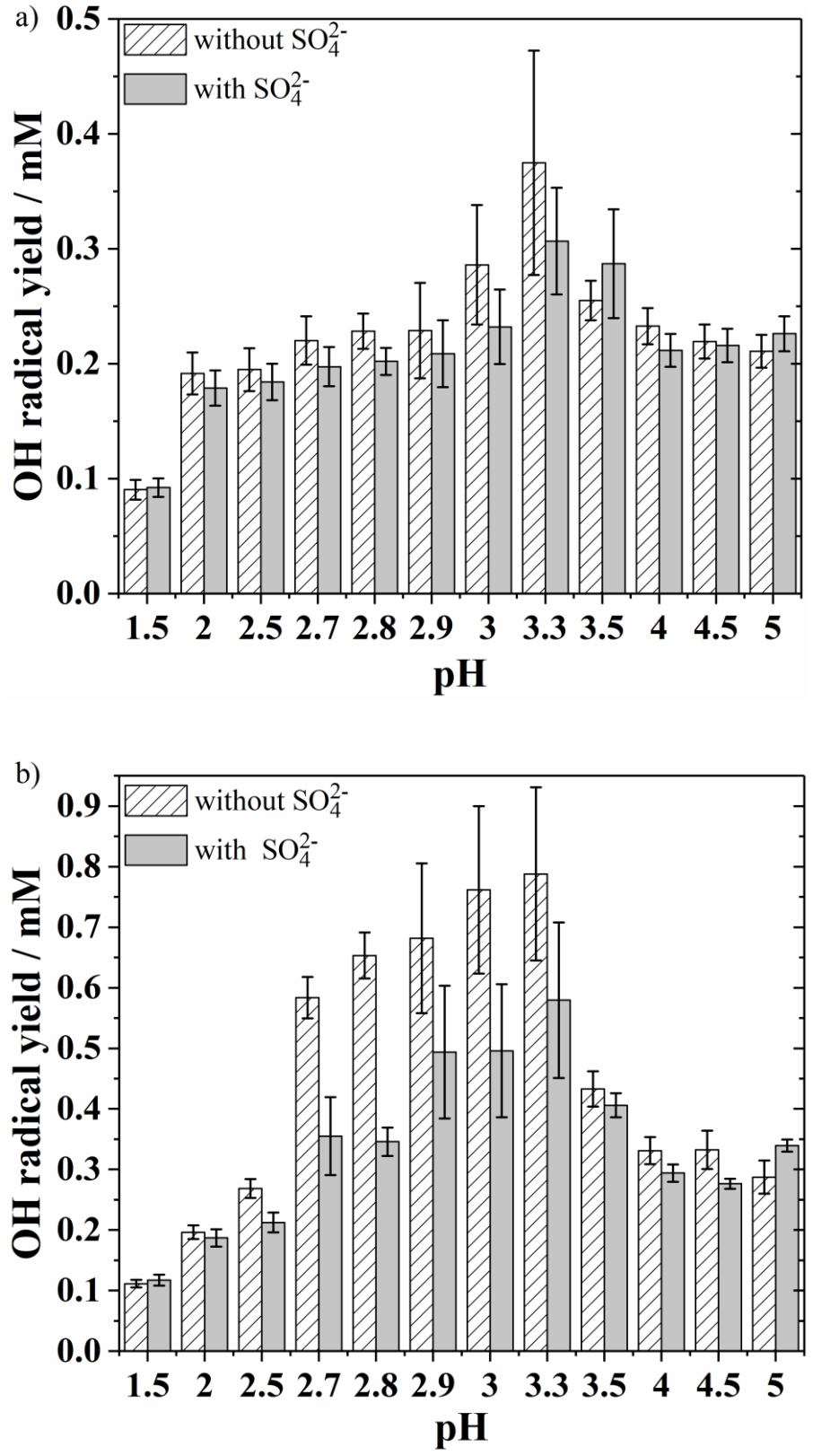

Figure S3-2: ˙OH yields calculated from the product analysis of the reaction of ˙OH with DMSO at a molar H_2O_2:Fe^{2+} ratio of 100:1 without any further addition of sulfate (molar SO_4^{2-}:Fe^{2+} ratio 1:1) and with the addition of sulfate (molar SO_4^{2-}:Fe^{2+} ratio 21:1); a) quenched after 3 h reaction time and b) 24 h.

Chapter 4

THE •OH RADICAL YIELD IN THE $H_2O_2 + O_3$ (PEROXONE) REACTION

Redrafted from "Fischbacher, A.; von Sonntag, J.; von Sonntag, C.; Schmidt, T. C., The •OH Radical Yield in the $H_2O_2 + O_3$ (Peroxone) Reaction. *Environ. Sci. Technol.*, ***2013***, *47*, (17), pp 9959-9964.", DOI: 10.1021/es402305r,

4.1 ABSTRACT

The peroxone process is one of the AOPs that lead to •OH. Hitherto, it has been generally *assumed* that the •OH yield is unity with respect to O_3 consumption. Here, experimental data are presented that suggest that it must be near 0.5. The first evidence is derived from competition experiments. The consumption of *p*-chlorobenzoic acid (*p*CBA), *p*-nitrobenzoic acid (*p*NBA) and atrazine present in trace amounts (1 µM) has been followed as a function of the O_3 concentration in a solution containing H_2O_2 (1 mM) and tertiary butanol (*t*BuOH, 0.5 mM) in excess over the trace compounds. With authentic •OH generated by γ-radiolysis such a competition can be adequately fitted by known •OH rate constants. Fitting the peroxone data, however, the consumption of the trace indicators can only be rationalized if the •OH yield is near 0.5 (*p*CBA: 0.51; *p*NBA: 0.45; atrazine: 0.6). Additional information for an •OH yield much below unity has been obtained by a product analysis of the reactions of *t*BuOH with •OH and dimethyl sulfoxide with •OH. The mechanistic interpretation for the low •OH yield is as follows (Merényi et al. *Environ. Sci. Technol.* **2010**, *44*, 3505-3507). In the reaction of O_3 with HO_2^- an adduct (HO_5^-) is formed that decomposes into $O_3^{\bullet-}$ and $HO_2^\bullet$ in competition with 2 O_2 + OH^-. The latter process reduces the free-radical yield.

4.2 INTRODUCTION

The reaction of H_2O_2 with O_3, often termed peroxone process, is one of the 'Advanced Oxidation Processes' (AOPs) that produce hydroxyl radicals (•OH) in aqueous solution and make use of its high reactivity in pollution abatement by transformation of organic micropollutants. Other AOPs include UV/H_2O_2, UV/O_3, Fe^{2+}/H_2O_2 (Fenton reaction), ionizing radiation and ultrasound. For any technical application, the process should be economically feasible. Besides equipment and reactant costs, a major factor is the •OH yield as it is the reactive species. In the UV/H_2O_2 process, it is 50 %,(Legrini *et al.*, 1993) in the UV/O_3 process merely 10 %,(Reisz *et al.*, 2003) and in the Fenton reaction it is negligible at pH 7 (Hug and Leupin, 2003). For an adequate efficiency the latter process has to be carried out at pH < 3 (Pignatello *et al.*, 2006). Regarding physical processes, energy efficiency of •OH formation is high with ionizing radiation (von Sonntag, 2006), but very low with ultrasound (von Sonntag *et al.*, 1999). For the peroxone process, it has always been *assumed* that the •OH yield per O_3 is 100 % (Staehelin and Hoigné, 1982). Yet, based on preliminary data it has been already noted that it might be much lower, close to 50 % (von Sonntag, 2008). This much lower yield has to

be taken into account when the technical application of the peroxone process is considered and warrants a detailed discussion of the mechanism.

A method for cost comparison of AOPs is the E_{EO} concept, which calculates the required electrical energy per order of magnitude of pollutant degradation per m^3 (Bolton *et al.*, 2001, Müller *et al.*, 2001). In addition, the cost for H_2O_2 is a major factor (Rosenfeldt *et al.*, 2006). The reaction of H_2O_2 ($pK_a = 11.8$) with O_3 is slow ($k < 0.01\ M^{-1}\ s^{-1}$), but that of its anion, HO_2^-, is fast ($k = 5.5 \times 10^6\ M^{-1}\ s^{-1}$) (Staehelin and Hoigné, 1982, Sein *et al.*, 2007). Due to large difference in rate constants for reactions leading to $^{\bullet}OH$ only reaction with HO_2^- is relevant. Originally, reactions (4-1) – (4-6) have been suggested to account for the formation of $^{\bullet}OH$ (Staehelin and Hoigné, 1982). In this concept, it has been assumed that the stoichiometry of the peroxone reaction is $H_2O_2 + 2\ O_3 \rightarrow 2\ ^{\bullet}OH + 3\ O_2$, that is, per each O_3 one $^{\bullet}OH$ is formed, as there were no reactions foreseen that would compete with reactions (4-1) – (4-6).

$$H_2O_2 \rightleftharpoons H^+ + HO_2^- \quad (4\text{-}1)$$

$$HO_2^- + O_3 \rightarrow HO_2^{\bullet} + O_3^{\bullet-} \quad (4\text{-}2)$$

$$HO_2^{\bullet} \rightleftharpoons O_2^{\bullet-} + H^+ \quad (4\text{-}3)$$

$$O_2^{\bullet-} + O_3 \rightarrow O_2 + O_3^{\bullet-} \quad (4\text{-}4)$$

$$O_3^{\bullet-} + H^+ \rightleftharpoons HO_3^{\bullet} \quad (4\text{-}5)$$

$$HO_3^{\bullet} \rightarrow {}^{\bullet}OH + O_2 \quad (4\text{-}6)$$

Recently, this mechanism has been modified by assuming that the electron transfer in reaction (4-2) is preceded by adduct formation (reaction 4-7), and the conversion of $O_3^{\bullet-}$ into $^{\bullet}OH$ must proceed via reactions (4-9) and (4-10) rather than by reactions (4-5) and (4-6) (Sein *et al.*, 2007, Merenyi *et al.*, 2010).

$$HO_2^- + O_3 \rightleftharpoons HO_5^- \quad (4\text{-}7)$$

$$HO_5^- \rightarrow HO_2^{\bullet} + O_3^{\bullet-} \quad (4\text{-}8)$$

$$O_3^{\bullet-} \rightleftharpoons O_2 + O^{\bullet-} \quad (4\text{-}9)$$

$$O^{\bullet-} + H_2O \rightleftharpoons {}^{\bullet}OH + OH^- \quad (4\text{-}10)$$

With the formation of an adduct as an intermediate in the rate-determining step (reaction 4-7), it has been discussed (thermokinetic and quantum-chemical considerations (Merenyi *et al.*, 2010)) that the adduct can also decay into OH^- and two molecules of O_2 in their ground state ($^3O_2$), reaction (4-11), in competition to radical formation (reaction 4-8).

$$HO_5^- \rightarrow 2\ ^3O_2 + OH^- \qquad (4\text{-}11)$$

In the following, experimental evidence will be given that the •OH formation efficiency of the peroxone process is only 50 %.

4.3 MATERIAL AND METHODS

Tertiary butanol (Merck), H_2O_2 (30%, Merck), dimethyl sulfoxide (Prolabo), *p*-chlorobenzoic acid (Aldrich), *p*-nitrobenzoic acid (Aldrich), atrazine (Riedel-de Haën) and 2,4-dinitrophenylhydrazine (Merck) were of the highest quality available and used as received. Ozone stock solutions were prepared by generating ozone with the help of an oxygen-fed ozonator (BMT 802X, BMT Messtechnik, Berlin) and passing it through Milli-Q-filtered (Millipore) water. Depending on the desired concentration, Milli-Q-filtered water was ice-cooled, as lower temperatures lead to higher solubility of ozone in water. The ozone concentration of these stock solutions was determined spectrophotometrically using ε(260 nm) = 3300 M^{-1} cm^{-1}. Radiolytic experiments were carried out in a ^{60}Co-γ-source at the IOM at a dose rate of 0.1 Gy s^{-1} as determined by Fricke dosimetry (Fricke and Hart, 1935, Mark *et al.*, 1998).

The destruction of the tracers was followed by HPLC-UV (column: C18RP 250 × 4mm, eluent for atrazine: acetonitrile/water (1:1 v/v) pH 3, for *p*CBA: acetonitrile/water (63:37 v/v) pH 3, for *p*NBA: acetonitrile/water (1:1 v/v) pH 3). The retention times for atrazine, *p*CBA and *p*NBA are under these conditions 12.7, 5.5 and 6.7 minutes, respectively.

Formaldehyde and 2-hydroxy-2-methylpropanal were determined as their 2,4-dinitrophenylhydrazones by HPLC-UV (Lipari and Swarin, 1982). 0.2 mL 2,4-DNPH solution (6 mM in acetonitrile) and 0.1 mL perchloric acid (1 M in acetonitrile) were added to 1.7 mL sample. After standing 45 minutes in the dark, the solutions were measured at a wavelength of 350 nm (column: C18RP 250 × 3 mm, eluent: acetonitrile/water pH 3 60/40 v/v). The retention times for 2,4-DNPH, 2-hydroxy-2-methylpropanal-2,4-DNPH and formaldehyde-2,4-DNPH were 6.6, 8.7 and 11.6 minutes, respectively. Another product is

acetone. It could not be quantified due to contaminations in the lab air but was not required in the context of this study.

The formation of methanesulfinic acid and methanesulfonic acid was measured by ion chromatography (column: Metrosep A Supp 4 – 250/4; eluent: 1.8 mM Na_2CO_3/1.7 mM $NaHCO_3$). Their retention times were 4.6 and 5.1 minutes, respectively.

Experiments were conducted keeping all concentrations constant beside ozone, which was varied between 10 and 400 µM.

4.4 RESULTS AND DISCUSSION

4.4.1 DETERMINATION OF THE ˙OH YIELD BY COMPETITION

The formation of ˙OH can be investigated by a competition of two ˙OH scavengers (Yurkova *et al.*, 1999), and this competition can also be used for a quantification of the ˙OH yield. In the present system, one is restricted to ˙OH scavengers with a low reactivity toward O_3. For a compilation of rate constants relevant to the present study see Table 4-1.

Table 4-1: Compilation of rate constants relevant for the present study

Reaction	Rate constant $M^{-1}\ s^{-1}$	pK_a	Reference
2-methyl-2-propanol (*t*BuOH) + $O_3 \rightarrow$ products	1.3×10^{-3}		(Neta *et al.*, 1988)
2-methyl-2-propanol (*t*BuOH) + ˙OH $\rightarrow$ products	6×10^{8}		(Buxton *et al.*, 1988)
p-chlorobenzoate ion (*p*CBA) + $O_3 \rightarrow$ products	0.15		(Neta *et al.*, 1988)
p-chlorobenzoate ion (*p*CBA) + ˙OH $\rightarrow$ products	5×10^{9}		(Buxton *et al.*, 1988)
p-chlorobenzoic acid (*p*CBA)		3.98	(Weast, 1971-1972)
p-nitrobenzoate ion (*p*NBA) + $O_3 \rightarrow$ products	< 0.15		*
p-nitrobenzoate ion (*p*NBA) + ˙OH $\rightarrow$ products	2.6×10^{9}		(Buxton *et al.*, 1988)
p-nitrobenzoic acid (*p*NBA)		3.41	(Weast, 1971-1972)
atrazine + $O_3 \rightarrow$ products	6.0		(Neta *et al.*, 1988)

atrazine + $^{\bullet}OH \rightarrow$ products	3×10^9		(Buxton *et al.*, 1988)
atrazine		1.71	(Vermeulen *et al.*, 1982)
$e_{aq}^- + N_2O + H_2O \rightarrow {}^{\bullet}OH + N_2 + OH^-$	1.9×10^9		(Buxton *et al.*, 1988)
$e_{aq}^- + H_2O_2 \rightarrow {}^{\bullet}OH + OH^-$	1×10^{10}		(Buxton *et al.*, 1988)
$H^{\bullet} + O_2 \rightarrow HO_2^{\bullet}$	1.2×10^{10}		(Buxton *et al.*, 1988)
$^{\bullet}OH + H_2O_2 \rightarrow H_2O + O_2^{\bullet-}$	2.7×10^7		(Buxton *et al.*, 1988)
$^{\bullet}OH + HO_2^- \rightarrow H_2O + O_2^{\bullet-}$	5.6×10^9		(Buxton, 1969)
dimethyl sulfoxide (DMSO) + $^{\bullet}OH \rightarrow$ products	7×10^9		(Veltwisch *et al.*, 1980)
dimethyl sulfoxide (DMSO) + $O_3 \rightarrow$ products	8.1		(Pryor *et al.*, 1984)

* less reactive than *p*CBA, as $–NO_2$ is more-electron withdrawing than –Cl

As competitors were chosen tertiary butanol (*t*BuOH) and the anion of *p*-chlorobenzoic acid (*p*CBA), the anion of *p*-nitrobenzoic acid (*p*NBA) that is less reactive than *p*CBA, and atrazine. In these competition experiments, *t*BuOH was in large excess (500 µM) over the other component and the decay of the minor partner, *e.g.*, *p*CBA (1 µM), was followed as a function of the O_3 concentration at a constant H_2O_2 concentration (1 mM).

The rate of disappearance of a tracer compound **A** due to a second-order reaction with $^{\bullet}OH$ is given by equation (4-12),

$$d[\mathrm{A}] = \left[{}^{\bullet}\mathrm{OH}\right](k_{\mathrm{A}}[\mathrm{A}])dt \qquad (4\text{-}12)$$

while the rate of disappearance of $^{\bullet}OH$ is caused by three reactants, **A**, **B** and **C**, and given by equation (4-13).

$$d\left[{}^{\bullet}OH\right] = \left[{}^{\bullet}OH\right](k_A[A] + k_B[B] + k_C[C])dt \qquad (4\text{-}13)$$

In this study, **A** is the tracer present at a very low concentration (*p*CBA, *p*NBA and atrazine), **B** and **C** (here *t*BuOH and H_2O_2, respectively) are in large excess over $^{\bullet}OH$, that is, that their concentrations remain practically unchanged. Rearrangement of equation (4-12) and substitution for $[^{\bullet}OH]dt$ in equation (4-13) gives the well-known competition kinetics (equation 4-14).

$$d[A]\frac{k_A[A]+k_B[B]+k_C[C]}{k_A[A]} = d[^{\bullet}OH] \tag{4-14}$$

Since equation (4-14) is already separated in variables, it can directly be integrated within the limits starting concentrations and end concentrations (in theory at infinite time, corresponding to complete consumption of •OH), equation (4-15).

$$\int_{[A]_0}^{[A]_\infty}\left(1+\frac{k_B[B]+k_C[C]}{k_A[A]}\right)d[A] = \int_{[^{\bullet}OH]_0}^{[^{\bullet}OH]_\infty} d[^{\bullet}OH] \tag{4-15}$$

The symbolic integration of equation (4-15) is straightforward (Bronstein *et al.*, 2001) and yields equation (4-16).

$$[A]_0 - [A]_\infty + \frac{k_B[B]+k_C[C]}{k_A} ln\left(\frac{[A]_0}{[A]_\infty}\right) = [^{\bullet}OH]_0 = \Phi_{\bullet OH}[O_3]_0 \tag{4-16}$$

For testing the above approach, •OH radicals with a known concentration were generated by ionizing radiation. In the radiolysis of water, •OH, solvated electrons (e_{aq}^-) and H• are formed as reactive intermediates (reaction 4-17). There are also low yields of the so-called molecular products H_2O_2 and H_2 besides transient H^+ to balance the charge of e_{aq}^- (von Sonntag, 2006).

$$H_2O + \text{ionizing radiation} \rightarrow {}^{\bullet}OH, e_{aq}^-, H^{\bullet}, H_2O_2, H_2, H^+ \tag{4-17}$$

The solvated electron is converted into •OH by saturating the solution with N_2O (reaction 4-18; $k = 1.9 \times 10^9$ M^{-1} s^{-1}) (Buxton *et al.*, 1988) and in some experiments by the addition of H_2O_2 (reaction 4-19; $k = 1 \times 10^{10}$ M^{-1} s^{-1}) (Buxton *et al.*, 1988).

$$e_{aq}^- + N_2O \rightarrow {}^{\bullet}OH + N_2 + OH^- \tag{4-18}$$

$$e_{aq}^- + H_2O_2 \rightarrow {}^{\bullet}OH + OH^- \tag{4-19}$$

In the presence of O_2, H• is converted to $HO_2^{\bullet}/O_2^{\bullet-} + H^+$ (reaction 4-20; $k = 1.2 \times 10^{10}$ M^{-1} s^{-1} (Buxton *et al.*, 1988); $pK_a(HO_2^{\bullet}) = 4.8$ (Bielski *et al.*, 1985)) that would not react with any of the substrates.

$$H^{\bullet} + O_2 \rightarrow HO_2^{\bullet}\ (O_2^{\bullet-} + H^+) \tag{4-20}$$

In γ-irradiated aqueous solution, the effective •OH yield (*G* value) depends somewhat on its •OH scavenging capacity. For the present system, it can be read from a nomogram (von Sonntag,

1987) to be $G = 5.3 \times 10^{-7}$ mol J^{-1}. Based on this G value, the observed and calculated *p*CBA, *p*NBA and atrazine decay as a function of the •OH concentration agrees well (Figure 4-1 A-C, solid squares and corresponding dashed line, respectively). As the radiolytic data (solid squares) fall well on the calculated curve (dashed lines), we conclude that the approach works well and that the •OH rate constants on which the competition is based must be correct.

The same solutions have also been subjected to the peroxone process. Here, the *p*CBA data can only be adequately interpreted if the •OH yield is 56 %. The two further scavengers, atrazine and *p*NBA, were also used. As their •OH rate constants are lower, higher O_3 (•OH) concentrations are required for obtaining the same level of degradation. These data are adequately fitted using the available rate constant by taking •OH yields of 60 % (atrazine) and 49 % (*p*NBA), respectively. In order to compare the results of both systems (peroxone process and γ-radiolysis) the data for each competitor were plotted in one figure. This shows that approximately twice as much ozone is needed to gain the same results as obtained with •OH from γ-radiolysis (Figure 4-1 A-C).

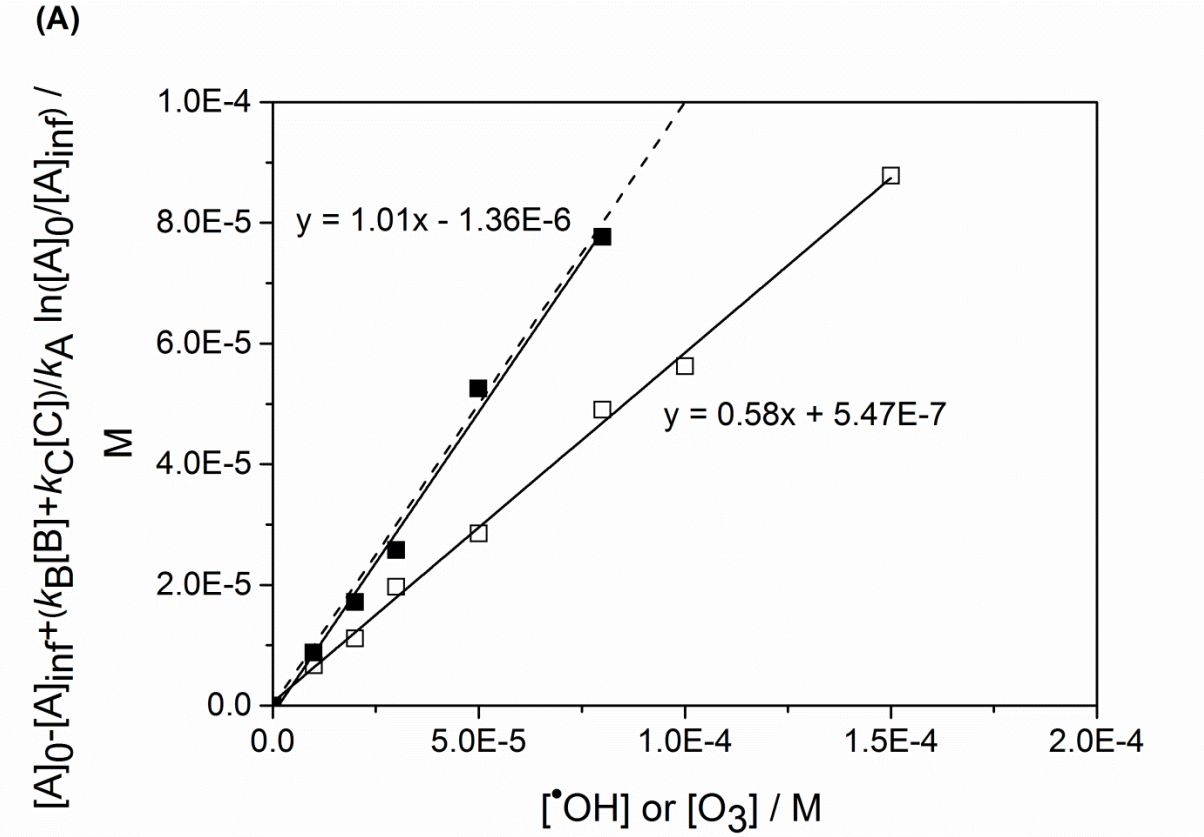

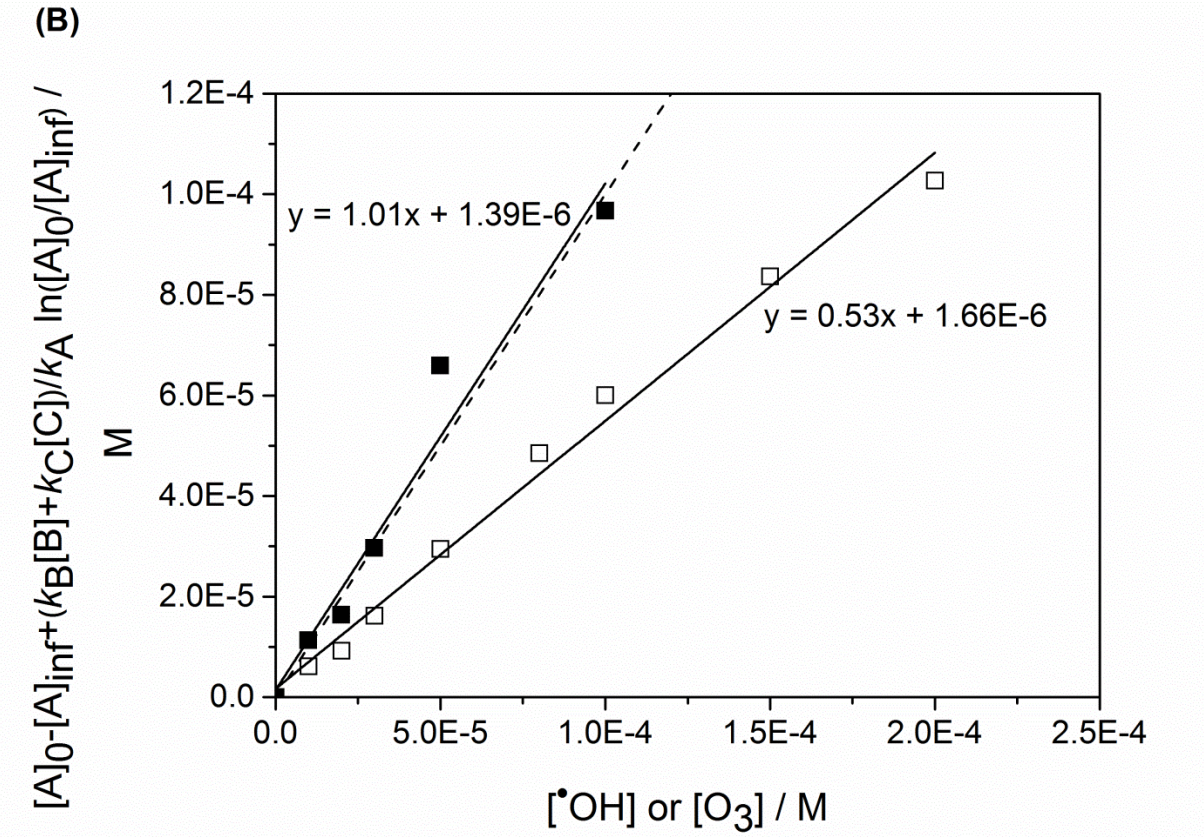
(B)
[A]0-[A]inf+(kB[B]+kC[C])/kA ln([A]0/[A]inf) / M
y = 1.01x + 1.39E-6
y = 0.53x + 1.66E-6
[•OH] or [O3] / M

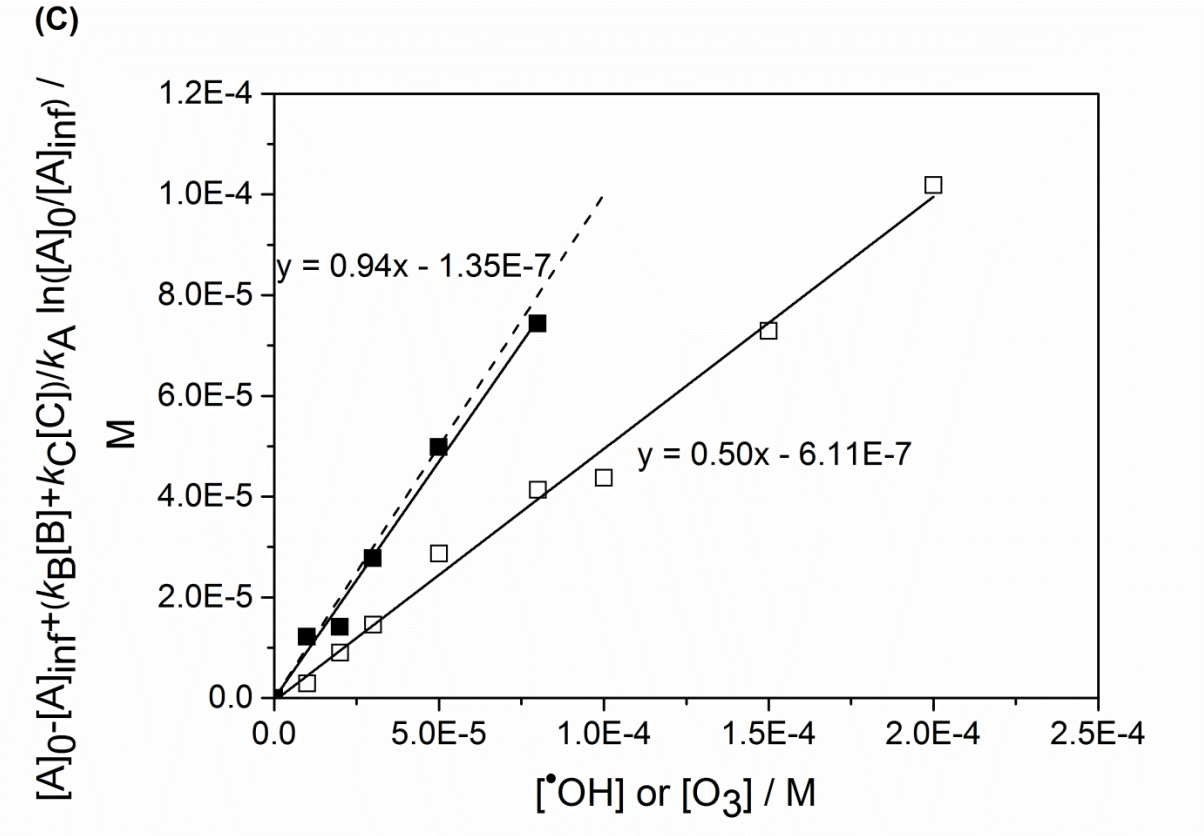
(C)
[A]0-[A]inf+(kB[B]+kC[C])/kA ln([A]0/[A]inf) / M
y = 0.94x - 1.35E-7
y = 0.50x - 6.11E-7
[•OH] or [O3] / M

Figure 4-1: Competition between *t*BuOH (0.5 mM) and the ˙OH scavengers present in trace amount (1 µM): atrazine (A), *p*CBA (B) and *p*NBA (C) for the ˙OH produced in the peroxone process (open squares). Consumption of scavengers is given as a function of the O_3 concentration. The solid squares represent the consumption of the scavengers by ˙OH generated in the γ-radiolysis. It is given as a function of the ˙OH concentration. The dashed lines are calculated on the basis of an unreduced yield (100 %) of ˙OH in the peroxone process, which corresponds to the applied ˙OH concentration in the γ-radiolysis system. The solid lines are fitted to experimental data.

Table 4-2: Relative ˙OH yields calculated point for point by equation 4-16 giving the percentage of the obtained ˙OH yield of the originally assumed.

$[O_3]$	˙OH yields / %		
	*p*CBA	*p*NBA	Atrazine
1.0×10^{-5}	62	-	67
2.0×10^{-5}	46	45	56
3.0×10^{-5}	54	49	66
5.0×10^{-5}	59	57	57
8.0×10^{-5}	61	51	61
1.0×10^{-4}	60	44	56
1.5×10^{-4}	56	49	59
2.0×10^{-4}	51	51	57
Mean	56	49	60
Standard deviation	5.3	4.6	4.3

The rate of decay of *p*CBA, *p*NBA and atrazine is markedly lower than is calculated on the basis of the above concentrations, rate constants and the original assumption that the ˙OH yield per O_3 is unity. The reason for this could be (i) a major uncertainty in the rate constants, (ii) an

uncertainty in the ozone concentration and (iii) a lower than 100 % ˙OH yield in the peroxone process. The rate constants have been determined by pulse radiolysis and are most likely correct within an error of 10 %. The O_3 concentration has been determined spectrophotometrically taking an absorption coefficient of ε(260 nm) = 3300 M^{-1} cm^{-1}. There are other values around 3000 M^{-1} cm^{-1} also in common use. The difference between these two values is only near 10 % and cannot account for the large difference between observed and calculated decay rates. Thus, the most likely reason for this difference is an ˙OH yield of the peroxone process of markedly below 100 %. The ˙OH yields in the peroxone process were calculated relative to the assumed yield by equation (4-16) (Table 4-2). The yields were calculated point for point and hence allow a conclusion without repeating the experiments many times. Their calculated mean values give a representative yield for the peroxone process. Considering that the ˙OH rate constants are flawed with an inherent error of ±10 %, these three data sets agree well and show that the ˙OH yield in the peroxone process must be near 50 %. To corroborate this assumption, further experiments were performed.

4.4.2 Determination of the ˙OH Yield by Product Analysis: *t*BuOH-System

Another experimental approach is to scavenge ˙OH with *t*BuOH and to quantify the *t*BuOH-derived products. The ensuing reactions in the presence of O_2 have been elucidated with the help of radiation techniques (pulse radiolysis and product analysis) (Schuchmann and von Sonntag, 1979). They are depicted in reaction (4-21) – (4-31).

$$\text{˙OH} + (CH_3)_3COH \rightarrow H_2O + \text{˙}CH_2C(CH_3)_2OH \quad (4\text{-}21)$$

$$HOC(CH_3)_2CH_2\text{˙} + O_2 \rightarrow HOC(CH_3)_2CH_2OO\text{˙} \quad (4\text{-}22)$$

$$2\ HOC(CH_3)_2CH_2OO\text{˙} \rightarrow (HOC(CH_3)_2CH_2OO)_2 \quad (4\text{-}23)$$

$$(HOC(CH_3)_2CH_2OO)_2 \rightarrow HOC(CH_3)_2C(O)H + O_2 + HOC(CH_3)_2CH_2OH \quad (4\text{-}24)$$

$$(HOC(CH_3)_2CH_2OO)_2 \rightarrow 2\ HOC(CH_3)_2C(O)H + H_2O_2 \quad (4\text{-}25)$$

$$(HOC(CH_3)_2CH_2OO)_2 \rightarrow 2\ HOC(CH_3)_2CH_2O\text{˙} + O_2 \quad (4\text{-}26)$$

$$HOC(CH_3)_2CH_2O\text{˙} \rightarrow \text{˙}C(CH_3)_2OH + H_2C{=}O \quad (4\text{-}27)$$

$$\text{˙}C(CH_3)_2OH + O_2 \rightarrow \text{˙}OOC(CH_3)_2OH \quad (4\text{-}28)$$

$$^{\bullet}OOC(CH_3)_2OH \rightarrow (CH_3)_2C{=}O + HO_2^{\bullet} \quad (4\text{-}29)$$

$$^{\bullet}OOC(CH_3)_2OH + OH^- \rightarrow (CH_3)_2C{=}O + O_2^{\bullet-} + H_2O \quad (4\text{-}30)$$

$$HOC(CH_3)_2CH_2O^{\bullet} \rightarrow HOC(CH_3)_2{}^{\bullet}CH(OH) \quad (4\text{-}31)$$

The *t*BuOH-derived radical formed in reaction (4-21) reacts with O_2 giving rise to the corresponding peroxyl radical (reaction 4-22). These decay bimolecularly (reaction 4-23). The tetroxide thus formed may decay by various pathways. The Russell-type reaction gives O_2, one molecule of 2-hydroxy-2-methyl-propanal and 2-hydroxy-2-methylpropanol (reaction 4-24). The Bennett-type reaction (4-25) yields two molecules of 2-hydroxy-2-methyl-propanal and H_2O_2. The pathway that has oxyl radicals (reaction 4-26) as intermediates ultimately yields acetone and formaldehyde (reactions 4-27 – 4-30). The 1,2-shift reaction (4-31) seems to be of minor importance compared to the β-fragmentation reaction (4-27).

Since in ozonation processes O_2 is always in excess over O_3, the above peroxyl radical reactions also dominate here, and in the peroxone process the two key products, 2-hydroxy-2-methylpropanal (MHP) and formaldehyde, (Flyunt *et al.*, 2003) were detected. In the present study, the *t*BuOH concentration was 20 mM and the H_2O_2 concentration 1 mM. Under such conditions, H_2O_2 not only serves as an $^{\bullet}OH$ source in the peroxone process but also converts e_{aq}^- into $^{\bullet}OH$ in the radiolytic system (reaction 4-19).

In the following, γ-radiolysis served as a quantitative standard of $^{\bullet}OH$. In principle, the $^{\bullet}OH$ yield can be estimated based on the formaldehyde yield alone ($^{\bullet}OH$ yield is about twice the formaldehyde yield) (Flyunt *et al.*, 2003). In the present study however, it seemed worthwhile to put it on a broader footing. It is of importance that the ratio of the *t*BuOH products must be independent of the $^{\bullet}OH$ source, γ-radiolysis or O_3/H_2O_2. This has been tested for the two aldehydes (formaldehyde and MHP). An authentic standard for 2-hydroxy-2-methylpropanal was not available, but the aldehyde ratio can be determined by measuring the peak areas of the 2,4-dinitrophenylhydrazine derivatives of formaldehyde and 2-hydroxy-2-methylpropanal under these two conditions. It was constant with both increasing applied radiation dose and applied O_3 dose (data not shown), confirming that the chemistries are essentially identical under these two conditions.

In the present study, the *t*BuOH-derived product yields were based on formaldehyde and 2-hydroxy-2-methylpropanal determinations. The combined peak areas of their 2,4-dinitrophenylhydrazine derivatives from the peroxone process and γ-radiolysis are compared in

Figure 4-2. The error of the slope for the radiolysis system is 1.7 and that for the peroxone system 1.0. This indicates the reliability of the systems.

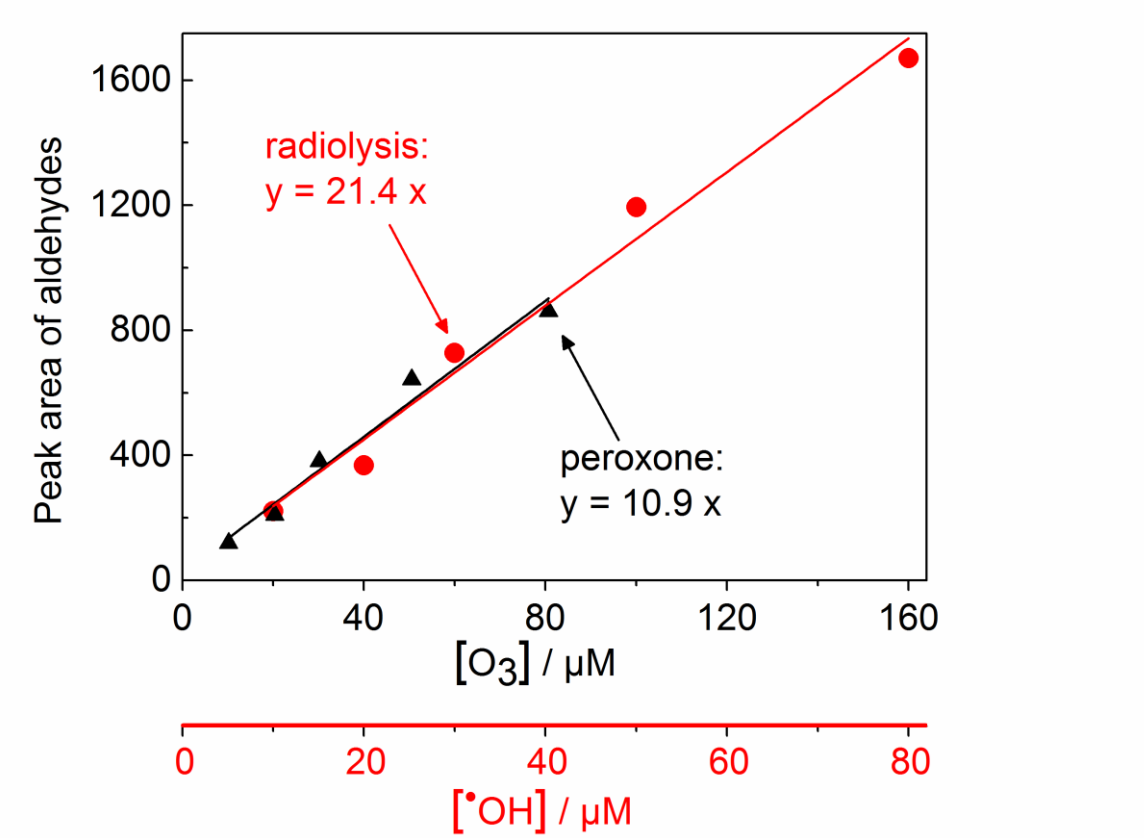

Figure 4-2: Reaction of *t*BuOH (20 mM) with •OH produced in the peroxone process and in γ-radiolysis. The formation of formaldehyde and 2-hydroxy-2-methyl-propanal in sum as a function of the O_3 concentration (upper scale) and •OH concentration (lower scale). The circles represent the aldehydes formed in the reaction of *t*BuOH with •OH produced in γ-radiolysis (lower scale), while the triangles show the aldehyde yield obtained from the reaction of *t*BuOH with •OH produced in the peroxone process (upper scale).

The dose/yield plots are linear (Figure 4-2). The peroxone data fall well on the radiation data, if the ozone x-axis is compressed by a factor of 2, i.e., 80 µM ozone corresponds to 40 µM •OH. That means that twice as much ozone is necessary to obtain the expected concentration of aldehydes as under the assumption that 1 mol ozone yields 1 mol •OH. This is the next evidence that the yield is not unity and the original assumption has to be revised.

4.4.3 DETERMINATION OF THE ˙OH YIELD BY PRODUCT ANALYSIS: DMSO-SYSTEM

A further approach to quantify ˙OH is the reaction of ˙OH with dimethyl sulfoxide (DMSO) (reaction 4-32). Its product methanesulfinic acid is formed in 92 % yield (Veltwisch *et al.*, 1980). The methanesulfinic acid can be further oxidized to methanesulfonic acid by peroxyl radicals (e.g., the peroxyl radical anticipated to from upon reaction of O_2 with the methyl radical generated in reaction (4-32)) (Flyunt *et al.*, 2001). Thus, the sum of both acids represents 92 % of the ˙OH yield. These acids were quantified by ion chromatography.

$$\text{˙OH} + (CH_3)_2S{=}O \rightarrow CH_3S(O)OH + \text{˙}CH_3 \qquad (4\text{-}32)$$

In these experiments DMSO was present in large excess (150 mM) over ozone (0.1 to 0.4 mM) at a constant H_2O_2 concentration (50 mM).The solutions were prepared in 10mM phosphate buffer (KH_2PO_4/Na_2HPO_4) at pH 8 to accelerate the reaction of O_3 with H_2O_2 (at pH 8: k = 870 $^{-1}$ s^{-1}) and avoid the competition with reaction O_3 + DMSO (k = 8.1 M^{-1} s^{-1}). Even if the concentrations of H_2O_2 and DMSO are taken into account the reaction of H_2O_2 with O_3 is still favored (k_{app} (H_2O_2 + O_3) = 43s^{-1}; k_{app} (DMSO + O_3) = 1.2 s^{-1}). The ˙OH yield is plotted against the ozone concentration and the resulting graph has a slope of 0.495 with an error of 0.017, which shows that the ˙OH yield in the peroxone process measured with the DMSO system is round 50 % of ozone consumed (Figure 4-3). This further confirms the results mentioned above.

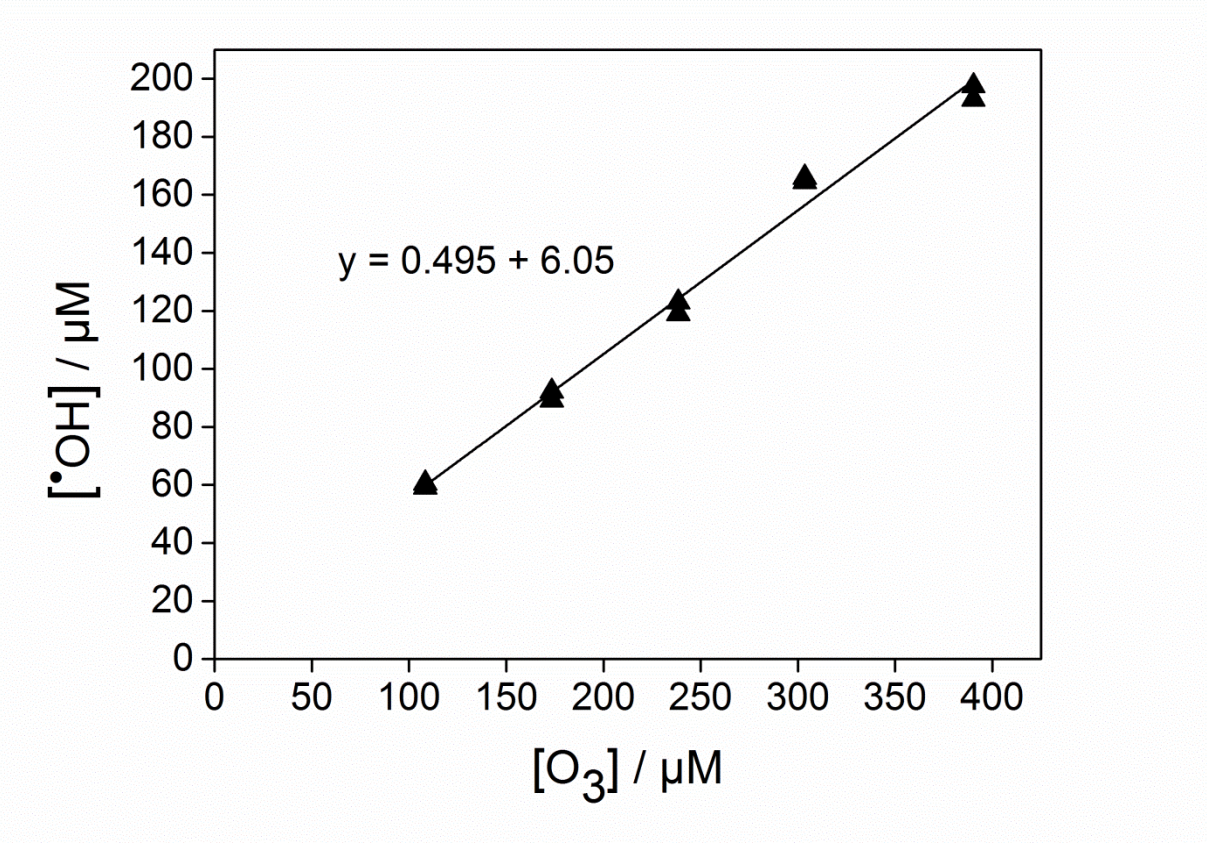

Figure 4-3: Reaction of DMSO (150 mM) with •OH produced in the peroxone process. •OH yield calculated from measured concentrations of methanesulfinic acid and methanesulfonic acid as a function of the O_3 concentration.

4.4.4 PRACTICAL IMPLICATIONS

The present paper shows that the •OH yield of the peroxone process is only around 0.5. It has to be taken into account that in real water matrix not only the reaction of O_3 with H_2O_2 leads to •OH generation. In addition •OH are generated in the reaction of ozone with dissolved organic matter (DOM) (Noethe *et al.*, 2009). Especially in wastewater (high DOM content) •OH formation from ozone is most effective and the benefit of H_2O_2 addition is negligible (Pocostales *et al.*, 2010). Therefore, the peroxone process is not used for wastewater treatment but in drinking water production. There it is not only applied for the •OH production, but also for the reduction of HOBr/OBr^-, a critical key intermediate in the bromate formation (von Gunten and Oliveras, 1997). Therefore, it is not easy to give a general statement about the effect of these findings for practical implication, but it has to be taken into account when using the peroxone process as an AOP for remediation or assessing its contribution to micropollutant elimination in water treatment. Consequently, the cost of this process could be much higher for some applications than hitherto assumed.

4.5 REFERENCES

Bielski, B. H. J., Cabelli, D. E., Arudi, R. L. and Ross, A. B. (1985). Reactivity of HO_2/O_2^- radicals in aqueous solution. Journal of Physical and Chemical Reference Data, **14**(4), 1041-1100.

Bolton, J. R., Bircher, K. G., Tumas, W. and Tolman, C. A. (2001). Figures-of-merit for the technical development and application of advanced oxidation technologies for both electric- and solar-driven systems - (IUPAC technical report). Pure and Applied Chemistry, **73**(4), 627-637.

Bronstein, I. N., Semendjajew, K. A., Musiol, G. and Mühlig, H. (2001). Taschenbuch der Mathematik. Harri Deutsch, Frankfurt am Main.

Buxton, G. V. (1969). Pulse radiolysis of aqueous solutions. Some rates of reaction of OH and O^- and pH dependence of the yield of O_3^-. Transactions of the Faraday Society, **65**(560P), 2150-2158.

Buxton, G. V., Greenstock, C. L., Helman, W. P. and Ross, A. B. (1988). Critical review of rate constants for reactions of hydrated electrons, hydrogen atoms and hydroxyl radicals ($\cdot OH/\cdot O^-$) in aqueous solution. Journal of Physical and Chemical Reference Data, **17**(2), 513-886.

Flyunt, R., Leitzke, A., Mark, G., Mvula, E., Reisz, E., Schick, R. and von Sonntag, C. (2003). Determination of $\cdot OH$, $O_2^{-\cdot}$, and hydroperoxide yields in ozone reactions in aqueous solution. Journal of Physical Chemistry B, **107**(30), 7242-7253.

Flyunt, R., Makogon, O., Schuchmann, M. N., Asmus, K. D. and von Sonntag, C. (2001). OH-radical-induced oxidation of methanesulfinic acid. The reactions of the methanesulfonyl radical in the absence and presence of dioxygen. Journal of the Chemical Society, Perkin Transactions 2(5), 787-792.

Fricke, H. and Hart, E. J. (1935). The oxidation of Fe^{++} to Fe^{+++} by the irradiation with X-rays of solutions of ferrous sulfate in sulfuric acid. Journal of Chemical Physics, **3**(1), 60-61.

Hug, S. J. and Leupin, O. (2003). Iron-catalyzed oxidation of arsenic(III) by oxygen and by hydrogen peroxide: pH-dependent formation of oxidants in the fenton reaction. Environmental Science & Technology, **37**(12), 2734-2742.

Legrini, O., Oliveros, E. and Braun, A. M. (1993). Photochemical processes for water treatment. Chemical Reviews, **93**(2), 671-698.

Lipari, F. and Swarin, S. J. (1982). Determination of formaldehyde and other aldehydes in automobile exhaust with an improved 2,4-dinitrophenylhydrazine method. Journal of Chromatography, **247**(2), 297-306.

Mark, G., Tauber, A., Rudiger, L. A., Schuchmann, H. P., Schulz, D., Mues, A. and von Sonntag, C. (1998). OH-radical formation by ultrasound in aqueous solution - part II: terephthalate and Fricke dosimetry and the influence of various conditions on the sonolytic yield. Ultrasonics Sonochemistry, **5**(2), 41-52.

Merenyi, G., Lind, J., Naumov, S. and von Sonntag, C. (2010). Reaction of ozone with hydrogen peroxide (peroxone process): a revision of current mechanistic concepts based on thermokinetic and quantum-chemical considerations. Environmental Science & Technology, **44**(9), 3505-3507.

Müller, J. P., Gottschalk, C. and Jekel, M. (2001). Comparison of advanced oxidation processes in flow-through pilot plants (part II). Water Science and Technology, **44**(5), 311-315.

Neta, P., Huie, R. E. and Ross, A. B. (1988). Rate constants for reactions of inorganic radicals in aqueous solution. Journal of Physical and Chemical Reference Data, **17**(3), 1027-1284.

Noethe, T., Fahlenkamp, H. and von Sonntag, C. (2009). Ozonation of wastewater: rate of ozone consumption and hydroxyl radical yield. Environmental Science & Technology, **43**(15), 5990-5995.

Pignatello, J. J., Oliveros, E. and MacKay, A. (2006). Advanced oxidation processes for organic contaminant destruction based on the Fenton reaction and related chemistry. Critical Reviews in Environmental Science and Technology, **36**(1), 1-84.

Pocostales, J. P., Sein, M. M., Knolle, W., von Sonntag, C. and Schmidt, T. C. (2010). Degradation of ozone-refractory organic phosphates in wastewater by ozone and ozone/hydrogen peroxide (peroxone): the role of ozone consumption by dissolved organic matter. Environmental Science & Technology, **44**(21), 8248-8253.

Pryor, W. A., Giamalva, D. H. and Church, D. F. (1984). Kinetics of ozonation. 2. amino acids and model compounds in water and comparisons to rates in nonpolar solvents. Journal of the American Chemical Society, **106**(23), 7094-7100.

Reisz, E., Schmidt, W., Schuchmann, H. P. and von Sonntag, C. (2003). Photolysis of ozone in aqueous solutions in the presence of tertiary butanol. Environmental Science & Technology, **37**(9), 1941-1948.

Rosenfeldt, E. J., Linden, K. G., Canonica, S. and von Gunten, U. (2006). Comparison of the efficiency of OH radical formation during ozonation and the advanced oxidation processes O_3/H_2O_2 and UV/H_2O_2. Water Research, **40**(20), 3695-3704.

Schuchmann, M. N. and von Sonntag, C. (1979). Hydroxyl radical-induced oxidation of 2-methyl-2-propanol in oxygenated aqueous solution. A product and pulse radiolysis study. Journal of Physical Chemistry, **83**(7), 780-784.

Sein, M. M., Golloch, A., Schmidt, T. C. and von Sonntag, C. (2007). No marked kinetic isotope effect in the peroxone ($H_2O_2/D_2O_2+O_3$) reaction: mechanistic consequences. Chemphyschem, **8**(14), 2065-2067.

Staehelin, J. and Hoigné, J. (1982). Decomposition of ozone in water: rate of initiation by hydroxide ions and hydrogen peroxide. Environmental Science & Technology, **16**(10), 676-681.

Veltwisch, D., Janata, E. and Asmus, K. D. (1980). Primary processes in the reaction of OH-radicals with sulphoxides. Journal of the Chemical Society-Perkin Transactions 2(1), 146-153.

Vermeulen, N. M. J., Apostolides, Z., Potgieter, D. J. J., Nel, P. C. and Smit, N. S. H. (1982). Separation of atrazine and some of its degradation products by high-performance liquid chromatography. Journal of Chromatography, **240**(1), 247-253.

von Gunten, U. and Oliveras, Y. (1997). Kinetics of the reaction between hydrogen peroxide and hypobromous acid: implication on water treatment and natural systems. Water Research, **31**(4), 900-906.

von Sonntag, C. (1987). The chemical basis of radiation biology. Taylor & Francis, London.

von Sonntag, C. (2006). Free-radical-induced DNA damage and its repair: a chemical perspective. Springer Verlag, Berlin, Heidelberg.

von Sonntag, C. (2008). Advanced oxidation processes: mechanistic aspects. Water Science and Technology, **58**(5), 1015-1021.

von Sonntag, C., Mark, G., Tauber, A. and Schuchmann, H. P. (1999). OH radical formation and dosimetry in the sonolysis of aqueous solutions. In: Advances in Sonochemistry. T. J. Mason (ed.), 5, pp. 109-145.

Weast, R. C., Ed. (1971-1972). Handbook of chemistry and physics. Ohio, The Chemical Rubber Co.

Yurkova, I. L., Schuchmann, H. P. and Von Sonntag, C. (1999). Production of OH radicals in the autoxidation of the Fe(II)-EDTA system. Journal of the Chemical Society. Perkin Transactions 2(10), 2049-2052.

Chapter 5

HYDROXYL RADICAL FORMATION IN THE REACTION OF BROMIDE WITH OZONE

Redrafted from " Fischbacher, A.; Löppenberg, K.; von Sonntag, C.; Schmidt, T. C., A New Reaction Pathway for Bromite to Bromate in the Ozonation of Bromide. *Environ. Sci. Technol.*, **2015**, *49* (19), pp 11714–11720.", DOI: 10.1021/acs.est.5b02634,

5.1 ABSTRACT

Ozone is often used in drinking water treatment. This may cause problems if the water to be treated contains bromide, as its reaction with ozone leads to the formation of bromate, which is considered to be carcinogenic. Bromate formation is a multistep process resulting from the reaction of ozone with bromite. Although this process seemed to be established, it has been shown that ozone reacts with bromite not by the previously assumed mechanism via O-transfer but via electron-transfer. Besides bromate, the electron transfer reaction also yields $O_3^{\bullet-}$, the precursor of OH radicals. The experiments were setup in such a way that OH radicals are not produced from ozone self-decomposition but solely by the electron-transfer reaction. This study shows that hydroxyl radicals are indeed generated by using *t*BuOH as the OH radical scavenger and measuring its product, formaldehyde. HOBr and bromate yields were measured in systems with and without *t*BuOH. As OH radicals contribute to bromate formation, higher bromate and HOBr yields were observed in the absence of *t*BuOH than in its presence, where all OH radicals are scavenged. Based on the results presented here, a pathway from bromide to bromate, revised in the last step, was suggested.

5.2 INTRODUCTION

Ozone is often used for disinfection and oxidation purposes and has a wide application in drinking water treatment. However, its use in water treatment may cause problems when the water to be treated contain bromide at concentrations higher than 50 µg/L (von Gunten, 2003), as the reaction of ozone with bromide leads to bromate formation. Bromide concentrations in natural waters usually range between 4 and 1000 µg/L (in some cases, e.g., oceans even more) (von Gunten and Hoigne, 1992) and thus the critical value for bromide of 50 µg/L is environmentally relevant. Therefore, the bromide concentration must be controlled before applying an ozone-based treatment step. Bromate is considered a potential carcinogen, with a threshold limit value in drinking water of 10 µg/L in the United States and Europe (U.S.EPA, 1994, Council-Directive-98/83/EC, 1998). Therefore, it is of great interest to elucidate the mechanism of bromate formation in drinking water treatment. The low drinking water standard may not be justified anymore, as preliminary experiments conducted in real and synthetic gastric juices predict a short lifetime for bromate in human stomach (Keith et al., 2006b, Keith et al., 2006a, Cotruvo et al., 2010). It was shown that at H^+, Cl^- and H_2S concentrations typically found in gastric juices, 99 % of bromate is reduced within its retention time of 20 - 30 minutes in the stomach. However, as long as the low drinking water standard is still present, bromate is

one of the most relevant by-products formed in ozone-based processes. Furthermore, once formed, it is neither biodegradable nor removable by conventional treatment.

Bromate formation is a multistep process that has been so far described in reactions (5-1) – (5-4) (Haag and Hoigné, 1983).

$$Br^- + O_3 \rightarrow BrO^- + O_2 \qquad k = 160\ M^{-1}\ s^{-1} \qquad (5\text{-}1)$$

$$BrO^- + O_3 \rightarrow BrO_2^- + O_2 \qquad k = 100\ M^{-1}\ s^{-1} \qquad (5\text{-}2)$$

$$BrO^- + O_3 \rightarrow Br^- + 2\ O_2 \qquad k = 330\ M^{-1}\ s^{-1} \qquad (5\text{-}3)$$

$$BrO_2^- + O_3 \rightarrow BrO_3^- + O_2 \qquad k > 1 \times 10^5\ M^{-1}\ s^{-1} \qquad (5\text{-}4)$$

This mechanistic concept has been studied in detail and seems to be well established. However, it has been suggested that bromite reacts with ozone by electron transfer (reaction 5-5) (Nicoson *et al.*, 2002) and not by O-transfer (reaction 5-4), as previously assumed. The authors investigated the reaction of bromite with ozone and postulated that electron-transfer provides a lower kinetic barrier than the breakage of the O–O bond, and, therefore, the reaction (5-4) is unlikely to proceed despite comparable reaction rate constants. The authors provided experimental evidence for the electron-transfer reaction by measuring the intermediate $BrO_2^{\bullet}$ (reaction 5-5). However, a further experimental or theoretical corroboration is missing.

$$BrO_2^- + O_3 \rightarrow BrO_2^{\bullet} + O_3^{\bullet -} \qquad k = 8.9 \times 10^4\ M^{-1}\ s^{-1} \qquad (5\text{-}5)$$

The electron transfer (reaction 5-5) yields $BrO_2^{\bullet}$ and $O_3^{\bullet -}$, the precursor of $^{\bullet}OH$ (overall, eq (5-6); for details see Merenyi *et al.* (2010)).

$$O_3^{\bullet -} + H_2O \rightarrow {}^{\bullet}OH + O_2 + OH^- \qquad (5\text{-}6)$$

$BrO_2^{\bullet}$ disproportionates into bromite and bromate (reactions 5-7a and 5-7b) (Buxton and Dainton, 1968, Naumov and von Sonntag, 2011).

$$2\ BrO_2^{\bullet} \rightleftharpoons Br_2O_4 \qquad k = 1.4 \times 10^9\ M^{-1}\ s^{-1} \qquad (5\text{-}7a)$$

$$Br_2O_4 + OH^- \rightarrow BrO_2^- + BrO_3^- + H^+ \qquad k = 7 \times 10^8\ M^{-1}\ s^{-1} \qquad (5\text{-}7b)$$

In the ozone-based reaction pathway from bromide to bromate, $^{\bullet}OH$ can also act as an oxidation agent and contribute to bromate formation (von Gunten and Hoigné, 1994). In a cascade of reactions (5-8) – (5-12) bromide reacts with $^{\bullet}OH$, yielding relevant intermediates (e.g., HOBr) that can further react with ozone or $^{\bullet}OH$, giving bromate (reactions 5-13 – 5-16, 5-7a, and 5-

7b) (see (Zehavi and Rabani, 1972) for reactions (5-8) – (5-10), (Matheson *et al.*, 1966) for reaction (5-11), (Klaning and Wolff, 1985) for reaction (5-13), and (Buxton and Dainton, 1968) for reaction (5-14) – (5-16)).

$$Br^- + {}^\bullet OH \rightleftharpoons BrOH^{\bullet -} \qquad k = 1.06 \times 10^{10}\ M^{-1}\ s^{-1} \qquad (5\text{-}8)$$

$$BrOH^{\bullet -} + H^+ \rightleftharpoons Br^\bullet + H_2O \qquad k = 4.4 \times 10^{10}\ M^{-1}\ s^{-1} \qquad (5\text{-}9)$$

$$Br^\bullet + Br^- \rightarrow Br_2^{\bullet -} \qquad k \simeq 10^{10}\ M^{-1}\ s^{-1} \qquad (5\text{-}10)$$

$$Br_2^{\bullet -} + Br_2^{\bullet -} \rightarrow Br^- + Br_3^- \qquad k = 1.8 \times 10^{9}\ M^{-1}\ s^{-1} \qquad (5\text{-}11)$$

$$Br_3^- + H_2O \rightarrow HOBr + 2\ Br^- + H^+ \qquad (5\text{-}12)$$

$$HOBr + {}^\bullet OH \rightarrow BrO^\bullet + H_2O \qquad k = 2 \times 10^{9}\ M^{-1}\ s^{-1} \qquad (5\text{-}13)$$

$$OBr^- + {}^\bullet OH \rightarrow BrO^\bullet + OH^- \qquad k = 4.5 \times 10^{9}\ M^{-1}\ s^{-1} \qquad (5\text{-}14)$$

$$2\ BrO^\bullet + H_2O \rightarrow OBr^- + BrO_2^- + 2\ H^+ \qquad k = 4.9 \pm 1.0 \times 10^{9}\ M^{-1}\ s^{-1} \qquad (5\text{-}15)$$

$$BrO_2^- + {}^\bullet OH \rightarrow BrO_2^\bullet + OH^- \qquad k = 1.8 \times 10^{9}\ M^{-1}\ s^{-1} \qquad (5\text{-}16)$$

The impact of $^\bullet OH$ on the bromate formation is negligible if H_2O_2 is present (von Gunten and Oliveras, 1998). As H_2O_2 is always in large excess over $^\bullet OH$, the formed HOBr is not oxidized further but reduced to bromide (reaction 5-17) (von Gunten and Oliveras, 1997), outcompeting the further oxidation.

$$HOBr + HO_2^- \rightarrow Br^- + H_2O + O_2 \qquad k = 7.6 \times 10^{8}\ M^{-1}\ s^{-1} \qquad (5\text{-}17)$$

As $^\bullet OH$ contribute to bromate formation, an indication for $^\bullet OH$ being formed in the system could be the comparison of the bromate formation with and without a suitable $^\bullet OH$ scavenger. If $^\bullet OH$ are present, the bromate yield should be higher than in systems without $^\bullet OH$. The same would apply to HOBr formation. Due to the fast reaction of bromide with $^\bullet OH$, higher HOBr concentrations should be found in the absence of an $^\bullet OH$ scavenger. A prerequisite for formation of $^\bullet OH$ is the intermediate ozonide radical anion ($O_3^{\bullet -}$). If the experimental conditions are chosen in a way that no ozone self-decomposition occurs, $O_3^{\bullet -}$ is only generated in pure water if reaction (5-5) occurs.

Ozone self-decomposition in water is initiated by the reaction of ozone with hydroxide ions (reaction 5-18). Therefore, it is strongly pH-dependent. At pH 6.5, the second-order rate

constant for ozone decomposition in water is 2.42 M^{-1} s^{-1}, while the second order rate constant for the reaction of bromide with ozone is 160 M^{-1} s^{-1}. When ozone decomposes, $^{\bullet}OH$ are generated (reactions 5-18 – 5-21). The ozone concentration was chosen not to be higher than the bromide concentration, so no ozone is present in excess. The fraction of ozone self-decomposition was calculated for the worst-case scenario, in which the ozone concentration was equal to the bromide concentration and was only around 1.5 %. If reactions of ozone with other bromine species are considered (alongside bromide), the fraction would be even smaller. Therefore, self-decomposition of ozone can be excluded as an $^{\bullet}OH$ source in the present study (Ershov and Morozov, 2009).

$$O_3 + OH^- \rightarrow HO_2^- + O_2 \quad (5\text{-}18)$$

$$O_3 + HO_2^- \rightarrow O_2^{\bullet-} + {}^{\bullet}OH + O_2 \quad (5\text{-}19)$$

$$O_3 + O_2^{\bullet-} \rightarrow O_3^{\bullet-} + {}^{\bullet}O_2 \quad (5\text{-}20)$$

$$O_3^{\bullet-} + H_2O \rightarrow {}^{\bullet}OH + O_2 + OH^- \quad (5\text{-}21)$$

Even though the electron-transfer reaction was suggested about a decade ago based on UV-Vis spectroscopic observation of $BrO_2^{\bullet}$, in the context of water treatment, the previously established concept of the O-transfer reaction in the last step of the pathway is still prevalent (Antoniou and Andersen, 2012, Han *et al.*, 2014). It is the intention of the present paper to determine the $^{\bullet}OH$ yield and based on these data, to provide further evidence of electron transfer occurring in the oxidation of bromite on route to bromate formation. This seems essential to establishing a correct mechanistic concept for bromate formation and has consequently already been picked up in the recent textbook by von Sonntag and von Gunten (2012) that, however, does not provide any experimental details.

5.3 MATERIAL AND METHODS

Ozone stock solutions (0.9 mM) were prepared by generating ozone with an oxygen-fed ozonator (BMT 802X, BMT Messtechnik, Berlin) and passing it through ice-cooled (4 °C) ultra pure water (Purelab Ultra, Elga LabWater, Celle). The ozone concentration of these stock solutions was determined spectrophotometrically using $\varepsilon(260\ nm) = 3300\ M^{-1}\ cm^{-1}$ (Hart *et al.*, 1983).

5.3.1 ˙OH QUANTIFICATION

Hydroxyl radicals (˙OH) are highly reactive and, therefore, short-lived, so they cannot be quantified by direct measurement. As direct measurement of ˙OH is difficult an appropriate indirect method must be selected. The indirect quantification is performed by scavenging ˙OH by a suitable probe compound and determining the formed products. Such a probe compound must react rapidly with ˙OH and barely with other substances present in the sample solution. Furthermore, the yield of the products from this reaction must be known so that the ˙OH yield can be derived from these results. In the present system, *t*BuOH was selected as a scavenger, as it complies with the requirements. It reacts readily with ˙OH ($k = 6 \times 10^8$ M^{-1} s^{-1}) (Buxton *et al.*, 1988) but barely with ozone ($k \approx 3 \times 10^{-3}$ M^{-1} s^{-1}) (Hoigne and Bader, 1983). In all experiments, the concentrations of *t*BuOH (180 mM) and bromide (0.6 mM) were kept constant, while ozone concentration was varied (0.15 - 0.6 mM). The *t*BuOH concentration was chosen to be 200 times higher than that of bromide for assuring that 99 % of the formed ˙OH are scavenged by *t*BuOH and do not react with any intermediates present in the solution (the calculation of the ˙OH fraction reacting with *t*BuOH is shown in the Supporting Information). As nearly all ˙OH react with *t*BuOH their quantification is possible. One of the main products of the reaction of ˙OH with *t*BuOH is formaldehyde, which can be determined after derivatization as its 2,4-dinitrophenylhydrazone by a high-performance liquid chromatographic system equipped with an UV detector (HPLC-UV) at $\lambda = 350$ nm (Lipari and Swarin, 1982). For the derivatization, 0.1 mL of perchloric acid (1 M in acetonitrile) and 0.2 mL of 2,4-DNPH solution (6 mM in acetonitrile) were added to 1.7 mL of the sample. After standing for 45 min in the dark, the solutions were measured by HPLC-UV (Agilent 1100, *Agilent Technologies*, Santa Clara, CA; column: NUCLEODUR 5 µm C18 ec 250 x 3 mm (Macherey-Nagel), eluent: gradient acetonitrile/water pH 3 within 20 minutes from 45 to 80 % acetonitrile at 0.5 mL/min). The retention times for 2,4-DNPH and derivatized formaldehyde were 5.5 and 9.3 minutes, respectively. The quantification was performed using formaldehyde standards derivatized in the same way as the samples. To control whether DNPH was contaminated with formaldehyde, blank samples were measured containing perchloric acid, DNPH solution and deionized water. The contamination of the DNPH solution was negligible. As the samples were always in the same concentration range as the standards, the impact of an incomplete derivatization can also be neglected.

As an alternative probe compound methanol was tested, as it has been applied as ˙OH scavenger in ozone-based systems (Liu *et al.*, 2015). It reacts fast with ˙OH ($k = 9.7 \times 10^8$ M^{-1} s^{-1}) (Buxton

et al., 1988) and barely with ozone ($k \approx 2 \times 10^{-2}\ M^{-1}\ s^{-1}$) (Hoigne and Bader, 1983). To obtain formaldehyde as the main product, HPO_4^{2-} and/or OH^- are required as the reaction is base-catalyzed (reactions 28 – 31) (Goldstein *et al.*, 2007). Therefore, all experiments were conducted in 2 mM $H_2PO_4^-/HPO_4^{2-}$ buffered water (pH 7 and 8). The concentration of methanol (470 mM) and bromide (0.6 mM) were kept constant, while ozone was varied between 0.15 and 0.6 mM. The fraction of $^{\bullet}OH$ reacting with methanol is calculated to be 99 % in the given system (the calculation of the $^{\bullet}OH$ fraction reacting with methanol is shown in the Supporting Information). Formaldehyde, the product of this reaction, was determined as described above.

5.3.2 Quantification of Bromate and HOBr

Bromate was determined by ion chromatography (883 Basic IC Plus, Metrohm, Filderstadt) using a Metrosep A Supp 4 – 250/4 column and an eluent consisting of 0.17 mM $NaHCO_3$ and 0.18 mM Na_2CO_3 at 1 mL/min. Retention times for bromate and bromide were 12 and 19.3 min, respectively.

HOBr stock solution was prepared from a 1 mM pH 4 buffered ozone solution (100 mM phosphate buffer) by the addition of 0.8 mM potassium bromide solution (Pinkernell *et al.*, 2000). This solution was stored for 24 h in the dark, and residual ozone was removed by purging the solution with nitrogen gas for 15 min. The first prepared HOBr solution was standardized iodometrically and by direct photometric determination of hypobromite at 329 nm (ε = 332 L mol^{-1} cm^{-1}) after adjusting the pH to 11 by sodium hydroxide (Troy and Margerum, 1991). Both methods gave consistent results and further standardization of HOBr solutions was only done photometrically before every use.

A photometric determination of HOBr formed in the samples was not possible due to other possible constituents of the samples, which might absorb light in the same range. Therefore, HOBr formed in the samples was determined by measuring its derivatization products with phenol, which yields 2- and 4-bromophenol (Tee *et al.*, 1989, Acero *et al.*, 2005). The pH for derivatization was varied from 2 to 5.

Calibration for 2- and 4-bromophenol was prepared from purchased ≥98 % pure 2- and 4-bromophenol, respectively. To investigate the reaction of HOBr with phenol and determine the bromophenol yield per HOBr, standards with defined HOBr concentrations were prepared from the produced HOBr stock solution. These solutions were buffered at pH 4 (100 mM phosphate buffer). 15 µL of phenol (0.5 M) was added to 1 mL of the buffered standards. After 2 h (once the reaction was completed), the solutions were measured by HPLC-UV.

2- and 4-bromophenol were determined using HPLC-UV at a wavelength of 271 nm and a flow rate of 0.4 mL min^{-1} (column: NUCLEODUR 5 µm C18 ec 250 x 3 mm (Macherey-Nagel) eluent: gradient acetonitrile/water within 18 min from 30 to 70 % acetonitrile). The retention times for phenol, 2- and 4-bromophenol were 9.2, 14.1, and 15.2 min, respectively.

5.4 RESULTS AND DISCUSSION

5.4.1 •OH QUANTIFICATION BY *t*BUOH

The reaction of *t*BuOH with •OH initiates a radical chain reaction (Schuchmann and von Sonntag, 1979). In the presence of O_2, a cascade of reactions leads to stable products. One of these products that can be easily quantified is formaldehyde (Schuchmann and von Sonntag, 1979, Flyunt *et al.*, 2003). Since in ozonation processes O_2 is always present in excess over O_3 (due to the generation of O_3 from O_2), the reactions yielding formaldehyde dominate here.

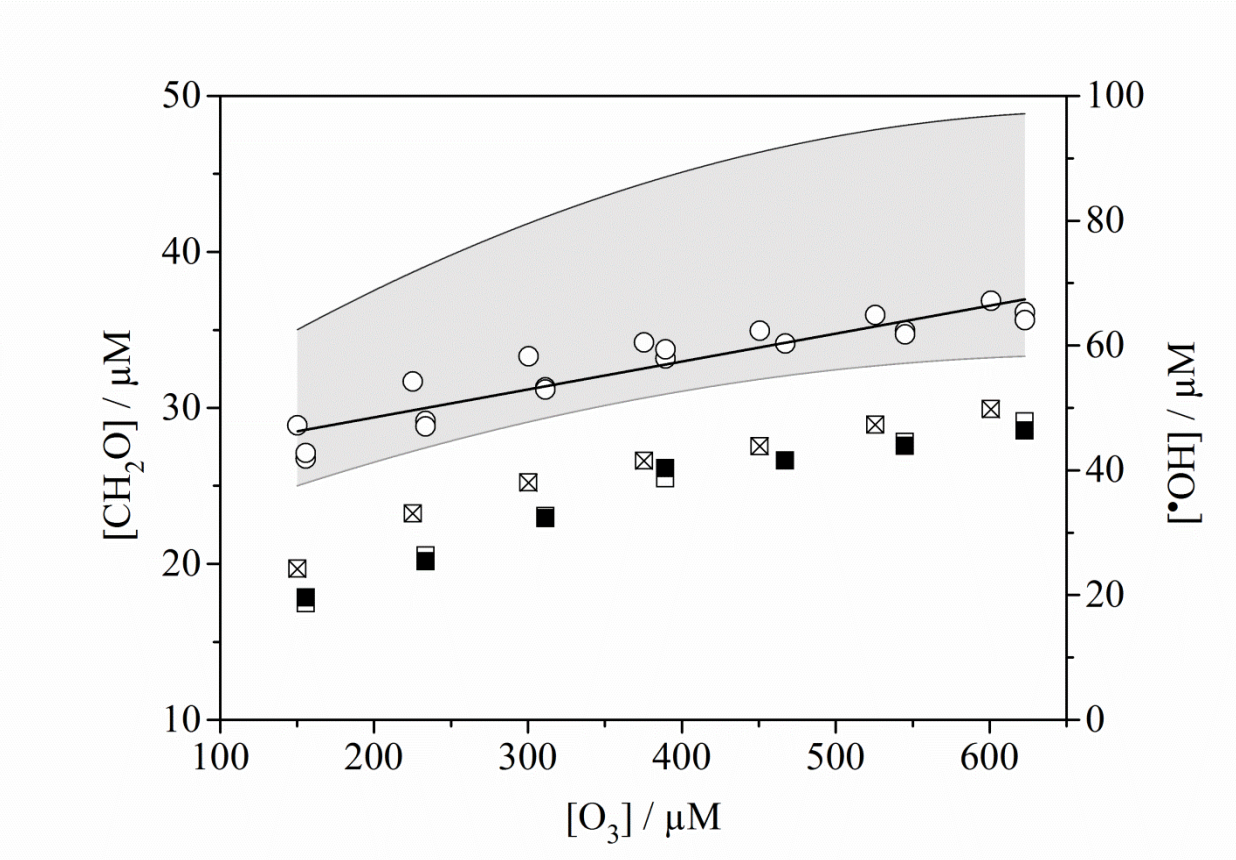

Figure 5-1: Formation of formaldehyde (⊠, ■ and □ correspond to 3 independent experiments and cannot be shown as mean values as the ozone concentrations differ slightly) in the reaction of •OH and *t*BuOH (left y-axis). •OH are generated in the reaction of ozone with bromite. The shaded area represents the possible range of •OH yield (right y-axis). The upper limit

corresponds to the highest possible yield if the •OH yield is 3.3 times the formaldehyde yield. The lower limit corresponds to the lowest possible •OH yield if the •OH yield is twice of the formaldehyde yield. Circles and the linear trend line correspond to the possible calculated •OH yields using a correction factor of 2.29±0.06 (for details, see the text).

The results obtained from the *t*BuOH /•OH system show that •OH were formed (Figure 5-1) as indicated by reaction (5-6). As the formation of bromate from bromide occurs not via one step (reactions 5-1 – 5-5), the yields are not linear. The formaldehyde yield always depends on the system generating •OH, as superoxide ($O_2^{\bullet-}$) is formed in the sequence of reactions of *t*BuOH with •OH (Flyunt *et al.*, 2003). It reacts fast with ozone, giving rise to additional •OH (reaction 5-22) that contribute to higher formaldehyde yields. This additional formaldehyde source has to be taken into account when calculating the •OH yield. The formaldehyde yield is about 30±4 % of •OH (•OH yield is 3.3 times the formaldehyde yield), if no ozone is present. In the presence of ozone, it is estimated to be around 50 % (•OH yield is 2 times the formaldehyde yield) (Flyunt *et al.*, 2003). If the yield is not corrected, it leads to overestimation of •OH yields. In this system, the •OH yield is just an approximate value, as $O_2^{\bullet-}$ reacts not only with ozone but also with other species present in the sample (reactions 5-22 – 5-27). HOBr must be the most relevant bromine species reacting with $O_2^{\bullet-}$ due to its high concentration in the sample and its fast reaction rate with $O_2^{\bullet-}$. As the pH of the solution is 6.5 and the pK_a of HOBr is 8.69 (Weast, 1971-1972), the slower reaction with OBr^- can be neglected, as under these conditions HOBr (99%) is present in excess over OBr^- (1%). $O_2^{\bullet-}$ reacts with HOBr ($k = 3.5 \times 10^9$ M^{-1} s^{-1}) even faster than with ozone; hence, HOBr acts here as competitor for ozone and makes it difficult to define the formaldehyde yield per •OH, as it is not possible to use the known correction factor for the formaldehyde yield in ozone-based processes.

$$O_3 + O_2^{\bullet-} \xrightarrow[Br^-]{} O_3^{\bullet-} + O_2 \qquad k = 1.6 \times 10^9\ M^{-1}\ s^{-1} \qquad (22)$$

$$HOBr + O_2^{\bullet-} \xrightarrow[Br^-]{} O_2 + OH^- + Br_2^{\bullet-} \qquad k = 3.5 \times 10^9\ M^{-1}\ s^{-1} \qquad (23)$$

$$OBr^- + O_2^{\bullet-} \longrightarrow O_2 + 2\ OH^- + Br_2^{\bullet-} \qquad k > 2 \times 10^8\ M^{-1}\ s^{-1} \qquad (24)$$

$$Br_2^{\bullet-} + O_2^{\bullet-} \rightarrow O_2 + 2\ Br^- \qquad k = 1.7 \times 10^8\ M^{-1}\ s^{-1} \qquad (25)$$

$$Br_3^{\bullet-} + O_2^{\bullet-} \rightarrow O_2 + Br^- + Br_2^{\bullet-} \qquad k = 1.5 \times 10^9\ M^{-1}\ s^{-1} \qquad (26)$$

$$Br_2^{\bullet-} + Br_2^{\bullet-} \rightarrow Br^- + Br_3^- \qquad k = 1.8 \times 10^9\ M^{-1}\ s^{-1} \qquad (27)$$

The •OH yield is shown in Figure 5-1. Due to the reaction of $O_2^{\bullet-}$ with ozone and HOBr, it is not possible to give an exact •OH yield per ozone. The shaded area indicates the possible range for the yield. The lower line gives the lowest limit, considering solely the reaction of $O_2^{\bullet-}$ with ozone, and the upper line indicates the highest yield, excluding the reaction of $O_2^{\bullet-}$ with ozone. As the system is very complex, it cannot be surely predicted to what extent $O_2^{\bullet-}$ reacts with ozone and to what extent it reacts with bromine species. If one assumes that the most important bromine species reacting with superoxide is HOBr, a possible •OH yield can be calculated. Therefore, the fractions of superoxide reacting with ozone and HOBr were calculated, from which the correction factors were adapted for every ozone concentration. The calculated correction factor is 2.29 ±0.06 (•OH yield is 2.29 times the formaldehyde yield), if the only bromine species reacting with $O_2^{\bullet-}$ is HOBr. The calculated possible •OH yields are shown in Figure 5-1 (white circles and corresponding linear trend line).

The exact quantification of •OH would be possible using the DMSO/•OH system, which gives methanesulfinic acid, that is formed in 92 % yield (Veltwisch *et al.*, 1980). However, this system could not be used here, as high DMSO concentrations would have to be present to scavenge all •OH, but at the same time it would compete with bromide for O_3. To comply with the prerequisites of an •OH scavenger, the DMSO concentration must be at least 100 times higher than the bromide concentration. Under these conditions, the fraction of •OH reacting with DMSO would be 99 %, but the fraction of ozone reacting with bromide would be only 45 %.

5.4.2 •OH QUANTIFICATION BY MEOH

The reaction of methanol with •OH yields formaldehyde (ractions 5-28 – 5-31) (Goldstein *et al.*, 2007). The formaldehyde yield per •OH is unity. Once an $^{\bullet}OOCH_2OH$ is formed, it reacts with HPO_4^{2-} and OH^- to form formaldehyde (reactions 5-30 and 5-31).

$$^{\bullet}OH + CH_3OH \rightarrow {}^{\bullet}CH_2OH + H_2O \qquad k = 9.7 \times 10^8\ M^{-1}\ s^{-1} \quad (5\text{-}28)$$

$$^{\bullet}CH_2OH + O_2 \rightarrow {}^{\bullet}OOCH_2OH \qquad k = 4.5 \times 10^9\ M^{-1}\ s^{-1} \quad (5\text{-}29)$$

$$^{\bullet}OOCH_2OH + HPO_4^{2-} \rightarrow HCHO + O_2^{\bullet-} + H_2PO_4^- \qquad k \approx 2 \times 10^6\ M^{-1}\ s^{-1} \quad (5\text{-}30)$$

$$^{\bullet}OOCH_2OH + OH^- \rightarrow HCHO + O_2^{\bullet-} + H_2O \qquad k = 1.8 \times 10^{10}\ M^{-1}\ s^{-1} \quad (5\text{-}31)$$

In the present system, the formaldehyde yield (and, thus, the •OH yield) is 83 % with respect to the applied ozone (Figure 5-2). Such a high •OH yield could not exclusively emerge from the

reaction of ozone with bromide. Thus, there must be another relevant source of •OH in the system. In the sequence of the reactions between methanol and •OH, $O_2^{\bullet-}$ is formed. Once it is formed, it reacts readily with ozone (reaction 5-22) and outcompetes the reaction of bromide with ozone. Hence, nearly all ozone is consumed by $O_2^{\bullet-}$, giving •OH that react with methanol yielding formaldehyde. This undesirable reaction leads to an overestimated •OH yield. Therefore, methanol cannot be used for the quantification of •OH in ozone-based reactions.

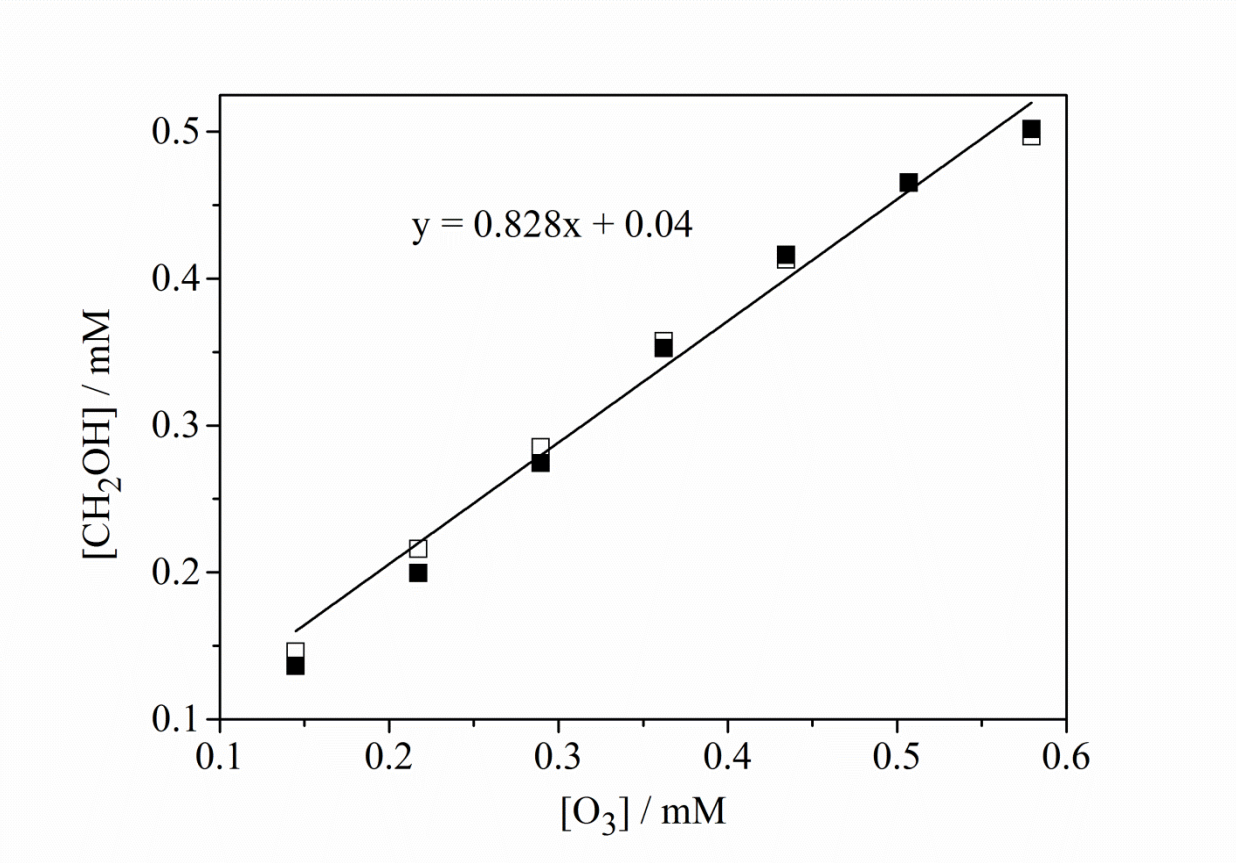

Figure 5-2: Formation of formaldehyde in the reaction of •OH with MeOH buffered at pH 7 (■) and 8 (□) with 2 mM $H_2PO_4^-/HPO_4^{2-}$.

5.4.3 Formation of Bromate and HOBr

Since •OH contribute to bromate formation (reactions 5-8 – 5-16), the scavenging of •OH must lead to a reduced bromate yield (von Gunten and Hoigné, 1994). This could be observed in experiments with and without the addition of *t*BuOH as an •OH scavenger (Figure 5-3). Such a significant difference between the bromate yield in the presence and absence of *t*BuOH is a further evidence for the •OH formation in the multistep reaction of ozone with bromide to bromate. The bromate yield without *t*BuOH is around twice its yield in the presence of *t*BuOH.

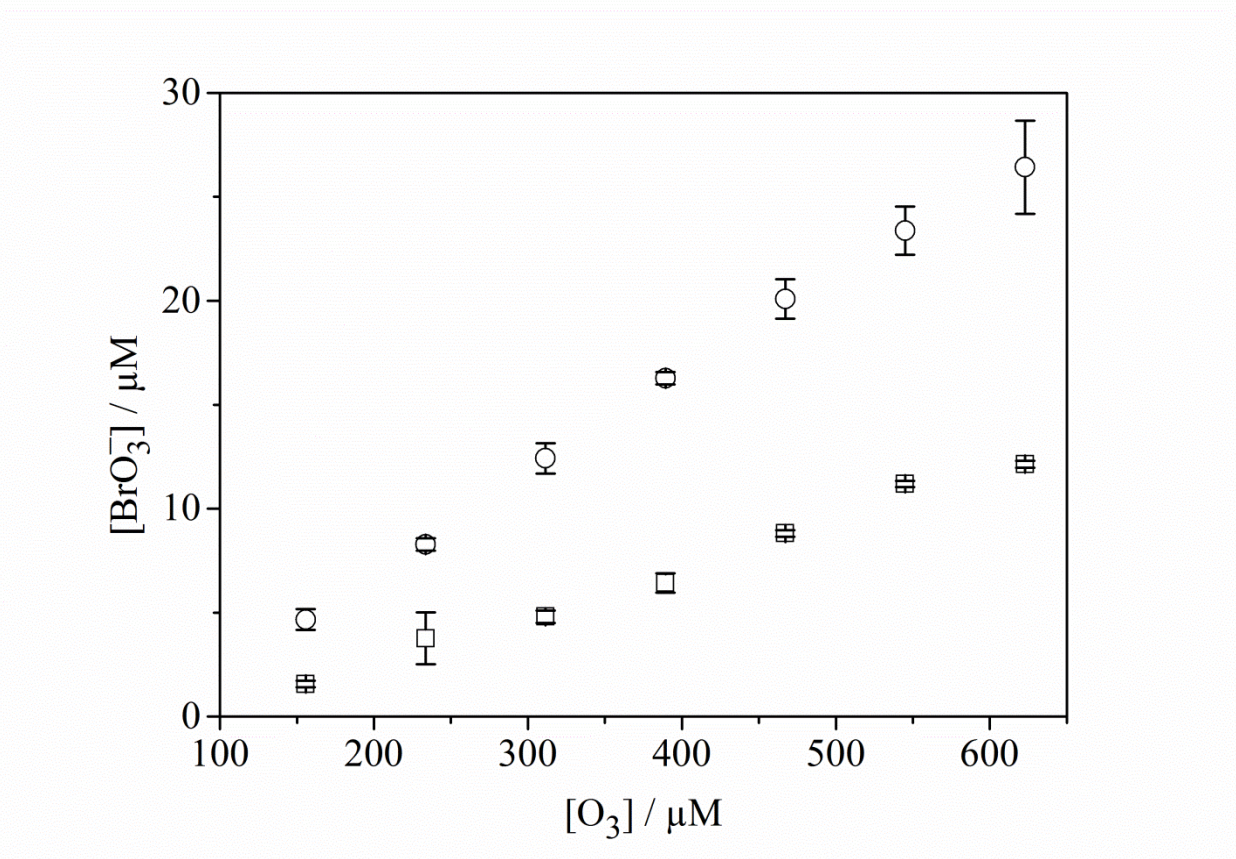

Figure 5-3: Formation of bromate in the presence of *t*BuOH as an •OH scavenger (squares) and in the absence of *t*BuOH (circles) in the reaction of ozone with bromide, plotted against the ozone concentration (n = 3).

HOBr is the most important and stable intermediate in the multistep process en route to bromate. Based on published results presenting the mechanism of the formation of 2- and 4-bromophenol as an example for the formation of brominated phenolic compounds in natural waters in ozone treatment, a well-working method for HOBr quantification was developed (Acero *et al.*, 2005). HOBr was quantified indirectly by measuring 2- and 4-bromophenol, the products from its reaction with phenol. The pH was varied from 2 to 5, and the highest yields were obtained at pH 4. The slope of the graph in Figure 5-4 gives the yield as 0.99 with an error of 0.026. Hence, the bromophenol yield with respect to the applied HOBr is ~100 %.

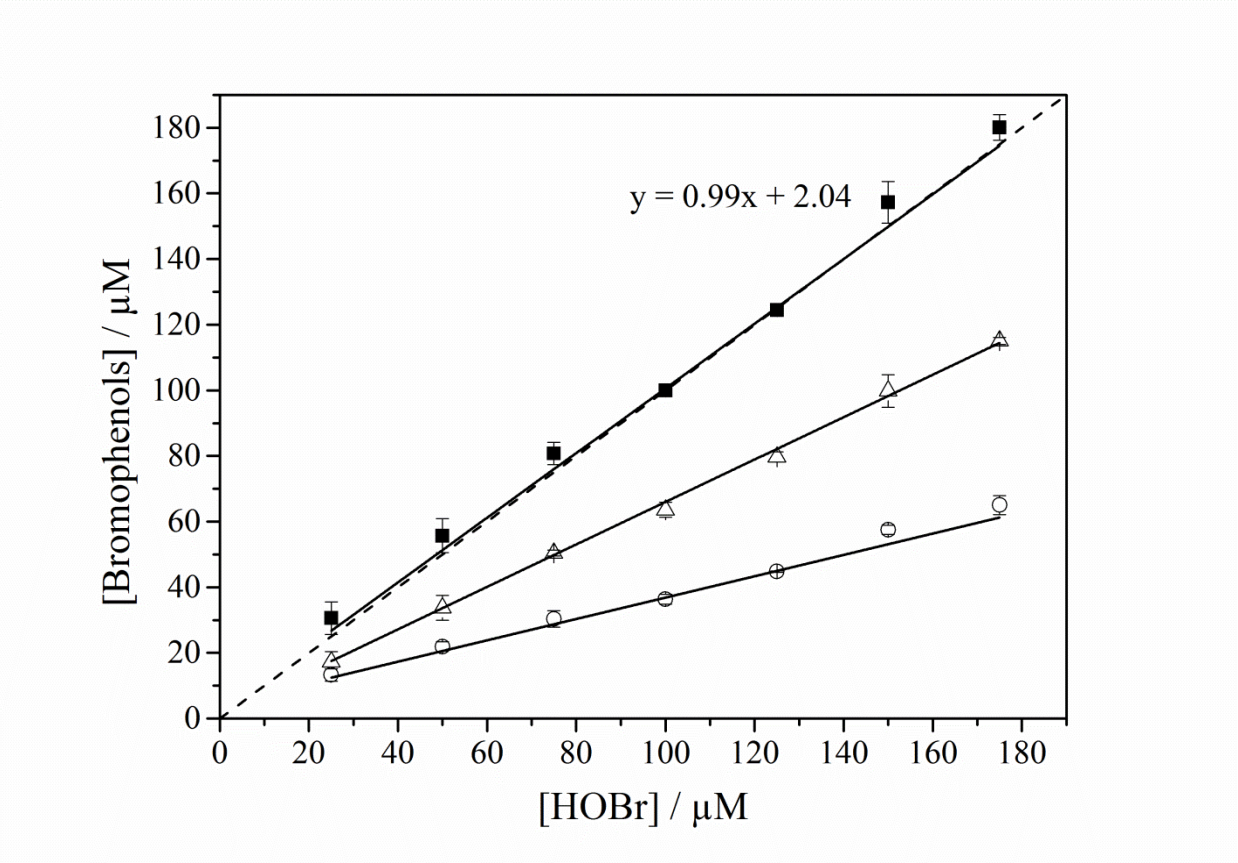

Figure 5-4: 2-Bromophenol (open circles), 4-bromophenol (open triangles), and the sum of both bromophenols (solid squares) yielded from the derivatization of HOBr with phenol at pH 4 (n = 3). Relative standard deviations are indicated but often smaller than symbol size. The dashed line indicates a 100 % yield of bromophenols per HOBr.

The ratio of 4-bromophenol and 2-bromophenol formed in the reaction of hypobromous acid with phenol is 1.64 at pH 4. This first appears to be contrary to the results of Acero *et al.* as they reported a ratio of 0.53 for experiments conducted at pH 8-9 (Acero *et al.*, 2005). However, the ratio of the two bromophenols is strongly pH-dependent, given that as Tee *et al.* (1989) published that 95% of formed bromophenols is parasubstituted at pH 0. This means that at a low pH, 4-bromophenol is prevalent, and at a high pH, 2-bromophenol is dominant. As the ratio of 2- and 4-bromophenol is pH-dependent, it is highly recommended to measure both bromophenols and use their sum concentration to determine the HOBr concentration. HOBr was measured after the reaction was completed and all ozone was consumed. Figure 5-5 shows the bromophenol yields in the samples. The sum of 2- and 4-bromophenol corresponds to the HOBr formed in the reaction of bromide and ozone. The HOBr concentration in the samples in the absence of *t*BuOH is higher than in its presence, as $^{\bullet}$OH are not scavenged and react rapidly with bromide that is present at a high concentration yielding HOBr (reaction 5-8). Furthermore,

if no *t*BuOH is added, no $O_2^{\bullet-}$ is formed in the sequence of the reaction between *t*BuOH and $^{\bullet}OH$ that could react with HOBr (reactions 5-23 and 5-24). Thus, the lower HOBr yield observed in the presence of *t*BuOH provides further evidence for $^{\bullet}OH$ formed from the reaction of bromite with ozone via electron transfer.

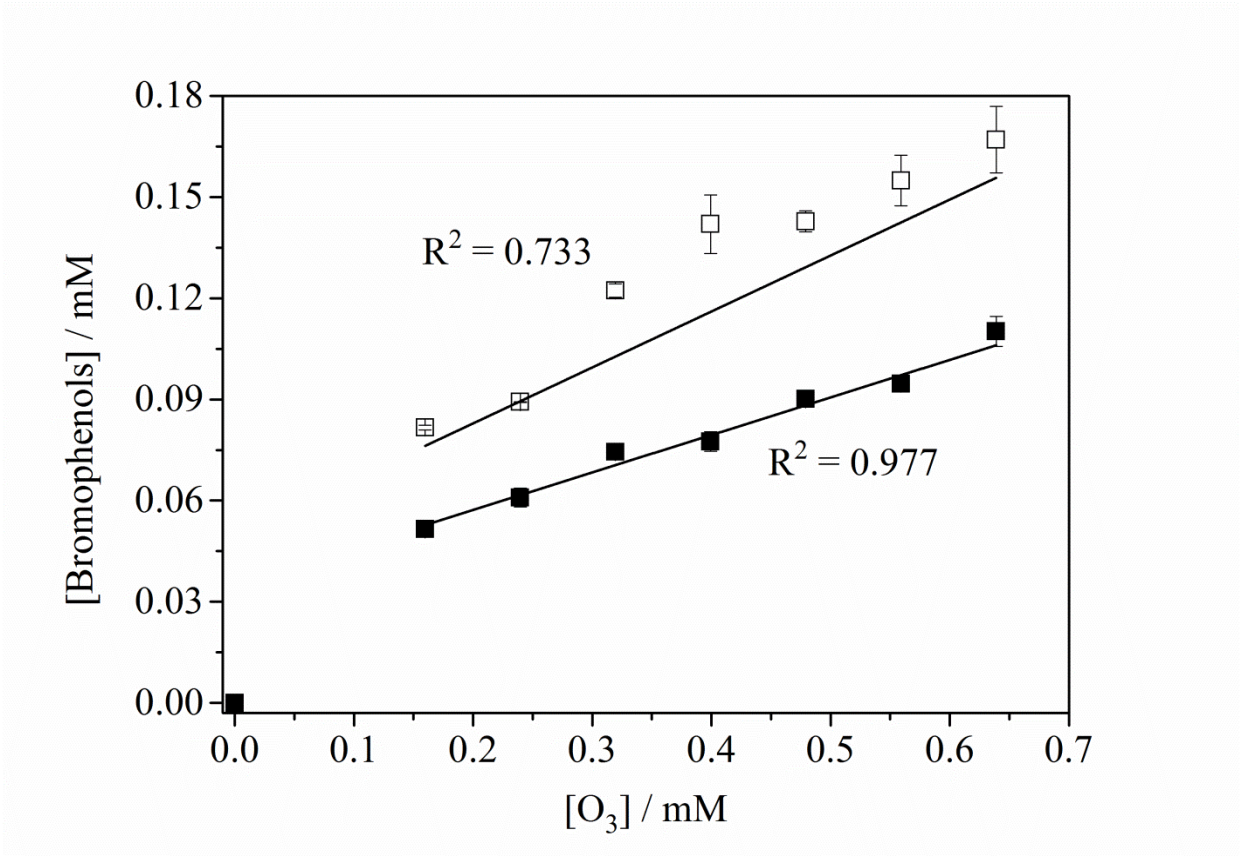

Figure 5-5: Formation of bromophenols at pH 4 from the reaction of phenol and HOBr, formed as intermediate from bromide and ozone. The sum of 2- and 4-bromophenol formed in the presence of *t*BuOH (solid squares) and in the absence of *t*BuOH (open squares) as a function of the applied ozone concentration (n = 3).

From the results discussed above, it can be concluded that in the sequence of the ozone reactions from bromide to bromate, $^{\bullet}OH$ must be generated. Thus, the original concept of bromate formation has to be revised. Based on the obtained results, the known pathway from bromide to bromate was modified (Figure 5-6). It was updated at the last ozone reaction step. The O-transfer reaction was replaced by the electron-transfer reaction.

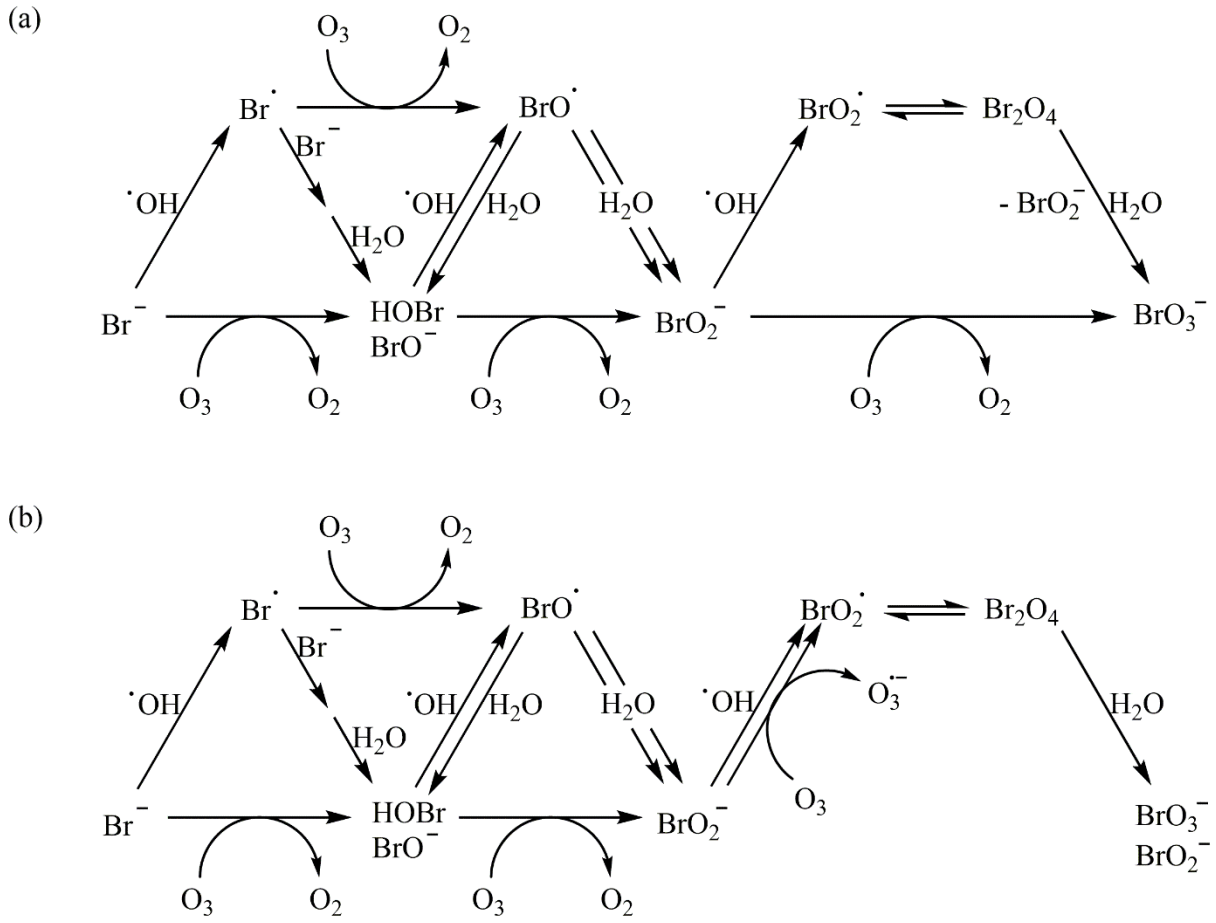

Figure 5-6: (a) The old pathway for the bromate formation in the reaction of ozone with bromide established by von Gunten (von Gunten and Hoigné, 1994, von Gunten, 2003) and (b) the new recommended pathway for the reaction of bromide with ozone based on this study adapted from von Gunten's reaction scheme (von Gunten and Hoigné, 1994, von Gunten, 2003). Note the difference between the old and the new mechanism in the last reaction of ozone on the right-hand side.

5.4.4 PRACTICAL IMPLICATIONS

The present paper shows that in the multistep reaction of ozone with bromide to bromate, ·OH are generated. This is due to the fact that the last of these steps is not as previously assumed an O-transfer reaction but rather an electron-transfer reaction. The electron-transfer reaction also yields bromate, but this new fact could be essential for reaction modeling. Until now, the modeling of the reaction of bromide with ozone does not give good results, as there are still too many not-well-known reactions included (von Gunten 2015, personal communication). In systems with low ·OH scavenger capacity (e.g., waters with low dissolved organic matter content) OH radical formation in the electron transfer step might enhance the bromate yield, as

the •OH formed on site may contribute to bromate formation. Under which conditions this is indeed relevant in natural waters requires further investigation.

5.5 REFERENCES

Acero, J. L., Piriou, P. and von Gunten, U. (2005). Kinetics and mechanisms of formation of bromophenols during drinking water chlorination: assessment of taste and odor development. Water Research, **39**(13), 2979-2993.

Antoniou, M. G. and Andersen, H. R. (2012). Evaluation of pretreatments for inhibiting bromate formation during ozonation. Environmental Technology, **33**(15), 1747-1753.

Buxton, G. V. and Dainton, F. S. (1968). The radiolysis of aqueous solutions of oxybromine compounds; the spectra and reactions of BrO and BrO_2. Proceedings of the Royal Society of London Series a-Mathematical and Physical Sciences, **304**(1479), 427-439.

Buxton, G. V., Greenstock, C. L., Helman, W. P. and Ross, A. B. (1988). Critical review of rate constants for reactions of hydrated electrons, hydrogen atoms and hydroxyl radicals ($\cdot OH/\cdot O^-$) in aqueous solution. Journal of Physical and Chemical Reference Data, **17**(2), 513-886.

Cotruvo, J. A., Keith, J. D., Bull, R. J., Pacey, G. E. and Gordon, G. (2010). Bromate reduction in simulated gastric juice. Journal American Water Works Association, **102**(11), 77-86.

Council-Directive-98/83/EC (1998). On the quality of water intended for human consumption. Official Journal of the European Communities. Brussels, Belgium, Council Directive 98/83/EC; European Commission Directorate-General for Environment.

Ershov, B. G. and Morozov, P. A. (2009). The kinetics of ozone decomposition in water, the influence of pH and temperature. Russian Journal of Physical Chemistry A, **83**(8), 1295-1299.

Flyunt, R., Leitzke, A., Mark, G., Mvula, E., Reisz, E., Schick, R. and von Sonntag, C. (2003). Determination of $\cdot OH$, $O_2^{-\cdot}$, and hydroperoxide yields in ozone reactions in aqueous solution. Journal of Physical Chemistry B, **107**(30), 7242-7253.

Goldstein, S., Aschengrau, D., Diamant, Y. and Rabani, J. (2007). Photolysis of aqueous H_2O_2: quantum yield and applications for polychromatic UV actinometry in photoreactors. Environmental Science & Technology, **41**(21), 7486-7490.

Haag, W. R. and Hoigné, J. (1983). Ozonation of bromide-containing waters: kinetics of formation of hypobromous acid and bromate. Environmental Science & Technology, **17**(5), 261-267.

Han, Q., Wang, H. J., Dong, W. Y., Liu, T. Z. and Yin, Y. L. (2014). Suppression of bromate formation in ozonation process by using ferrate(VI): batch study. Chemical Engineering Journal, **236**, 110-120.

Hart, E. J., Sehested, K. and Holcman, J. (1983). Molar absorptivities of ultraviolet and visible bands of ozone in aqueous solutions. Analytical Chemistry, **55**(1), 46-49.

Hoigne, J. and Bader, H. (1983). Rate constants of reactions of ozone with organic and inorganic compounds in water - I non-dissociating organic compounds. Water Research, **17**(2), 173-183.

Keith, J. D., Pacey, G. E., Cotruvo, J. A. and Gordon, G. (2006a). Experimental results from the reaction of bromate ion with synthetic and real gastric juices. Toxicology, **221**(2-3), 225-228.

Keith, J. D., Pacey, G. E., Cotruvo, J. A. and Gordon, G. (2006b). Preliminary data on the fate of bromate ion in simulated gastric juices. Ozone-Science & Engineering, **28**(3), 165-170.

Klaning, U. K. and Wolff, T. (1985). Laser flash-photolysis of HClO, ClO^-, HBrO, and BrO^- in aqueous solution - reactions of Cl- and Br-atoms. Berichte Der Bunsen-Gesellschaft-Physical Chemistry Chemical Physics, **89**(3), 243-245.

Lipari, F. and Swarin, S. J. (1982). Determination of formaldehyde and other aldehydes in automobile exhaust with an improved 2,4-dinitrophenylhydrazine method. Journal of Chromatography, **247**(2), 297-306.

Liu, Y., Jiang, J., Ma, J., Yang, Y., Luo, C., Huangfu, X. and Guo, Z. (2015). Role of the propagation reactions on the hydroxyl radical formation in ozonation and peroxone (ozone/hydrogen peroxide) processes. Water Research, **68**, 750-758.

Matheson, M. S., Mulac, W. A., Weeks, J. L. and Rabani, J. (1966). The pulse radiolysis of deaerated aqueous bromide solutions. Journal of Physical Chemistry, **70**(7), 2092-2099.

Merenyi, G., Lind, J., Naumov, S. and von Sonntag, C. (2010). Reaction of ozone with hydrogen peroxide (peroxone process): a revision of current mechanistic concepts based on

thermokinetic and quantum-chemical considerations. Environmental Science & Technology, **44**(9), 3505-3507.

Naumov, S. and von Sonntag, C. (2011). Standard Gibbs free energies of reactions of ozone with free radicals in aqueous solution: quantum-chemical calculations. Environmental Science & Technology, **45**(21), 9195-9204.

Nicoson, J. S., Wang, L., Becker, R. H., Huff Hartz, K. E., Muller, C. E. and Margerum, D. W. (2002). Kinetics and mechanisms of the ozone/bromite and ozone/chlorite reactions. Inorganic Chemistry, **41**(11), 2975-2980.

Pinkernell, U., Nowack, B., Gallard, H. and Von Gunten, U. (2000). Methods for the photometric determination of reactive bromine and chlorine species with ABTS. Water Research, **34**(18), 4343-4350.

Schuchmann, M. N. and von Sonntag, C. (1979). Hydroxyl radical-induced oxidation of 2-methyl-2-propanol in oxygenated aqueous solution. A product and pulse radiolysis study. Journal of Physical Chemistry, **83**(7), 780-784.

Tee, O. S., Paventi, M. and Bennett, J. M. (1989). Kinetics and mechanism of the bromination of phenols and phenoxide ions in aqueous solution. Diffusion-controlled rates. Journal of the American Chemical Society, **111**(6), 2233-2240.

Troy, R. C. and Margerum, D. W. (1991). Non-metal redox kinetics: hypobromite and hypobromous acid reactions with iodide and with sulfite and the hydrolysis of bromosulfate. Inorganic Chemistry, **30**(18), 3538-3543.

U.S.EPA (1994). U.S. Environmental Protection Agency. National primary drinking water regulations: disinfectants and disinfection byproducts. Federal Register. Washington, DC, Environmental Protection Agency. **59, (145)**.

Veltwisch, D., Janata, E. and Asmus, K. D. (1980). Primary processes in the reaction of OH-radicals with sulphoxides. Journal of the Chemical Society-Perkin Transactions 2(1), 146-153.

von Gunten, U. (2003). Ozonation of drinking water: part II. Disinfection and by-product formation in presence of bromide, iodide or chlorine. Water Research, **37**(7), 1469-1487.

von Gunten, U. and Hoigne, J. (1992). Factors controlling the formation of bromate during ozonation of bromide-containing waters. Journal of Water Supply: Research and Technology - AQUA, **41**(5), 299-304.

von Gunten, U. and Hoigné, J. (1994). Bromate formation during ozonation of bromide-containing waters: interaction of ozone and hydroxyl radical reactions. Environmental Science & Technology, **28**(7), 1234-1242.

von Gunten, U. and Oliveras, Y. (1997). Kinetics of the reaction between hydrogen peroxide and hypobromous acid: implication on water treatment and natural systems. Water Research, **31**(4), 900-906.

von Gunten, U. and Oliveras, Y. (1998). Advanced oxidation of bromide-containing waters: bromate formation mechanisms. Environmental Science & Technology, **32**(1), 63-70.

von Sonntag, C. and von Gunten, U. (2012). Chemistry of ozone in water and wastewater treatment - from basic principles to applications. IWA Publishing, London.

Weast, R. C., Ed. (1971-1972). Handbook of chemistry and physics. Ohio, The Chemical Rubber Co.

Zehavi, D. and Rabani, J. (1972). Oxidation of aqueous bromide ions by hydroxyl radicals. A pulse radiolytic investigation. Journal of Physical Chemistry, **76**(3), 312-319.

Chapter 6

THE SYNTHESIS OF 2-METHYL-2-HYDROXYPROPANOL AND 2-METHYL-2-HYDROXYPROPANAL

6.1 ABSTRACT

An established method for the determination of •OH in water is measuring the products of its reaction with *tert*-Butanol (*t*BuOH). Besides formaldehyde and acetone 2-methyl-2-hydroxypropanol and 2-methyl-2-hydroxypropanal are main products of this reaction. Since there are no authentic standards for 2-methyl-2-hydroxypropanol and 2-methyl-2-hydroxypropanal commercially available an indirect quantification of •OH is just possible by an assumed yield of formaldehyde formed per •OH. The synthesis of 2-methyl-2-hydroxypropanol was performed by adapting the synthesis presented by Steffan *et al.* (1997). The product was characterized by NMR and GC-MS and it could be shown that 2-methyl-2-hydroxypropanol was formed. A method to synthesize 2-methyl-2-hydroxypropanal is the oxidation of 2-methyl-2-hydroxy-propanol by Dess-Martin periodinane (DMP), l,l,l-triacetoxy-l,l-dihydro-l,2-benziodoxol-3(1H)-one. The product characterization was done by NMR and HPLC-UV after derivatization. The NMR spectra did not show any product which could be due to the low amount of product present in the solution and the results obtained from the HPLC show many impurities and therefore, 2-methyl-2-hydroxypropanal could not be identified.

6.2 INTRODUCTION

The determination of •OH in water occurs indirectly due to their short lifetime. One of several quantification approaches is the quantification of products from the reaction of •OH with *tert*-Butanol (*t*BuOH). Besides formaldehyde and acetone, that both can readily be quantified 2-methyl-2-hydroxypropanal and 2-methyl-2-hydroxy-propanol are the main degradation products in the reaction of *t*BuOH with •OH (Flyunt *et al.*, 2003). As there are no authentic standards for 2-methyl-2-hydroxypropanal and 2-methyl-2-hydroxypropanol available a precise quantification is not possible. Therefore, •OH in water are quantified by assuming that the formaldehyde yield corresponds to 30±4% of the formed •OH and when ozone is present its yield increases to 50% (Flyunt *et al.*, 2003). This assumption seems not to work for all systems as the attempt of quantifying •OH in the Fenton reaction via scavenging with *t*BuOH gives no plausible results. In such cases authentic standards of 2-methyl-2-hydroxypropanal and 2-methyl-2-hydroxypropanol would allow to quantify •OH without any assumptions.

Besides the quantification of •OH environmental research also requires an authentic standard for 2-methyl-2-hydroxypropanol, as it is found to be a degradation product of MTBE, a main gasoline component (Acero *et al.*, 2001, Ferreira *et al.*, 2006). 2-methyl-2-hydroxypropanal is found to be a degradation product from the oxidation of the biogenic hydrocarbon 2-methyl-3-

buten-2-ol (Spaulding *et al.*, 2002, Reisen *et al.*, 2003, Carrasco *et al.*, 2006). Spaulding *et al.* (2002) used 3-hydroxy-3-methyl-2-butanone as a surrogate for the quantification of 2-methyl-2-hydroxypropanal by GC-MS, while Reisen *et al.* (2003) used for the quantification of 2-methyl-2-hydroxypropanal by GC-FID the response factor of the measurement of 2,2-dimethylpropanal. (Alvarado *et al.*, 1999) quantified 2-methyl-2-hydroxypropanal by calculating its GC-FID response factor relative to the educt using the effective carbon number method. All these methods contain errors and an authentic 2-methyl-2-hydroxypropanal standard would facilitate its quantification.

Some synthesis routes for 2-methyl-2-hydroxypropanal and 2-methyl-2-hydroxypropanol have been reported in literature. Carrasco *et al.* (2006) described a route to synthesize 2-methyl-2-hydroxypropanal by ozonation of -78 °C cold 2-methyl-3-buten-2-ol. The products of the synthesis were 2-methyl-2-hydroxypropanal, formaldehyde and acetone.

Steffan *et al.* (1997) described a method to synthesize 2-methyl-2-hydroxypropanol from methyl-2-methylglycidate by reducing it with sodium borohydride (reaction 6-1).

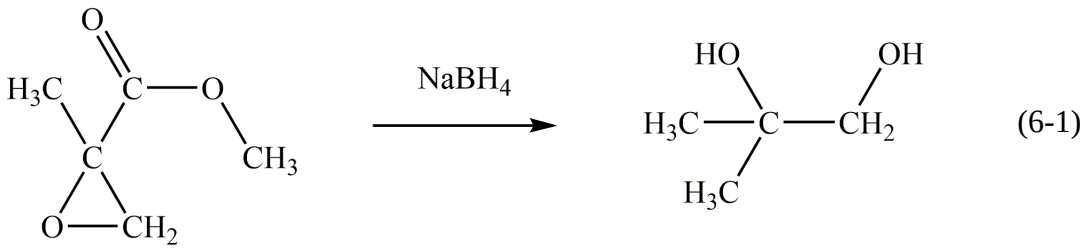

(6-1)

2-methyl-2-hydroxypropanal can also be obtained by oxidation of the primary alcoholic group of 2-methyl-2-hydroxypropanol. It is important to choose a mild oxidation method that allow the oxidation of the alcohol to the aldehyde and no further oxidation to the carboxylic acid. The oxidation of primary and secondary alcohols with, e.g., MnO_4^- in alkaline solution and Cr(VI) in acidic solution leads to a full oxidation to the carboxylic acid (Beckert *et al.*, 2004). A mild oxidation agent presented by Dess and Martin (1991) is l,l,l-triacetoxy-l,l-dihydro-l,2-benziodoxol-3(1H)-one (Dess-Martin periodinane). It oxidizes primary and secondary alcohols to aldehydes or ketones but not further to carboxylic acids. As tertiary alcohols are not oxidized by the Dess-Martin periodinane the OH group at C2 remains unoxidized.

The scope of the present work is the synthesis of 2-methyl-2-hydroxypropanol and 2-methyl-2-hydroxypropanal.

6.3 MATERIAL AND METHODS

6.3.1 CHEMICALS

Following chemicals were used as received without any further purification: Acetonitrile (≥ 99.8 %) VWR, Dess-Martin periodinane solution (0.3 M in methylene chloride) Aldrich, Diethyl ether (≥ 99.7 %) Sigma-Aldrich, Dimethylsulfoxide (99.9 %) VWR, 2,4-Dinitrophenylhydrazine (97 %) Merck, formaldehyde (~ 37 %) Supelco, hydrogen peroxide (30 %) Merck, methanol (99.8 %) Sigma-Aldrich, methyl-2-methylglycidate (99 %) Aldrich, perchloric acid (70 %) Fluka, pure water (18 MΩ cm) ELGA, sodium borohydride (≥ 98 %) Aldrich

6.3.2 SYNTHESIS

6.3.2.1 SYNTHESIS OF 2-METHYL-2-HYDROXYPROPANOL

The synthesis was performed after an adaption of the method described by Steffan *et al.* (1997) as the synthesis following the described procedure was not successful and did not yield 2-methyl-2-hydroxypropanol. Table 6-1 shows the difference of the original synthesis and the adapted synthesis used in this work. 228 µL (2.16 mmol) methyl-2-methylglycidate were dissolved in 2.5 mL methanol in a 50-mL round-bottomed flask under nitrogen atmosphere. The round-bottomed flask was placed in a water/ice bath and the solution was continuously stirred by a magnetic stirrer. Within 20 min small portions of $NaBH_4$ (in total 615 mg (16.26 mmol)) were added to the solution. During this time a strong gas evolvement was observed. As the mixture solidified additional 2.5 mL methanol were added. After another 20 min cooling and stirring the reaction seemed to be completed as no gas evolvement could be observed anymore. The water/ice bath was removed and the round-bottom flask was placed in a water bath (~ 20 °C) to keep the temperature constant. Under this condition the solution was stirred for another 5 h. After 30 min of stirring 2 mL methanol were added and after 2 h another 2 mL methanol. The reaction was quenched by adding 0.332 mL (4.46 mmol) formaldehyde. After stirring the solution for 5 min 10 mL water and 5 mL diethyl ether were added. The round-bottom flask was shaken and the diethyl ether phase was collected. The aqueous phase was extracted four times with 5 mL diethyl ether each and the extracts combined.

The diethyl ether phase was stored overnight in the fridge. The next day diethyl ether was evaporated in a rotary evaporator (Rotavapor R-210 (Büchi, Flawil)) at 40 °C and 850 mbar.

After the diethyl ether was evaporated the pressure was decreased to 30 mbar for short time to remove all moisture. The obtained product (189.18 mg) was a clear liquid.

The characterization of the obtained product was performed by measuring the product with GC-MS (Finnigan Trace GC Ultra, (Thermo Electron Corporation, Waltham)) and by NMR **(**DMX300 (Bruker, Rheinstetten) ^{1}H frequency: 300.13 MHz, ^{13}C frequency: 75.46 MHz.**).** The GC-MS settings were as follows: full scan measurements between 40 and 200 m/z, oven temperature: 40°C for 2 min, 10°C/min to 250°C held for 2 min, in splitless mode with a constant He flow of 1.3 ml/min and an ion source temperature of 230°C. The product was dissolved in DMSO prior to NMR measurements and in diethyl ether prior to GC-MS measurements.

Table 6-1: Comparison of the synthesis presented by Steffan *et al.* (1997) with the adapted synthesis used in this work

Synthesis by Steffan *et al.* (1997)	adapted synthesis
Dissolve 2 g methyl-2-methylglycidate in 20 mL methanol	Dissolve 228 µL methyl-2-methylglycidate in 2.5 mL methanol
Add 5 g $NaBH_4$	Add 615 mg $NaBH_4$ in small portions within 20 min while cooling and stirring the solution
	Add 2.5 mL methanol
Incubate on ice for 20 min	Cool and stir for 20 min
Incubate 5 h at room temperature	Stir 5 h at room temperature
	– Add 2 mL methanol after 30 min
	– Add 2 mL methanol after 2 h
Add 3 mL formaldehyde	Add 0.332 mL formaldehyde
	Stir 5 min
	Add 10 mL water
Evaporate methanol	
Extract product with diethyl ether	Extract four times with each time 5 mL diethyl ether
	Evaporate diethyl ether

6.3.2.2 OXIDATION OF 2-METHYL-2-HYDROXYPROPANOL TO 2-METHYL-2-HYDROXYPROPANAL

The oxidation of 2-methyl-2-hydroxypropanol to 2-methyl-2-hydroxypropanal was conducted according to Dess and Martin (1991). After 0.121 g (1.34 mmol) of 2-methyl-2-hydroxypropanol were dissolved in 7.5 mL dichloromethane 5 mL 3 M (15 mmol) Dess-Martin periodinane solution (Dess-Martin periodinane solution is commercially available but can also be prepared according to Ireland and Liu (1993)) were added while the solution was continuously stirred. The reaction solution was stirred over night for ~ 27 h. During this time a white powder precipitated and the solution smelled like acetic acid. The product was extracted with 3 mL water. The aqueous phase was clear. An aliquot of both phases was added to DMSO and measured by NMR **(**DMX300 (Bruker, Rheinstetten) ^{1}H frequency: 300.13 MHz, ^{13}C frequency: 75.46 MHz.**).** Additionally 1.7 mL of both phases (aqueous and dichloromethane) was derivatized with 2,4-dinitrophenylhydrazine (2,4-DNPH) and determined as its 2,4-dinitrophenylhydrazones by HPLC-UV (Agilent 1100, *Agilent Technologies*, Santa Clara, CA). The derivatization was conducted according to Lipari and Swarin (1982). 0.2 mL 2,4-DNPH solution (6 mM in acetonitrile) and 0.1 mL perchloric acid (1 M in acetonitrile) were added to 1.7 mL sample. After standing 45 minutes in the dark, the solutions were measured at a wavelength of 350 nm (column: NUCLEODUR 5 µm C18 ec 250 x 3 mm (Macherey-Nagel), flow: 0.4 mL/min, eluent: acetonitrile/water pH 3.5 45/55 (*v/v*) isocratic for 23 min followed by a gradient from 45 to 80 % acetonitrile within 17 min and afterwards keeping the acetonitrile content constant at 80 % for 5 min). The retention times for 2,4-DNPH and 2-hydroxy-2-methylpropanal-2,4-DNPH were 7.0 and 11.3 minutes, respectively. As no authentic standard for 2-methyl-2-hydroxypropanal was available a direct identification is not possible. Fischbacher *et al.* (2013) could identify 2-methyl-2-hydroxypropanal as its 2,4-dinitrophenylhydrazone in samples after reaction of $^{\bullet}OH$ (formed in the peroxone process) with *t*BuOH, as it is one of the main products from this reaction. Besides the formaldehyde concentration the amount of 2-methyl-2-hydroxypropanal increases with increasing $^{\bullet}OH$ concentration. To be able to compare the retention times of the synthesis products in the HPLC measurements a sample containing $^{\bullet}OH$ (formed in peroxone process) and *t*BuOH was prepared as standard according to Fischbacher *et al.* (2013). To 1 mL H_2O_2 (0.25 M) and 2 mL *t*BuOH (11 M) 7 mL O_3 enriched in pure water (0.85 mM) were added.

6.4 RESULTS AND DISCUSSION

6.4.1 SYNTHESIS OF 2-METHYL-2-HYDROXYPROPANOL

The product yielded by the reduction of methyl-2-methylglycidate was measured by GC-MS and by NMR. The GC-MS measurement gives a single peak at a retention time of 5.5 min. The corresponding mass spectrum showed mass fragments at m/z 59 ($C_3H_6OH^+$) and 75 ($C_3H_5(OH)_2^+$). As 2-methyl-2-hydroxypropanol is not included in any mass spectra library there was no direct comparison with library data possible. However, these fragments are in agreement with expected fragments for 2-methyl-2-hydroxypropanol. This is a first hint, that the product from the synthesis could be 2-methyl-2-hydroxypropanol.

The comparison of the obtained ^{1}H NMR spectrum (Figure 6-1) with a predicted one (Figure 6-2) and with data published by Murphy and Adam (1996) shows that the published peaks for 2-methyl-2-hydroxypropanol at 1.2 (2 × CH_3) and 3.4 ppm (1 × CH_2) agree well with the data obtained in this study. As the spectrum shows many more peaks and to confirm that the peaks of interest belong to 2-methyl-2-hydroxypropanol NMR blanks of DMSO (solvent used for NMR), methyl-2-methylglycidate (educt) and diethyl ether (extraction solvent in the synthesis) were run in addition.

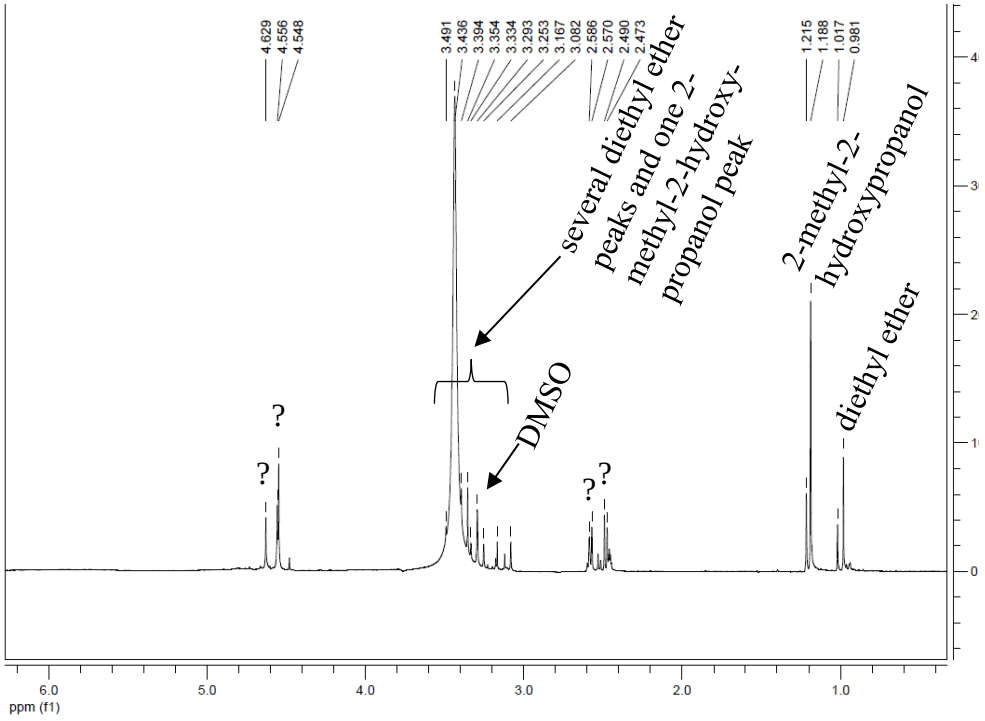

Figure 6-1: ^{1}H NMR spectrum of the product yielded in the synthesis of methyl-2-methylglycidat to 2-methyl-2-hydroxypropanol. Sample prepared in DMSO.

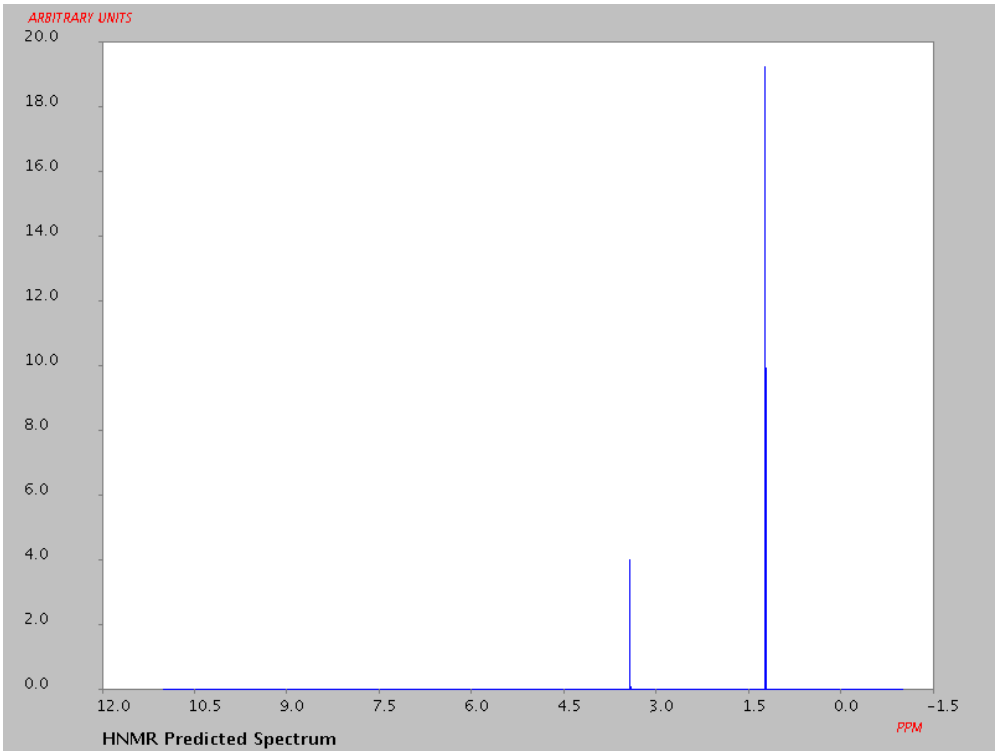

Figure 6-2: predicted ^{1}H NMR spectrum of 2-methyl-2-hydroxypropanol (Predicted NMR data calculated using Advanced Chemistry Development, Inc. (ACD/Labs) Software V11.01 (© 1994-2017 ACD/Labs) taken from SciFinder)

The ^{1}H NMR spectrum of diethyl ether (Figure 6-3) shows several peaks at 1.1 and 3.3 - 3.4 ppm. The peaks at 3.4 ppm interfere with one of the peaks of 2-methyl-2-hydroxypropanol. The spectrum of DMSO (Figure 6-4) shows a peak at 3.3 ppm. Both solvents show peaks in the range of 3.3 - 3.4, which explains the huge amount of peaks around 3.4 ppm in the spectrum of the product of the synthesis (Figure 6-1).

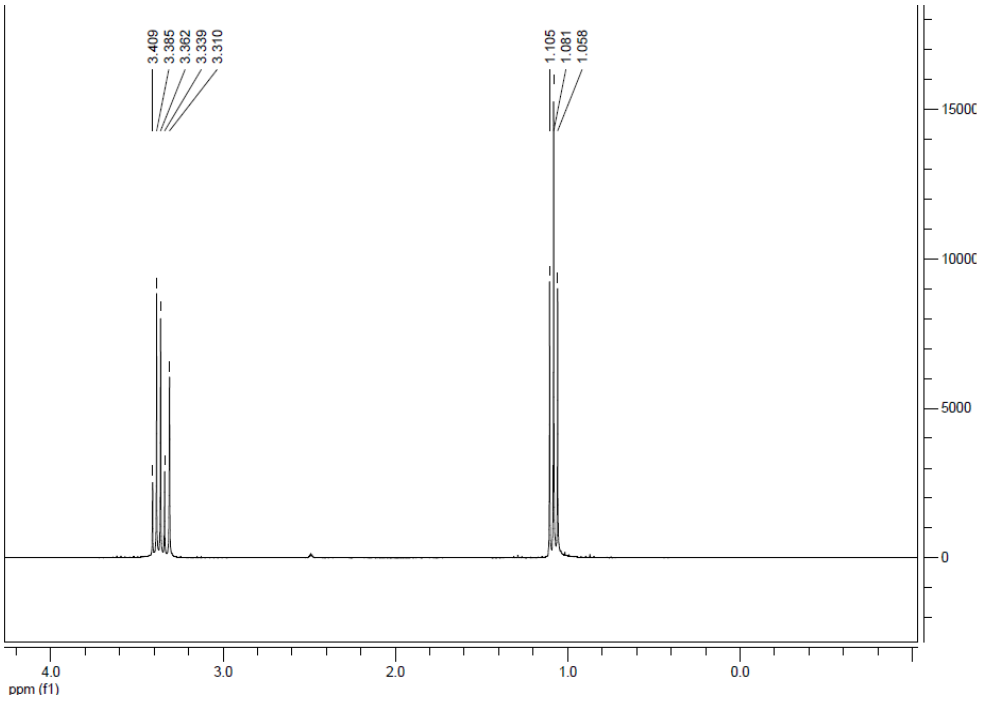

Figure 6-3: ^{1}H NMR spectrum of diethyl ether

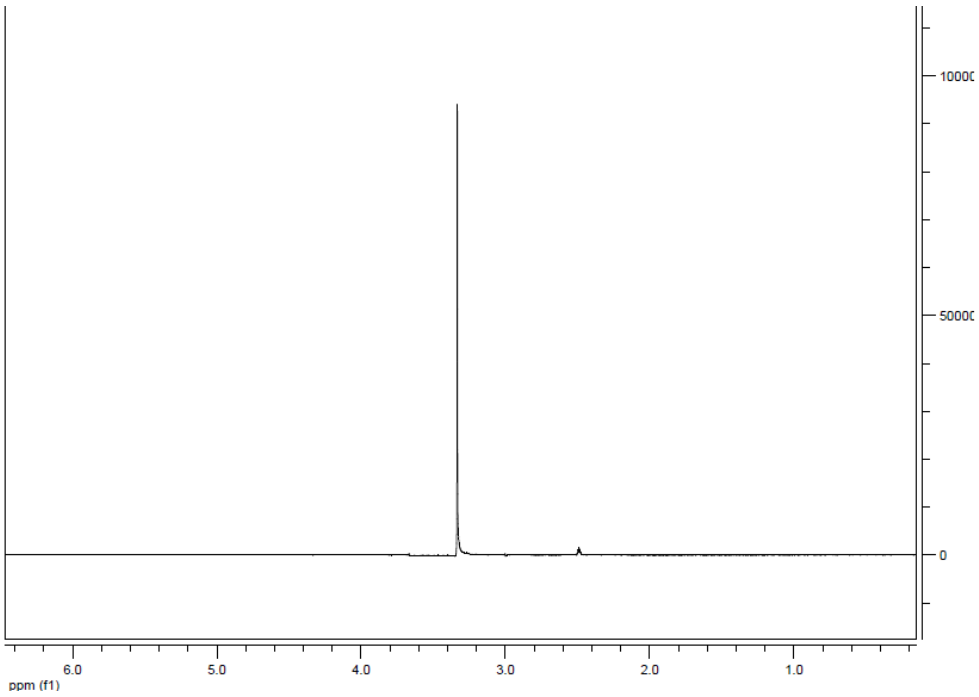

Figure 6-4: ^{1}H NMR spectrum of DMSO

The main peaks of the educt are at 1.45 and 3.65 ppm (Figure 6-5). As these are not present in the synthesis product spectrum, the educt seems to have completely reacted. Due to the results obtained from the GC-MS measurement and as none of the ^{1}H NMR spectra of the used solvents

show a peak at 1.2 ppm which is one of the relevant peaks of 2-methyl-2-hydroxylpropanol, it is assumed that the product of the synthesis is 2-methyl-2-hydroxypropanol.

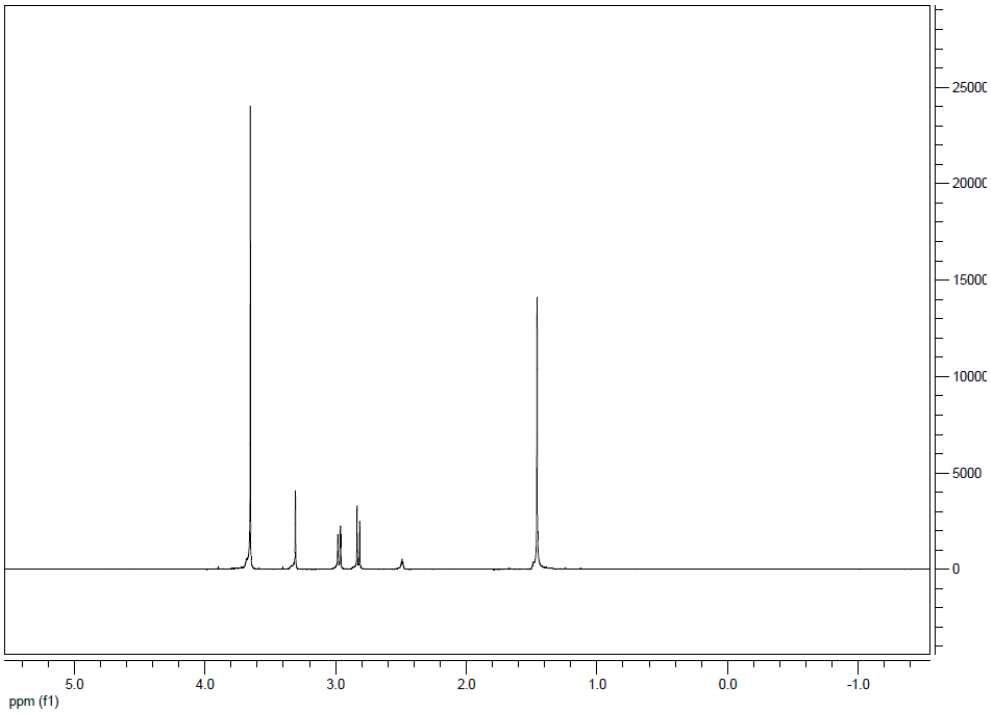

Figure 6-5: ^{1}H NMR spectrum of methyl-2-methylglycidate

6.4.2 Oxidation of 2-methyl-2-hydroxypropanol to 2-methyl-2-hydroxypropanal

The results obtained by the NMR measurement of the product obtained from the oxidation of 2-methyl-2-hydroxypropanol were compared with predicted data. It was found that neither in the ^{1}H NMR spectrum of the aqueous phase (Figure 6-6) nor in the dichloromethane phase (Figure 6-7) peaks corresponding to 2-methyl-2-hydroxypropanal (1.4 and 9.5 ppm see Figure 6-8) could be found. The spectrum of the dichloromethane phase (Figure 6-7) shows peaks that correspond to DMSO (3.4 ppm) and dichloromethane (5.7 ppm).

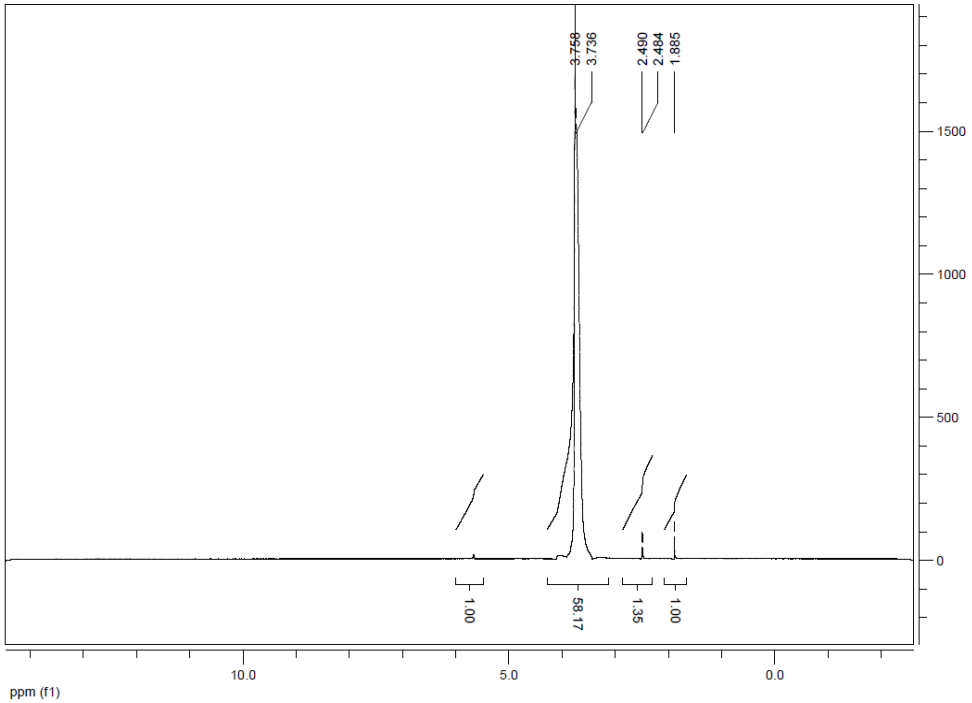

Figure 6-6: ^{1}H NMR spectrum of the aqueous phase obtained after extraction of the solution after oxidation of 2-methyl-2-hydroxypropanol to 2-methyl-2-hydroxypropanal

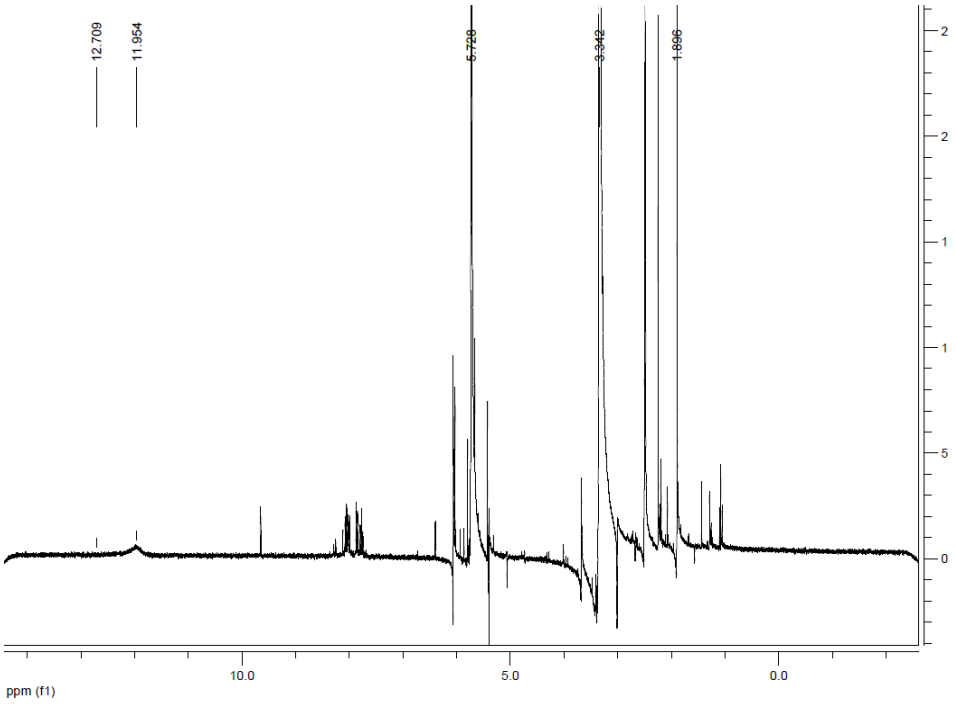

Figure 6-7: ^{1}H NMR spectrum of the dichloromethane phase obtained after extraction of the solution after oxidation of 2-methyl-2-hydroxypropanol to 2-methyl-2-hydroxypropanal

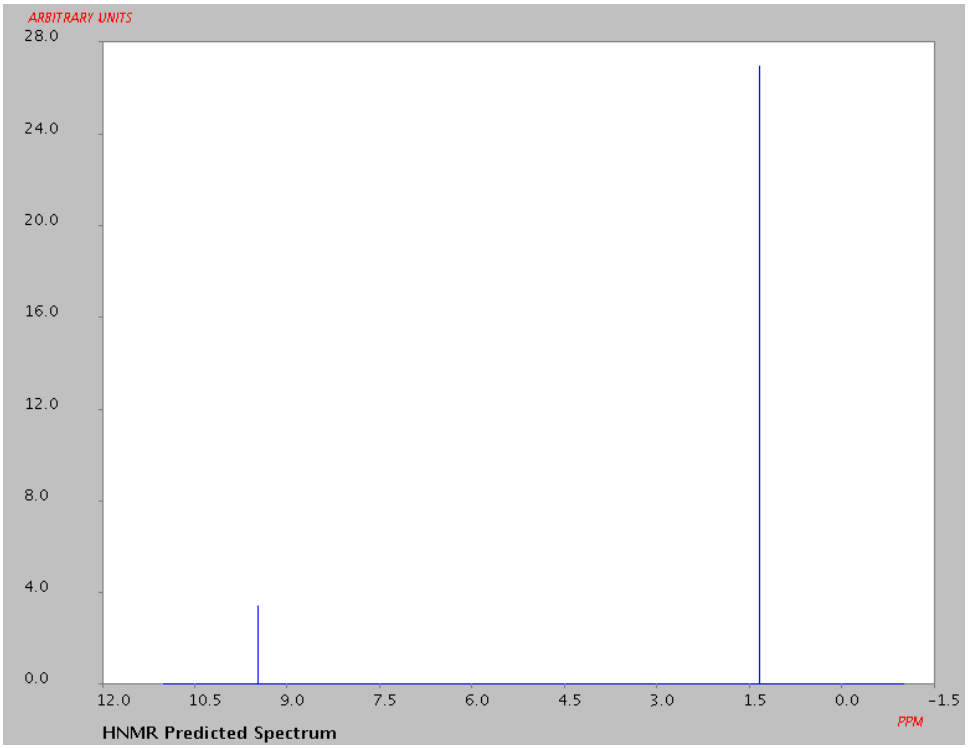

Figure 6-8: predicted ^{1}H NMR spectrum of 2-methyl-2-hydroxypropanal (Predicted NMR data calculated using Advanced Chemistry Development, Inc. (ACD/Labs) Software V11.01 (© 1994-2017 ACD/Labs) taken from SciFinder)

The same is valid for the ^{13}C NMR spectra. Both spectra (aqueous phase and dichloromethane phase) do not include peaks that correspond to 2-methyl-2-hydroxypropanal (see Figure 6-11). The spectrum of the aqueous phase just shows peaks of DMSO (~ 40 ppm) (Figure 6-9) and the spectrum of the dichloromethane phase includes peaks corresponding to DMSO and dichloromethane (~ 55 ppm) (Figure 6-10).

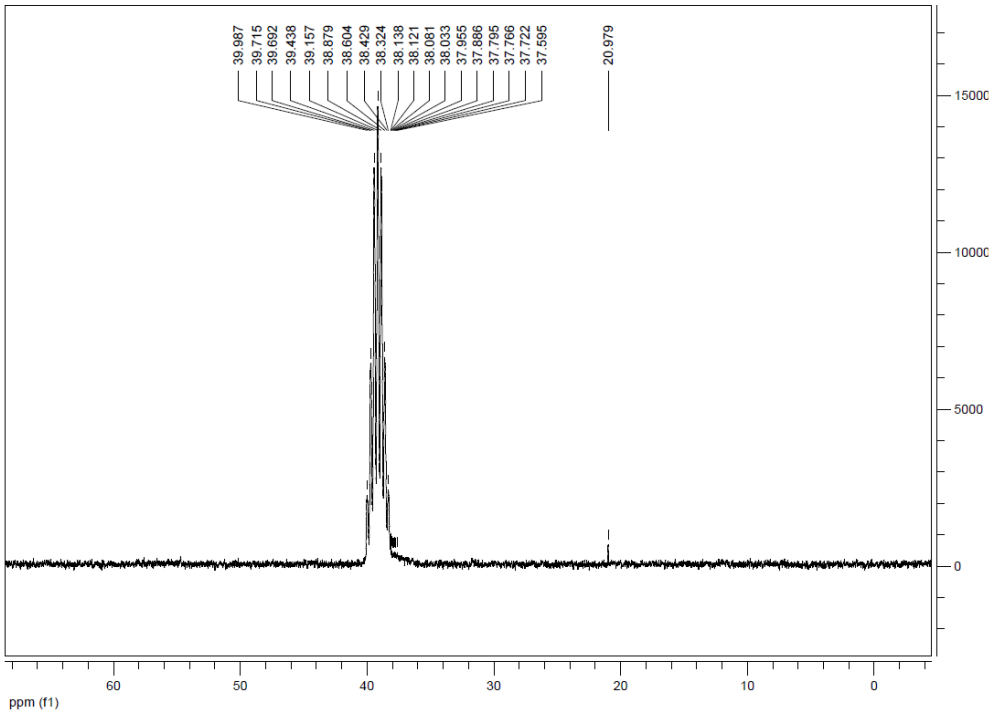

Figure 6-9: ^{13}C NMR spectrum of the aqueous phase obtained after extraction of the solution after oxidation of 2-methyl-2-hydroxypropanol to 2-methyl-2-hydroxypropanal

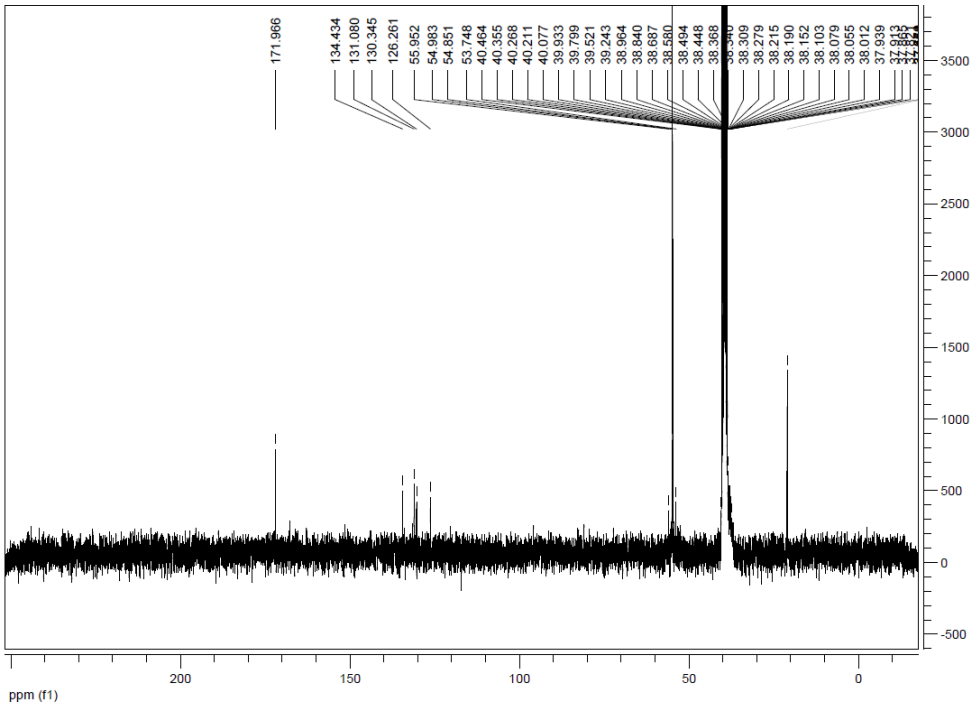

Figure 6-10: ^{13}C NMR spectrum of the dichloromethane phase obtained after extraction of the solution after oxidation of 2-methyl-2-hydroxypropanol to 2-methyl-2-hydroxypropanal

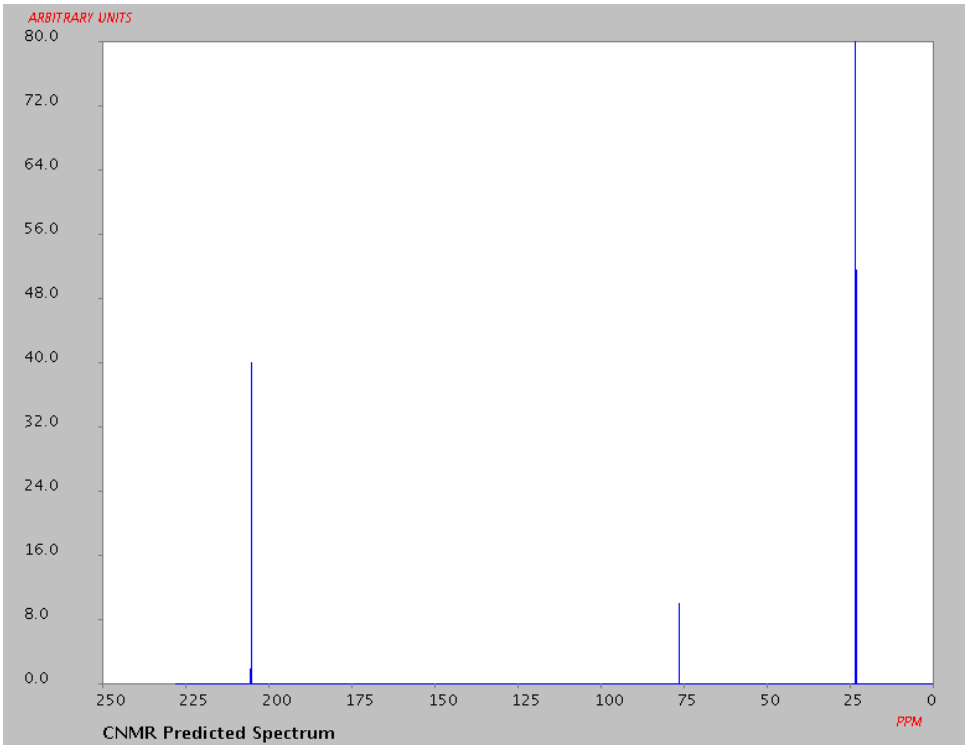

Figure 6-11: predicted ^{13}C NMR spectrum of 2-methyl-2-hydroxypropanal (Predicted NMR data calculated using Advanced Chemistry Development, Inc. (ACD/Labs) Software V11.01 (© 1994-2017 ACD/Labs) taken from SciFinder)

The derivatized standard (a sample after reaction of ˙OH with *t*BuOH) was measured by HPLC-UV to obtain the retention times for 2,4-DNPH and 2-methyl-2-hydroxypropanal-2,4-DNPH (Figure 6-12) for the comparison with the chromatogram of the derivatized product from the oxidation of 2-methyl-2-hydroxypropanol. These were 7.0 and 11.3 min, respectively. The peak eluting at 14.11 min corresponds to formaldehyde-2,4-DNPH.

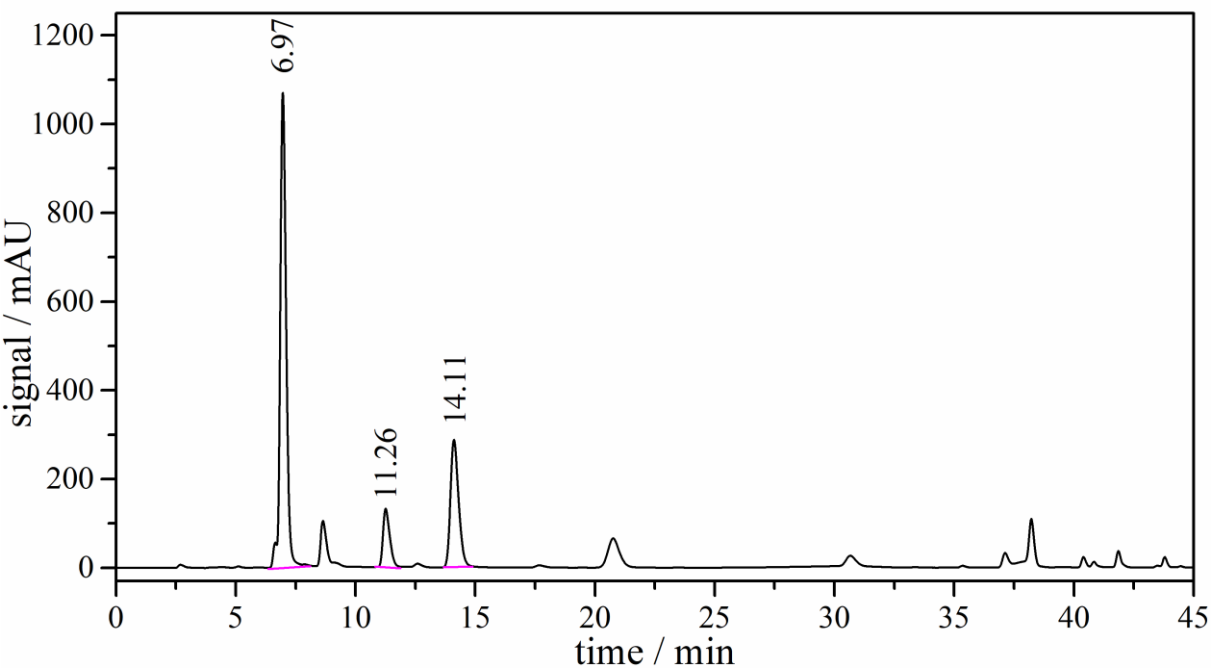

Figure 6-12: Chromatogram of derivatized products of a sample after reaction of •OH with *t*BuOH used as standard.

The measurement of the derivatized products of the oxidation of 2-methyl-2-hydroxypropanol shows a huge amount of peaks in the obtained chromatogram (Figure 6-13). This demonstrates that there are impurities in the obtained product.

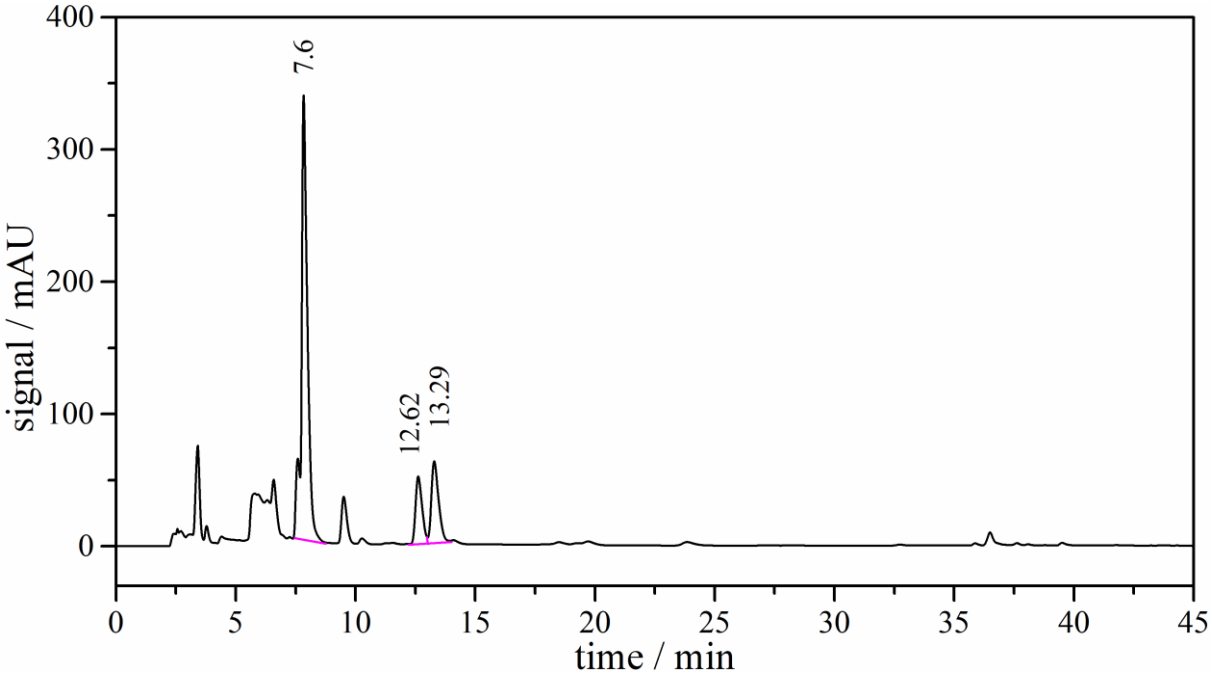

Figure 6-13: Chromatogram of the derivatized products of the oxidation of 2-methyl-2-hydroxypropanol after extraction in the aqueous phase

Overlapping both chromatograms (Figure 6-14) shows a shift in the retention time for 2,4-DNPH from 7.0 (standard) to 7.6 min (oxidation product). The shift can be caused by substances/solvents that were present in the injected sample, changing the elution strength while diluting the eluent. If so, one of the peaks eluted at 12.6 or 13.3 min could correspond to 2-methyl-2-hydroxypropanal-DNPH. But due to the fact, that the solution included many impurities an identification of 2-methyl-2-hydroxypropanal was impossible.

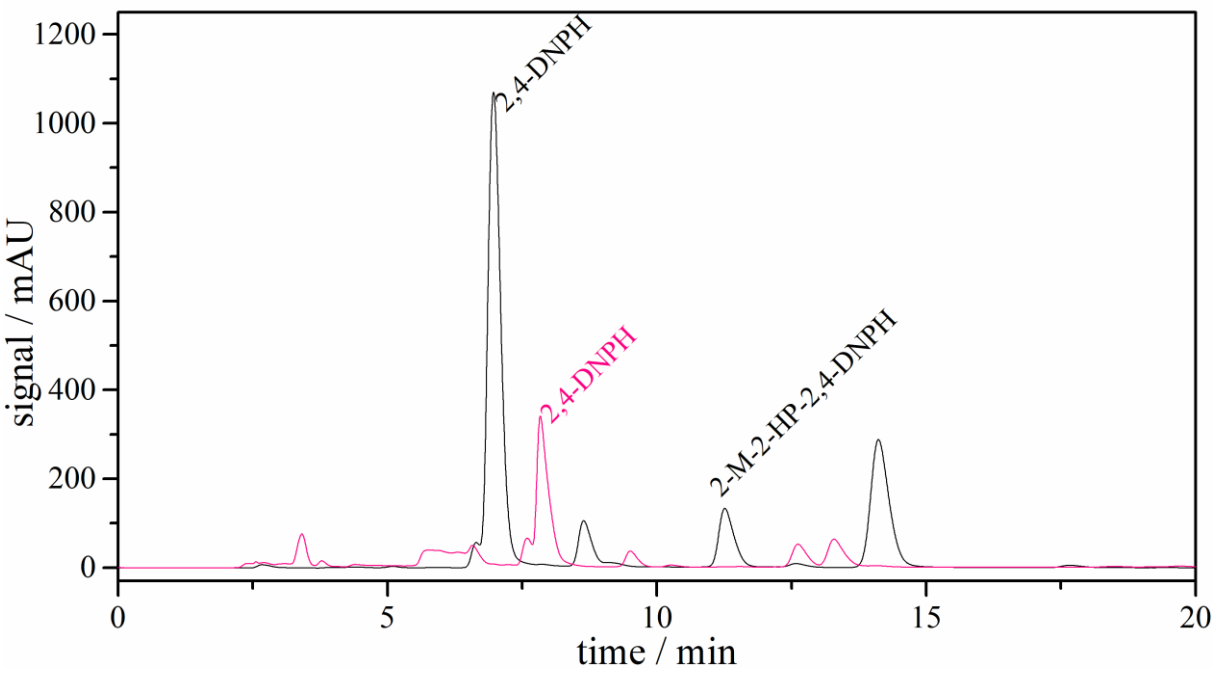

Figure 6-14: Overlapped chromatograms of the derivatized products of the reaction of •OH with *t*BuOH (black) and derivatized products from the oxidation of 2-methyl-2-hydroxypropanol (pink)

As shown in Figure 6-15 the results of the HPLC measurements of the dichloromethane phase (solvent of dichloromethane phase was evaporated under a nitrogen stream to dryness and replaced by water) cannot be evaluated. From these data no conclusion could be made.

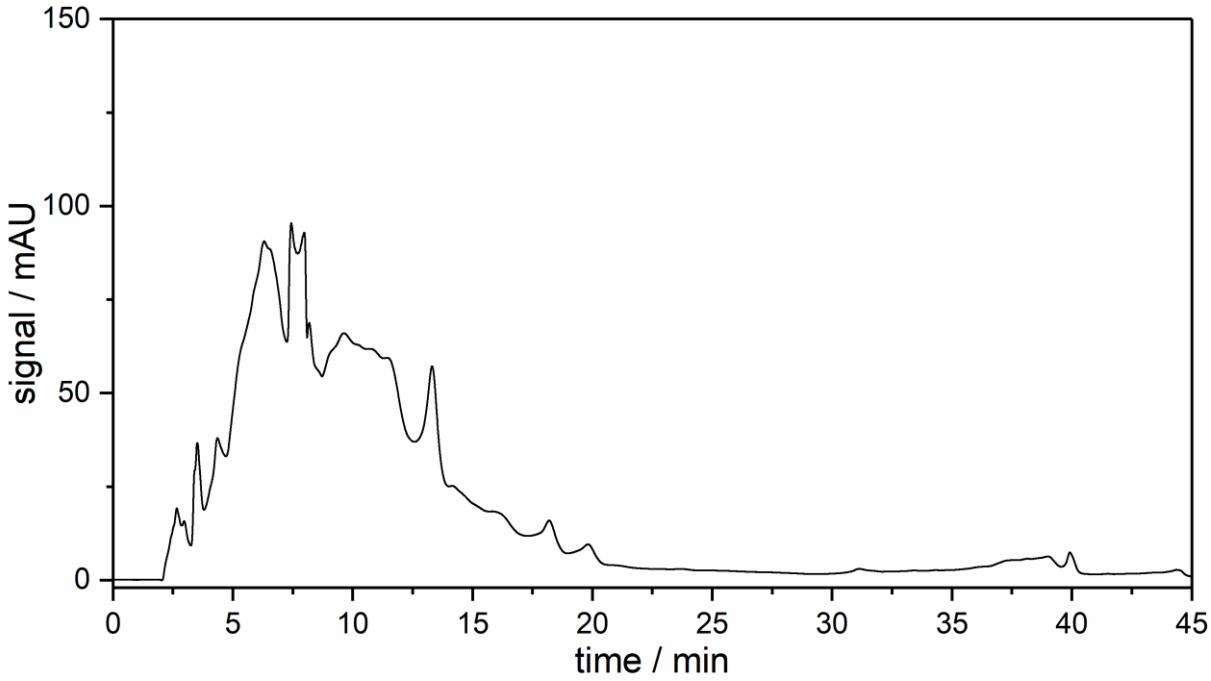

Figure 6-15: Chromatogram of the derivatized products of the oxidation of 2-methyl-2-hydroxypropanol after extraction in the dichloromethane phase

In summary one can say that there are no other main peaks in the NMR spectra present, but the HPLC measurements show that there are products (aldehydes or ketones) present in the aqueous phase. This discrepancy could be due to the fact that the amount of analyte in the NMR samples was too low. Hence, further development of the oxidation is needed to gain a pure product.

6.5 REFERENCES

Acero, J. L., Haderlein, S. B., Schmidt, T. C., Suter, M. J. F. and von Gunten, U. (2001). MTBE oxidation by conventional ozonation and the combination ozone/hydrogen peroxide: efficiency of the processes and bromate formation. Environmental Science & Technology, **35**(21), 4252-4259.

Alvarado, A., Tuazon, E. C., M. Aschmann, S., Arey, J. and Atkinson, R. (1999). Products and mechanisms of the gas-phase reactions of OH radicals and O_3 with 2-methyl-3-buten-2-ol. Atmospheric Environment, **33**(18), 2893-2905.

Beckert, R., Fanghänel, E. and Habicher, W. D. (2004). Organikum : organisch-chemisches Grundpraktikum; 22., vollst. überarb. und aktualisierte Aufl. Wiley-VCH, Weinheim.

Carrasco, N., Doussin, J.-F., Picquet-Varrault, B. and Carlier, P. (2006). Tropospheric degradation of 2-hydroxy-2-methylpropanal, a photo-oxidation product of 2-methyl-3-buten-2-

ol: kinetic and mechanistic study of its photolysis and its reaction with OH radicals. Atmospheric Environment, **40**(11), 2011-2019.

Dess, D. B. and Martin, J. C. (1991). A useful 12-I-5 triacetoxyperiodinane (the Dess-Martin periodinane) for the selective oxidation of primary or secondary alcohols and a variety of related 12-I-5 species. Journal of the American Chemical Society, **113**(19), 7277-7287.

Ferreira, N. L., Labbe, D., Monot, F., Fayolle-Guichard, F. and Greer, C. W. (2006). Genes involved in the methyl tert-butyl ether (MTBE) metabolic pathway of Mycobacterium austroafricanum IFP 2012. Microbiology-Sgm, **152**, 1361-1374.

Fischbacher, A., von Sonntag, J., von Sonntag, C. and Schmidt, T. C. (2013). The $^{\bullet}$OH radical yield in the $H_2O_2 + O_3$ (peroxone) reaction. Environmental Science & Technology, **47**(17), 9959-9964.

Flyunt, R., Leitzke, A., Mark, G., Mvula, E., Reisz, E., Schick, R. and von Sonntag, C. (2003). Determination of $^{\cdot}$OH, $O_2^{-\cdot}$, and hydroperoxide yields in ozone reactions in aqueous solution. Journal of Physical Chemistry B, **107**(30), 7242-7253.

Ireland, R. E. and Liu, L. (1993). An improved procedure for the preparation of the Dess-Martin periodinane. The Journal of Organic Chemistry, **58**(10), 2899-2899.

Lipari, F. and Swarin, S. J. (1982). Determination of formaldehyde and other aldehydes in automobile exhaust with an improved 2,4-dinitrophenylhydrazine method. Journal of Chromatography, **247**(2), 297-306.

Murphy, S. and Adam, W. (1996). The elusive 1,4-dioxy biradical: revised mechanism for the formation of diol from 3,3-dimethyldioxetane in cyclohexadiene. Journal of the American Chemical Society, **118**(51), 12916-12921.

Reisen, F., Aschmann, S. M., Atkinson, R. and Arey, J. (2003). Hydroxyaldehyde oroducts from hydroxyl radical reactions of Z-3-hexen-1-ol and 2-methyl-3-buten-2-ol quantified by SPME and API-MS. Environmental Science & Technology, **37**(20), 4664-4671.

Spaulding, R., Charles, M. J., Tuazon, E. C. and Lashley, M. (2002). Ion trap mass spectrometry affords advances in the analytical and atmospheric chemistry of 2-hydroxy-2-methylpropanal, a proposed photooxidation product of 2-methyl-3-buten-2-ol. Journal of the American Society for Mass Spectrometry, **13**(5), 530-542.

Steffan, R. J., McClay, K., Vainberg, S., Condee, C. W. and Zhang, D. L. (1997). Biodegradation of the gasoline oxygenates methyl tert-butyl ether, ethyl tert-butyl ether, and tert-amyl methyl ether by propane-oxidizing bacteria. Applied and Environmental Microbiology, **63**(11), 4216-4222.

Chapter 7

GENERAL CONCLUSIONS AND OUTLOOK

This thesis deals with •OH formation and quantification in two AOPs, the Fenton process and the peroxone process. Furthermore, the mechanisms of bromate (by-product) formation in the reaction of bromide with ozone is described. The synthesis of two products that could improve the quantification of •OH is also part of this thesis.

This thesis shows that ligands, e.g. pyrophosphate and sulfate can influence the Fenton process and its •OH yield. In the presence of pyrophosphate the •OH yield in the Fenton process is decreased. Pyrophosphate adds to Fe(III) forming a complex, which does not react with H_2O_2 back to Fe(II) and thus, terminates the Fenton reaction. Sulfate also influences the Fenton reaction but not to the same extent than pyrophosphate. In case of sulfate the complex with Fe(III) seems to be less reactive towards H_2O_2 than uncomplexed Fe(III) but still reacts with H_2O_2. Beside these two selected ligands there are many more organic and inorganic ligands that influence the Fenton process (Pignatello *et al.*, 2006). As sulfate and pyrophosphate decrease the reactivity of complexed Fe(III) with H_2O_2, but do not affect the reaction of Fe(II) with H_2O_2, other ligands, e.g. oxalate and EDTA enhance reactivity of Fe(II) towards H_2O_2 (Rush and Koppenol, 1986, Park *et al.*, 1997). The influence of ligands that may be present in wastewater, e.g. organic compounds, inorganic ions and complex forming agents, on the •OH yield has to be further investigated. Beside ligands the influence of the pH and H_2O_2/Fe(II) ratio on the •OH yield is discussed in this thesis. As present ligands may shift the optimal pH and H_2O_2/Fe(II) ratio, these factors have to be determined in dependency on the ligands. It is necessary to know more conditions that enhance or inhibit the Fenton reaction to be able to predict reactions that are involved in the Fenton reaction yielding •OH or other reactive species. This thesis is just a first step in a better understanding of constraints of the Fenton reaction needed for such a prediction. If industrial wastewater treated with the Fenton process contains compounds acting as ligands and inhibiting the •OH generation, one could consider another AOP for the treatment of such a water to make the process more efficient. In cases where the Fenton reaction occurs unintentionally, e.g. in fuel cells where the prerequisites for the Fenton reaction are given (Holton and Stevenson, 2013) ligands can be added to avoid the undesired •OH formation. To be able to control the reaction it is necessary to investigate the conditions leading to •OH.

The mechanism of the peroxone process is revised in this thesis. The present thesis shows that the •OH yield in the peroxone process is not as previously assumed unity with respect to applied O_3 (Staehelin and Hoigné, 1982), but only around 0.5. This is shown by different approaches. Based on the experiments presented in this thesis Merenyi *et al.* (2010) published a possible explanation for the reduced •OH yield. In the reaction of O_3 with HO_2^- HO_5^- is formed that

decomposes into $O_3^{\bullet-}$ and $HO_2^{\bullet}$ in competition with 2 O_2 + OH^-. $O_3^{\bullet-}$ is the precursor of $^{\bullet}OH$ and only the decomposition of the adduct to $O_3^{\bullet-}$ leads to $^{\bullet}OH$ formation. In water treatment processes $^{\bullet}OH$ are also formed from the reaction of ozone with matrix components, e.g. DOC (Noethe *et al.*, 2009). Therefore, the process is not applied in wastewater treatment processes as wastewater has a high content of DOC and the benefit of the addition of H_2O_2 is negligible (Pocostales *et al.*, 2010). Therefore, a general statement about the effect of the revised mechanism and reduced $^{\bullet}OH$ on practical implications is not possible, but it has to be taken into account when using the peroxone process as an AOP for micropollutant oxidation in water treatment. Consequently, the cost of this process could be much higher for some applications than hitherto assumed.

In this thesis it is shown that in the multistep reaction of ozone with bromide to bromate, $^{\bullet}OH$ are formed. Hitherto it was assumed that the last of these steps (bromate formation) is an O-transfer reaction (von Gunten and Hoigné, 1994, von Gunten, 2003). An electron-transfer reaction in the last step that also yields bromate could explain the $^{\bullet}OH$ formation in this multistep reaction. If not scavenged by other compounds present in the treated water the formed $^{\bullet}OH$ may contribute to bromate formation increasing its yield. As bromate is a critical by-product in the ozonation of waters reaction modelling is often performed before applying the treatment process. Hitherto, the modeling of the reaction of bromide with ozone does not give good results, as there are still too many not well known reactions included (von Gunten 2015, personal communication). The revised mechanism could enhance the reaction modeling. In systems with low $^{\bullet}OH$ scavenger capacity (e.g., waters with low DOC) $^{\bullet}OH$ formation in the electron transfer step might enhance the bromate yield, as the $^{\bullet}OH$ formed on site may contribute to bromate formation. It requires further investigation to find out under which conditions this is relevant in treatment of natural waters.

As $^{\bullet}OH$ cannot be quantified directly indirect methods are applied. One of these methods is the product analysis of the products from the reaction of *t*BuOH with $^{\bullet}OH$. These products are formaldehyde, acetone, 2-methyl-2-hydroxypropanol and 2-methyl-2-hydroxypropanal. The latter two are not commercially available and the quantification of $^{\bullet}OH$ is just based on the formaldehyde yield, but the quantification might be more exact if all products would be available. In this thesis the synthesis of 2-methyl-2-hydroxypropanol and 2-methyl-2-hydroxypropanal is presented, but just 2-methyl-2-hydroxypropanol could be successfully synthesized, while the synthesis of 2-methyl-2-hydroxypropanal failed. The unsuccessful synthesis of 2-methyl-2-hydroxypropanal was based on the oxidation of 2-methyl-2-

hydroxypropanol by Dess-Martin periodinane (Dess and Martin, 1991). To obtain the desired product further oxidation methods have to be applied. In addition the amount of 2-methyl-2-hydroxypropanol formed from the reaction of *t*BuOH with •OH should be determined, as in the cascade of reactions 2-methyl-hydroxypropanol is just formed in one reaction, that might be of minor importance.

Overall, the protection of the environment is in greater focus, which will lead to more regulations of micropollutants in treatment plant effluents and in drinking water. As the enhancement of analytical systems leads to more identified micropollutants in these waters more efficient processes for degradation of micropollutants, e.g. AOPs are requested. Hence, the mechanistic investigations in the field of AOPs are essential, as this knowledge may enhance the selection of a suitable treatment process for each water and lower the treatment costs.

7.1 REFERENCES

Dess, D. B. and Martin, J. C. (1991). A useful 12-I-5 triacetoxyperiodinane (the Dess-Martin periodinane) for the selective oxidation of primary or secondary alcohols and a variety of related 12-I-5 species. Journal of the American Chemical Society, **113**(19), 7277-7287.

Holton, O. T. and Stevenson, J. W. (2013). The role of platinum in proton exchange membrane fuel cells. Platinum Metals Review, **57**(4), 259-271.

Merenyi, G., Lind, J., Naumov, S. and von Sonntag, C. (2010). Reaction of ozone with hydrogen peroxide (peroxone process): a revision of current mechanistic concepts based on thermokinetic and quantum-chemical considerations. Environmental Science & Technology, **44**(9), 3505-3507.

Noethe, T., Fahlenkamp, H. and von Sonntag, C. (2009). Ozonation of wastewater: rate of ozone consumption and hydroxyl radical yield. Environmental Science & Technology, **43**(15), 5990-5995.

Park, J. S. B., Wood, P. M., Davies, M. J., Gilbert, B. C. and Whitwood, A. C. (1997). A kinetic and ESR investigation of iron(II) oxalate oxidation by hydrogen peroxide and dioxygen as a source of hydroxyl radicals. Free Radical Research, **27**(5), 447-458.

Pignatello, J. J., Oliveros, E. and MacKay, A. (2006). Advanced oxidation processes for organic contaminant destruction based on the Fenton reaction and related chemistry. Critical Reviews in Environmental Science and Technology, **36**(1), 1-84.

Pocostales, J. P., Sein, M. M., Knolle, W., von Sonntag, C. and Schmidt, T. C. (2010). Degradation of ozone-refractory organic phosphates in wastewater by ozone and ozone/hydrogen peroxide (peroxone): the role of ozone consumption by dissolved organic matter. Environmental Science & Technology, **44**(21), 8248-8253.

Rush, J. D. and Koppenol, W. H. (1986). Oxidizing intermediates in the reaction of ferrous EDTA with hydrogen peroxide. Reactions with organic molecules and ferrocytochrome c. Journal of Biological Chemistry, **261**(15), 6730-6733.

Staehelin, J. and Hoigné, J. (1982). Decomposition of ozone in water: rate of initiation by hydroxide ions and hydrogen peroxide. Environmental Science & Technology, **16**(10), 676-681.

von Gunten, U. (2003). Ozonation of drinking water: part II. Disinfection and by-product formation in presence of bromide, iodide or chlorine. Water Research, **37**(7), 1469-1487.

von Gunten, U. and Hoigné, J. (1994). Bromate formation during ozonation of bromide-containing waters: interaction of ozone and hydroxyl radical reactions. Environmental Science & Technology, **28**(7), 1234-1242.

Chapter 8

SUPPLEMENTS

8.1 LIST OF FIGURES

8.2 LIST OF TABLES

8.3 LIST OF ABBREVIATIONS

2-MIB	2-Methylisoborneol
2,4-DNPH	2,4-dinitrophenylhydrazine
AOC	Assimilable organic carbon
AOPs	Advanced oxidation processes
B. subtilis	*Bacillus subtilis*
BDE	Bond dissociation energy
BTEX	Benzene, toluene, ethylbenzene, and o-, m-, and p-xylenes
C. parvum	*Cryptosporidium parvum*
COD	Chemical oxygen demand
E. coli	*Escherichia coli*
EDC	Endocrine disrupting chemicals
EDTA	Ethylenediaminetetraacetic acid
E_{EM}	Electrical energy per mass of pollutant degradation per m^3
E_{EO}	Electrical energy per order of magnitude of pollutant degradation per m^3
EPR	Electron paramagnetic resonance
EU	European Union
G. lamblia	*Giardia lamlia*
G. muris	*Giardia muris*
DMS	N,N-dimethylsulfamide
DMSO	Dimethyl sulfoxide
DNA	Deoxyribonucleic acid

DOC	Dissolved organic carbon
GAC	Granulated activated carbon
HPLC-UV	High performance liquid chromatography with ultraviolet detection
IWR	In-well reactors
k	Reaction rate constant
LP-UV	Low pressure ultra violet (lamp)
MAR	Managed aquifer recharge
MeOH	Methanol
MHP	2-methyl-2-hydroxypropanal
MP	Micropollutant
MP-UV	Medium pressure ultra violet (lamp)
MTBE	Methyl tert-butyl ether
NDMA	N-Nitrosodimethylamine
NMR	Nuclear magnetic resonance
OMP	Organic micropollutant
*p*CBA	Para-chlorobenzoic acid
PCE	Tetrachloroethene
*p*NBA	Para-nitrobenzoic acid
PPCPs	Pharmaceuticals and personal care products
RNA	Ribonucleic acid
*t*BuOH	Tertiary butanol
T&O	Taste and odor
TCE	Trichloroethene

TOC	Total organic carbon
TPH-g	Total petroleum hydrocarbons – gasoline range organics
UK	United Kingdom
U.S. EPA	United States Environmental Protection Agency
UV	Ultra violet (light)
UV-Vis	Ultra violet and visible (light)
VOC	Volatile organic compound
VUV	Vacuum ultra violet
WTP	Water treatment plant

ε	Absorption coefficient [M^{-1} cm^{-1}]
λ	Wave length [nm]

8.4 LIST OF PUBLICATIONS

8.4.1 BOOK CHAPTERS

1. **Fischbacher, A.**; Lutze, H. V.; Schmidt, T. C., Ozone/H_2O_2 and Ozone/UV Processes. In *Advanced Oxidation Processes for Water Treatment: Fundamentals and Applications*, Stefan, M. I., Ed. IWA Publishing: 2017.

8.4.2 PEER-REVIEWED PUBLICATIONS

1. **Fischbacher, A.**; von Sonntag, C.; Schmidt, T. C., Hydroxyl Radical Yields in the Fenton Process Under Various pH, Ligand Concentrations and Hydrogen Peroxide/Fe(II) Ratios. Chemosphere 2017, 182, 738-744.

2. **Fischbacher, A.**; Löppenberg, K.; von Sonntag, C.; Schmidt, T. C., A New Reaction Pathway for Bromite to Bromate in the Ozonation of Bromide. Environmental science & technology 2015, 49, (19), 11714-20.

3. Reisz, E.; **Fischbacher, A.**; Naumov, S.; von Sonntag, C.; Schmidt, T. C., Hydride Transfer: A Dominating Reaction of Ozone with Tertiary Butanol and Formate Ion in Aqueous Solution. Ozone-Science & Engineering 2014, 36, (6), 532-539.

4. **Fischbacher, A.**; von Sonntag, J.; von Sonntag, C.; Schmidt, T. C., The $^{\bullet}OH$ Radical Yield in the $H_2O_2 + O_3$ (Peroxone) Reaction. Environmental science & technology 2013, 47, (17), 9959-9964.

5. Naumov, S.; Mark, G.; **Jarocki, A.**; von Sonntag, C., The Reactions of Nitrite Ion with Ozone in Aqueous Solution - New Experimental Data and Quantum-Chemical Considerations. Ozone-Science & Engineering 2010, 32, (6), 430-434.

6. Reisz, E.; Leitzke, A.; **Jarocki, A.**; Irmscher, R.; von Sonntag, C., Permanganate Formation in the Reactions of Ozone with Mn(II): A Mechanistic Study. Journal of Water Supply Research and Technology-Aqua 2008, 57, (6), 451-464.

8.4.3 POSTERS AND ORAL PRESENTATIONS

Poster presentation: Jarocki, A.; Löppenberg, K.; von Sonntag; C. Schmidt, T. C.; *Hydroxyl Radical Formation in the Reaction of Bromide with Ozone* - Wasser 2012 – Jahrestagung der Wasserchemischen Gesellschaft 2012; Neu-Ulm, Germany

Poster presentation: Jarocki, A.; Brünning, J.; von Sonntag, C.; Schmidt, T. C.; *Influence of Pyrophosphate on OH-Radical Yield in the Fenton Process* – Wasser 2011 – Jahrestagung der Wasserchemischen Gesellschaft 2011; Norderney, Germany

Oral presentation: Jarocki, A. Sein, M. M.; von Sonntag, J.; Golloch, A.; Schmidt, T. C.; von Sonntag, C.; *OH Radical Yield in the Peroxone Process (O_3 + H_2O_2)* – Ozone and UV: Leading-edge science and technologies 2011, Paris, France

Poster presentation: Jarocki, A.; Schmidt, T. C.; von Sonntag, C.; *OH-Radical Yield in the Fenton Process under Varied Conditions* – Wasser 2010 – Jahrestagung der Wasserchemischen Gesellschaft 2010; Bayreuth, Germany

Poster presentation: Jarocki, A. Sein, M. M.; von Sonntag, J.; Golloch, A.; Schmidt, T. C.; von Sonntag, C.; *OH Radical Yield in the Peroxone Process (O_3 + H_2O_2)* – 5th International Conference on Oxidation Technologies for Water and Wastewater Treatment 2009, Berlin, Germany

Poster presentation: Jarocki, A. Sein, M. M.; von Sonntag, J.; Golloch, A.; Schmidt, T. C.; von Sonntag, C.; *OH Radical Yield in the Peroxone Process (O_3 + H_2O_2)* – enviroWater 2009; Stellenbosch, South Africa

Poster presentation: Jarocki, A. Sein, M. M.; von Sonntag, J.; Golloch, A.; Schmidt, T. C.; von Sonntag, C.; *OH Radical Yield in the Peroxone Process (O_3 + H_2O_2)* – Wasser 2008 – Jahrestagung der Wasserchemischen Gesellschaft 2008; Trier, Germany

8.5 CURRICULUM VITAE

Der Lebenslauf ist in der Online-Version aus Gründen des Datenschutzes nicht enthalten.

8.6 ERKLÄRUNG

Hiermit versichere ich, dass ich die vorliegende Arbeit mit dem Titel:

„Formation and Quantification of ˙OH in Oxidative Water Treatment"

selbst verfasst und keine außer den angegebenen Hilfsmitteln und Quellen benutzt habe, und dass die Arbeit in dieser oder ähnlicher Form noch bei keiner anderen Universität eingereicht wurde.

Essen, im Dezember 2017

8.7 DANKSAGUNG

Mein besonderer Dank gilt Prof. Dr. Torsten C. Schmidt, der mir die Möglichkeit gab diese Arbeit in seiner Arbeitsgruppe anzufertigen, für die vielen wertvollen Diskussionen und die wissenschaftliche Freiheit. Ich danke Herrn Prof. Dr. Malte Behrens für die Übernahme des Zweitgutachtens.

Ausdrücklich möchte ich Herrn Prof. Dr. Clemens von Sonntag, der meine wissenschaftliche Herangehensweise geprägt hat, posthum danken. Ich danke ihm für seine Inspiration, seine mitreißende Begeisterung für die Forschung und die vielen und langen Diskussionen und Gespräche.

Allen derzeitigen und ehemaligen Mitarbeitern der Instrumentellen Analytischen Chemie danke ich für die freundliche Atmosphäre, die guten Gespräche beim Essen und die schöne gemeinsame Zeit. Insbesondere aber möchte ich der „AOP+-Gang“ (Alexandra Beermann, Dr. Maike Funke, Dr. Thorsten Hüffer, Robert Knierim, Dr. Holger Lutze, Florian Metzelder, Dr. Uschi Telgheder, Jens Terhalle, Laura Wiegand, Sarah Willach und Vanessa Wirzberger) für den hilfreichen, fachlichen Austausch und die vielen schönen AOP-Ausflüge danken. Ein großes Dankeschön gebührt Frau Katja Löppenberg, die mir im Labor eine große Hilfe war.

Des Weiteren danke ich meiner Familie, insbesondere meinen Eltern, und meinen Freunden, die immer hinter mir standen.

Zu guter Letzt gilt ein ganz besonderer, unendlicher Dank meinem Ehemann, Marcel Fischbacher, für die Unterstützung, das Verständnis, die Liebe und Geduld.